in Graham & Wilcox. Algae. 2000

# Chapter 22

# Phytoplankton Ecology

Dr. James M. Graham

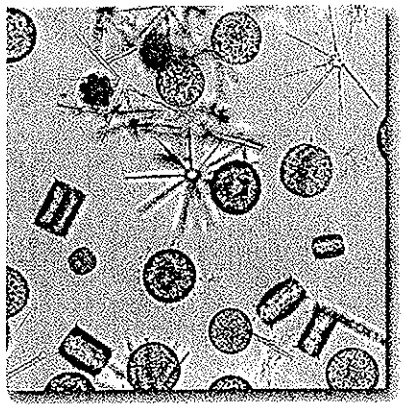

freshwater planktonic diatoms

What are phytoplankton? The prefix "phyto" comes from the Greek word for plant, *phytos*. "Plankton" derives from another Greek word meaning wanderer. Hence phytoplankton refers to organisms that wander in the surface waters of lakes, rivers, and the oceans.

The previous chapters have described many groups of algae. Among these groups, cyanobacteria, greens, diatoms, dinoflagellates, haptophytes, and chrysophyceans are especially rich in planktonic species. The dominant taxonomic groups differ between freshwaters and oceans. In freshwaters, cyanobacteria and greens are conspicuous and morphologically diverse while in the oceans these groups are primarily represented by small coccoid cyanobacteria and green microflagellates. Dinoflagellates occur in both freshwater and marine environments but are much more dominant and diverse in the oceans. Diatoms are abundant in both aquatic systems.

Phytoplankton cover a vast range of sizes and forms, both as single cells and as colonies (Fig. 22–1). Generally, cells or colonies with a maximum linear dimension less than 2 $\mu$m are considered to be picoplankton. Those greater than 30 $\mu$m in length are considered net plankton or microplankton. Cells and colonies between these two extremes are nanoplankton. Individual cells and colonies may possess flagella and be motile or lack flagella and be nonmotile. *Chlamydomonas* and *Ochromonas* are examples of small flagellated motile cells while *Chlorella* is a small nonmotile cell. *Scenedesmus* is a small nonmotile colony, and *Gonium* is a small motile one. *Staurastrum* and many other genera of desmids are large nonmotile cells. The dinoflagellate *Ceratium hirundinella* is an exceptionally large (> 100 $\mu$m), single-celled, motile alga. Large colonial phytoplankton include the nonmotile cyanobacterium *Microcystis aeruginosa* and diatom *Asterionella formosa* and the flagellated green *Volvox aureus*. Planktonic filamentous algae such as *Anabaena flos-aquae* can be thought of as long linear colonies. Why do phytoplankton vary so much in size?

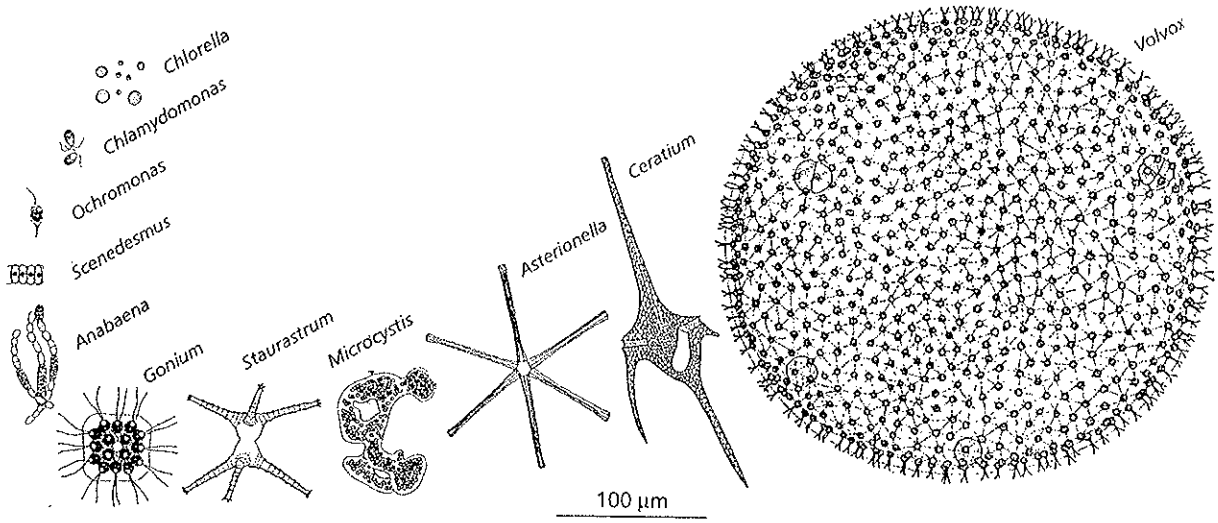


**Figure 22–1** Sizes and types of phytoplankton (approximately to scale). (Drawings from Smith, G. M. 1950. *Freshwater Algae of the United States*. McGraw-Hill. Reproduced with permission of the McGraw-Hill Companies, except for *Anabaena*: originally from G. M. Smith, in Prescott, G. W. 1951. *Algae of the Western Great Lakes Area*. Cranbrook Institute of Science, a division of Cranbrook Educational Community)

Size is the most important single characteristic affecting the ecology of phytoplankton. Table 22–1 presents volumes and surface areas of a number of phytoplanktonic species (Reynolds, 1984). As phytoplankton become larger, their volumes increase as the cube of their radius, while their surface areas increase in proportion to only the square of the radius. Consequently, as algal species become larger, their surface-to-volume ratio (SA/V) becomes smaller. Note the high SA/V ratios for tiny *Synechococcus* and *Ankistrodesmus* compared to the low SA/V ratios for *Microcystis* and *Volvox*. Since growth of phytoplankton involves the exchange of materials at the cell surface, there is a close relationship between cell volume and maximum rate of reproduction (Table 22–2). Large cells and colonies generally have low rates of reproduction, although the correlation holds less well for flagellates (Sommer, 1981).

Size affects more than just phytoplankton growth rates. Small cells can respond to a pulse of nutrients with a rapid burst of growth. Large cells, however, can take up and store more nutrients such as phosphate than can small cells. These size-related phenomena result in a spectrum of competitive strategies among phytoplankton species from small, fast-growing cells to large, slow-growing cells able to store nutrients through periods of scarcity. Between these extremes lie a range of intermediate adaptations. The danger of sinking out of the lighted (euphotic) zone in a body of water is a continual problem. Large cells tend to sink more rapidly through water than small cells (see below). To avoid losses due to sinking, phytoplankton have evolved a wide range of adaptations to increase buoyancy, reduce density, or increase physical-form resistance to sinking; these adaptations are more pronounced in large cells and colonies. In turn these same adaptations are responsible for much of the morphological diversity within the phytoplankton. Finally, the susceptibility of phytoplankton to losses due to grazing or predation is size-dependent. Small cells are generally rapidly consumed by grazers such as protozoa, rotifers, and crustaceans (see below). Large cells and colonies above about 50 $\mu$m in diameter are largely immune to predation by crustaceans (Burns, 1968), but are more prone to attack by parasites (see below). Intermediate cell and colony sizes may be free from predation by protozoa but susceptible to crustaceans. Many of the adaptations that reduce sinking rates also perform anti-herbivore roles.

The importance of cell size is one example of how scale factors into phytoplankton ecology. Different aspects of phytoplankton ecology occur at different scales of time and space. Nutrient regeneration and grazing of phytoplankton can take place at scales of seconds to minutes over distances of millimeters.

**Table 22–1 Volumes, surface areas, and surface-to-volume ratios for some selected phytoplanktonic algae (Data from Reynolds, 1984)**

| species | volume ($\mu m^3$) | surface area ($\mu m^2$) | SA/V ($\mu m^{-1}$) |
|---|---|---|---|
| *Synechococcus* sp. | 18 | 35 | 1.94 |
| *Aphanizomenon flos-aquae* | 610 | 990 | 1.62 |
| *Anabaena circinalis* | 2040 | 2110 | 1.03 |
| *Oscillatoria agardhii* | 46,600 | 24,300 | 0.52 |
| *Microcystis aeruginosa* | $4.2 \times 10^6$ | $1.26 \times 10^5$ | 0.03 |
| *Cryptomonas ovata* | 2710 | 1030 | 0.38 |
| *Certaium hirundinella* | 43,740 | 9600 | 0.22 |
| *Fragilaria crotonensis* | 6230 | 9290 | 1.48 |
| *Asterionella formosa* | 5160 | 6690 | 1.30 |
| *Tabellaria flocculosa* | 13,800 | 9800 | 0.71 |
| *Melosira granulata* | 8470 | 4915 | 0.58 |
| *Synedra ulna* | 7900 | 4100 | 0.52 |
| *Cyclotella meneghiniana* | 1600 | 780 | 0.49 |
| *Stephanodiscus astraea* | 5930 | 1980 | 0.33 |
| *Chrysochromulina parvula* | 85 | 113 | 1.33 |
| *Mallomonas caudata* | 4200 | 3490 | 0.83 |
| *Uroglena lindii* | $2.2 \times 10^6$ | $8.1 \times 10^4$ | 0.04 |
| *Ankistrodesmus falcatus* | 30 | 110 | 3.67 |
| *Ankyra judayi* | 24 | 60 | 2.50 |
| *Chlorella* sp. | 33 | 50 | 1.52 |
| *Pediastrum boryanum* | 16,000 | 18,200 | 1.14 |
| *Scenedesmus quadricauda* | 1000 | 908 | 0.91 |
| *Staurastrum pingue* | 9450 | 6150 | 0.65 |
| *Cosmarium depressum* | 7780 | 2770 | 0.36 |
| *Sphaerocystis schroederi* | $5.1 \times 10^4$ | $6.65 \times 10^3$ | 0.13 |
| *Eudorina unicocca* | $1.15 \times 10^6$ | $5.31 \times 10^4$ | 0.05 |
| *Volvox globator* | $4.77 \times 10^7$ | $6.36 \times 10^5$ | 0.01 |

Lehman and Scavia (1982) showed that zooplankton excrete nutrients in patches that significantly affect nutrient uptake by algae over scales of millimeters. Growth rates operate at scales of hours to days. Phytoplankton patches develop at scales of weeks and kilometers, and successions of species occur at scales of entire seasons across entire lake basins and oceans (Harris, 1986). Dynamic processes in lakes and oceans are very similar but operate on different scales. A patch of phytoplankton in a lake may extend for hundreds of meters whereas a patch in an ocean may be hundreds of kilometers across.

As an example of the importance of scale in phytoplankton ecology, consider the routine problem of determining the abundance of phytoplankton in a body of water. Counts of phytoplankton are usually done by collecting a sample of water and placing a subsample into a settling chamber. After the algae have settled overnight, they are counted and identified with an inverted microscope. The results are then reported as number of cells of each species per unit of volume (ml or l). If an alga were present at a density of one cell per liter, it would likely be missed or considered unimportant. But consider a typical lake like Lawrence Lake in southwestern Michigan (Wetzel, 1975). Lawrence Lake has a volume of 293,500 $m^3$, which is 293,500,000 liters! Thus even a rare alga existing at an average density of one per liter would have a total population of 293,500,000—more than the number of people in the United States! Many such rare species contribute to the high species diversity of phytoplankton in lakes and oceans.

**Table 22–2 Volumes and maximum rates of reproduction for selected phytoplankton (Data from Reynolds, 1984; Sandgren, 1988)**

| species | volume ($\mu m^3$) | $\mu_{max}$ ($day^{-1}$) |
|---|---|---|
| *Synechococcus* sp. | 18 | 2.01 |
| *Aphanizomenon flos-aquae* | 610 | 0.98 |
| *Oscillatoria agardhii* | 46,600 | 0.86 |
| *Microcystis aeruginosa* | $4.2 \times 10^6$ | 0.48 |
| *Cryptomonas ovata* | 2710 | 0.83 |
| *Certatium hirundinella* | 43,740 | 0.26 |
| *Stephanodiscus hantzschii* | 600 | 1.18 |
| *Cyclotella meneghiniana* | 1600 | 0.85 |
| *Asterionella formosa* | 5160 | 1.74 |
| *Tabellaria flocculosa* | 13,800 | 0.76 |
| *Monodus subterraneus* | 105 | 0.64 |
| *Dinobryon cylindricum* | 290 | 0.58 |
| *Synura petersenii* | 431 | 0.76 |
| *Mallomonas cratis* | 1516 | 0.55 |
| *Mallomonas caudata* | 10625 | 0.30 |
| *Ankistrodesmus falcatus* | 30 | 1.59 |
| *Chlorella* sp. | 33 | 2.15 |
| *Scenedesmus quadricauda* | 1000 | 2.84 |
| *Eudorina unicocca* | $1.15 \times 10^6$ | 0.62 |

Even though a phytoplankton species may be rare in a body of water at a particular time, the importance of temporal scale in phytoplankton ecology guarantees that it may not remain so for long. Rates of reproduction in phytoplankton vary from two to three doublings per day to one doubling every week to ten days. If an alga started at a density of one per liter with a reproduction rate of two doublings per day, it would reach a density of 16,384 cells $l^{-1}$ in one week (if we assume no losses during this time). It is therefore essential when planning a program to sample phytoplankton to be aware of the time scale at which events occur. In Figure 22–2, the upper graph shows the rapid changes in population densities of chrysophyceans as was determined by sampling every two to three days (Sandgren, 1988). Figure 22–2b shows what the same data would have looked like if these populations had been sampled at weekly intervals (which is a more common practice). The population maxima of several species would have been missed. The phenomenon of missing important phenomena by sampling at an inappropriate scale is called **aliasing**. Because of the short scales at which many events involving phytoplankton occur, aliasing is a persistent problem.

Phytoplankton ecology has been characterized by the development of a large body of theory and mathematical modeling. Theory and modeling have centered about two topics—competition theory and trophic dynamics. The original source of competition theory lies in the work of Gause (1934) on various microorganisms in test tubes and flasks. These experiments led to the development of the competitive exclusion principle and later to niche theory. The basic idea is that biological interactions—not physical and chemical external factors—are paramount in community dynamics. Species are assumed to exist close to their maximum density in the environment and to compete for scarce resources. If two species occupy the same niche, one must inevitably drive the other out through competitive displacement. These concepts entered plankton ecology when Hutchinson (1961) wrote his famous paper on the paradox of the plankton. If we assume that species are close to their

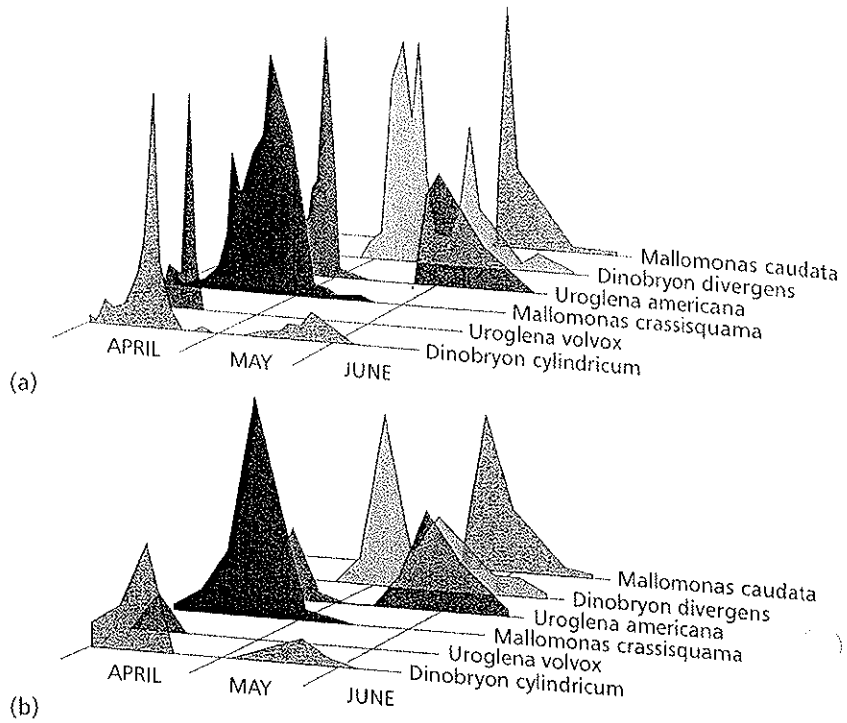


**Figure 22–2** (a) Patterns in populations of some opportunistic chrysophyceans sampled every two to three days. (Data from Sandgren, 1988) (b) A plot of the same data had sampling been conducted only every seven days. Several population maxima are missed.

maximum density in aquatic systems and competitive exclusion is a general rule, how can 50 to 100 species of phytoplankton possibly coexist in only a few milliliters of lake or ocean water? The controversy concerning this paradox has fueled experimental and theoretical research to the present and has even shaped aquatic management practices.

The second focus of theory and modeling is that of trophic dynamics. The concept of top-down control of phytoplankton communities originated with Porter (1977). Top-down theories assume phytoplankton are controlled by herbivory, which directs species compositions and seasonal patterns of biomass. The opposite concept of bottom-up control maintains that phytoplankton are fundamentally controlled by nutrients rather than herbivory. These concepts have also shaped management practices. We will discuss both competition theory and trophic dynamics in later sections. We will consider phytoplankton population dynamics under two general categories: (1) growth processes, including photosynthesis and nutrient uptake, and (2) loss processes, including competition, grazing, sedimentation, parasitism, washout, and death. But first, we will consider briefly the physical and chemical environment of lakes and oceans, the arena of phytoplankton ecology.

## The Physical Environment

### Water as a Fluid Medium

The physical environment in which phytoplankton reside is determined by the physical properties of water as a molecule and the interaction of water with solar radiation. In a molecule of water the two hydrogen atoms and single oxygen atom are arranged as if they were at the points of an isosceles triangle with an obtuse angle of 104.5° at the oxygen atom. Consequently, the hydrogen atoms bear a weak positive charge and the oxygen atom a weak negative charge. Water molecules are capable of forming hydrogen bonds between adjacent molecules. These bonds in turn allow water to act as a liquid crystal—a property that is almost unique among compounds. If water ($H_2O$) behaved like structurally similar compounds such as $H_2S$ or $NH_3$, it would be a gas at normal environmental temperatures.

Water is a highly effective solvent for inorganic salts, soluble hydrophilic organic compounds, and a wide array of gases including $O_2$, $N_2$, and $CO_2$. Therefore it is an ideal medium for a vast number of chemical interactions. The intermolecular bonding properties of water give it a high specific heat. This

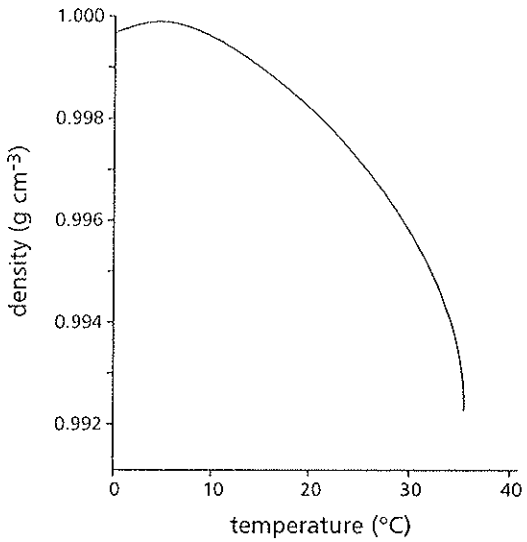


**Figure 22–3** The density of freshwater changes with temperature. Maximum density occurs at 4° C. (After Goldman, C. R., and A. J. Horne. 1983. *Limnology*. McGraw-Hill. Reproduced with permission of the McGraw-Hill Companies)

means that liquid water can store a large quantity of solar heat and that a large quantity of heat is required to raise the temperature of a body of water. Especially large inputs of heat (540 cal g$^{-1}$) are required for the phase transition from liquid to gas. Conversely, when a body of water cools, it gives off large amounts of heat to the overlying air and surrounding land. Aquatic environments are very stable thermal environments for phytoplankton, which are normally not subjected to sharp temperature changes over short periods of time as are terrestrial organisms.

Water shows very marked changes in density with temperature (Fig. 22–3). Density increases rapidly as temperature falls from 35° C, reaching a maximum density at 4° C. With further cooling, water becomes less dense until it freezes as ice, which floats because it is less dense than liquid water. The fact that ice floats is profoundly significant for aquatic life. If, like most substances, water had its greatest density when it became solid, ice would sink to the bottom of lakes or the oceans, which would consequently freeze from the bottom up. Bodies of water would be inhospitable places for life since few large organisms can withstand being frozen solid. Water ice furthermore has a specific heat (0.5) about half that of liquid water, and so ice forms and melts readily. The ease with which it forms means that the underlying warmer and denser water is quickly insulated from the cold air above and therefore remains liquid. Many lakes in Antarctica are covered by permanent ice caps up to 4 m thick; liquid water and phytoplankton survive under the ice. In the oceans, high salinity (on average, 35 g l$^{-1}$) increases density and depresses the freezing point to −1.91° C, but ice still floats and insulates the underlying waters.

Two final properties of water arise from hydrogen bonding. Surface tension is the tendency of water molecules to bond together at the air-liquid interface. This property makes it possible for a number of species of phytoplankton, including some diatoms and chrysophyceans, to hang from or sit atop the surface film. Collectively they are termed **neuston** (Wetzel, 1975). Viscosity is the tendency of water to resist flow and impose drag on organisms moving through it. Viscosity increases as temperature decreases. While water is much less viscous than maple syrup, it still has profound effects on the shapes of phytoplankton. If water

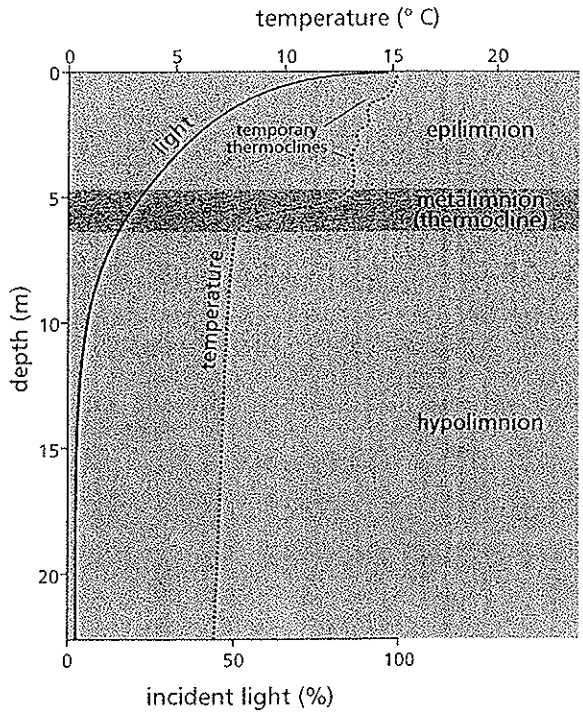


**Figure 22–4** Distribution of light and heat in a summer stratified lake. Light declines exponentially with depth. The thermocline divides the lake into upper mixed epilimnion, metalimnion, and lower, colder hypolimnion. Temporary thermoclines are due to warm, calm days. (After Goldman, C. R., and A. J. Horne. 1983. *Limnology*. McGraw-Hill. Reproduced with permission of the McGraw-Hill Companies)

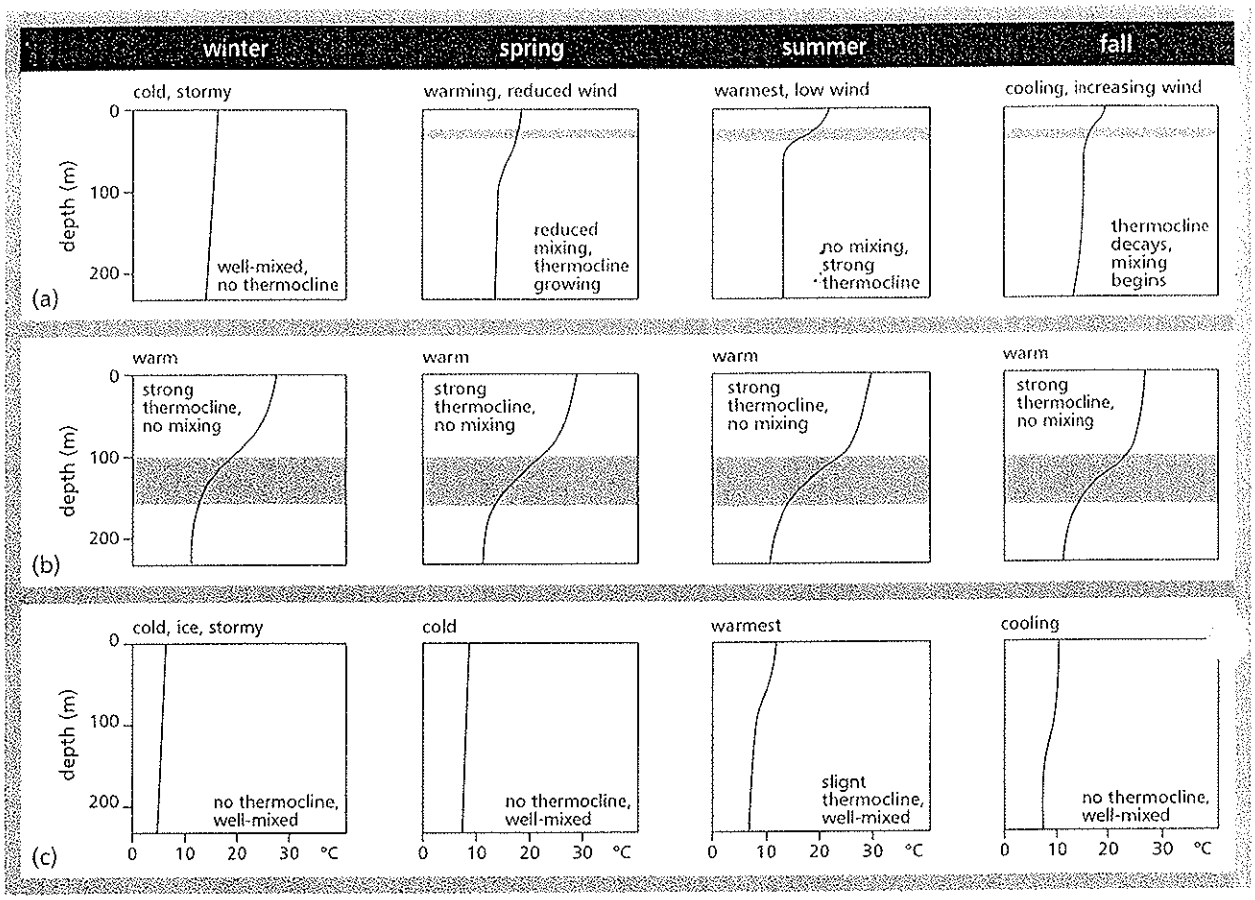


**Figure 22–5** Generalized patterns of temperature and mixing in (a) temperate, (b) tropical, and (c) polar oceans as functions of depth and seasonality. Line denotes temperature as a function of depth. Shaded zone indicates thermocline, which prevents mixing in the waters beneath it. (After MARINE BIOLOGY 2nd. Edition, by J. W. Nybakken. ©1987 by HARPER COLLINS PUBLISHERS. Reprinted by permission of Addison-Wesley Educational Publishers)

were significantly less viscous than it is, phytoplankton would have difficulty remaining in suspension.

## Light and Heat

Most of the solar radiation entering a lake or ocean is converted into heat. Light entering a body of water declines as a function of depth according to a simple exponential decay function.

$$I_z = I_o e^{-\eta z} \quad (1)$$

Here $I_z$ is the irradiance ($\mu$mol quanta $m^{-2}$ $s^{-1}$) at depth z. $I_o$ is the irradiance at the surface (about 2000 $\mu$mol quanta $m^{-2}$ $s^{-1}$), e the base of natural logarithms, and $\eta$ the extinction coefficient. The value of the extinction coefficient varies with the wavelength of light, being greater than 2.0 for red and infrared light and less than 0.01 for blue and violet light. Therefore most heat is absorbed near the surface, and only blue light penetrates to any depth. The penetration of light into a lake is shown in Figure 22–4. The depth at which light becomes too dim for photosynthesis defines the bottom of the **euphotic zone**. Temperature would follow a similar curve except that wind sets up currents in the water column that mix the heat down into the water column. This mixing process divides a lake or an ocean into distinct layers or strata and is called **stratification**. The upper warm and less dense layer is termed the **epilimnion** in lakes and the **epipelagic** in the oceans. In lakes the cooler denser lower layer is known as the **hypolimnion**. In the oceans there are four cold lower

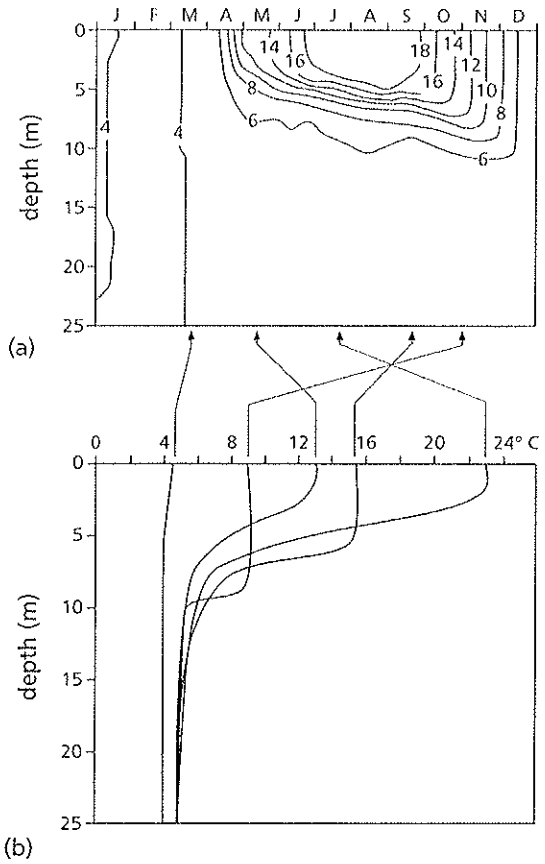


Figure 22–6 Mixing and thermal stratification in Lake Plußsee in Holstein, Germany, in 1986. (a) Temperatures are shown as isotherms—lines of equal temperature. (b) Temperature plotted as a function of depth on five dates. Lake Plußsee is an example of a dimictic lake (one that mixes twice a year, in the spring and fall). (After Lampert and Sommer, 1997 ©Georg Thieme Verlag)

strata—the **mesopelagic**, **bathypelagic**, **abyssal pelagic**, and **hadalpelagic** (see below). Between the upper and lower zones lies a region of sharp change in temperature and density (termed the **metalimnion** in lakes), which is marked by a decrease in temperature called the **thermocline** (Fig. 22–4). The depth of the epilimnion varies with the area of the lake; it may be as shallow as 2 m or greater than 20 m. Metalimnions are usually several meters in depth. A hypolimnion may be absent entirely in shallow lakes or extremely deep as in the Great Lakes or Lake Baikal in Russia. In oceans the epipelagic may be 20–100 m deep with its lower boundary marked by the thermocline. The mesopelagic extends from the epipelagic down to the 10° C isotherm at 700–1000 m depth, depending on geographic area. The bathypelagic lies between the 10° C and 4° C isotherms (2000–4000 m depth). The abyssal pelagic reaches to 6000 m, and the hadalpelagic occurs in deep trenches, from 6000–10,000 m. There are many patterns of formation and breakdown of stratification in lakes and oceans, which vary with size and latitude (Figs. 22–5, 22–6).

Stratification has important consequences for phytoplankton. The upper, warmer epilimnion is generally well mixed and well lighted. Phytoplankton will circulate within the epilimnion over 30 minutes to a few hours. In the metalimnion, however, the mixing time is on the order of weeks (Harris, 1986). Phytoplankton may occupy distinct vertical layers or patches within the epilimnion where light may be optimal for growth. Motile species may migrate up to the top of the epilimnion for photosynthesis during the day and back to the darker lower levels to acquire nutrients at night. Nonmotile species depend on vertical mixing to maintain position in the lighted water column. If the metalimnion is lighted (within the euphotic zone), species such as *Oscillatoria* may be concentrated there (Fig. 22–7). In the oceans, tropical and subtropical regions have a perennial thermocline that retards upward movement of nutrients (Fig. 22–5). Phytoplankton biomass in these regions is low year-round, except at coastal upwelling zones (Fig. 22–13) where it is enhanced and persistent. In temperate oceans the epipelagic is recharged with nutrients when the thermocline breaks down. In stratified open ocean waters phytoplankton typically show a deep chlorophyll maximum, which represents a trade-off between decreas-

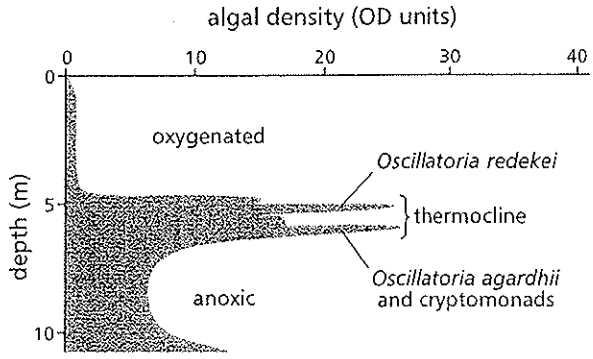


Figure 22–7 Vertical distribution of cryptomonads and *Oscillatoria* spp. in a stratified kettle lake. (Goldman, C. R., and A. J. Horne. 1983. *Limnology*. McGraw-Hill. Reproduced with permission of the McGraw-Hill Companies, based on Baker and Brook, 1971)

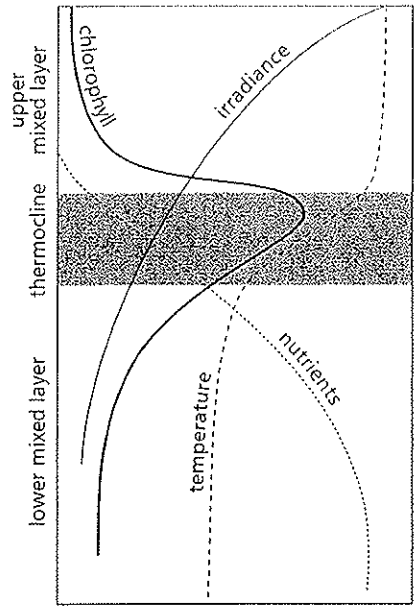


**Figure 22–8** Vertical profile of chlorophyll, temperature, irradiance, and nutrients in a stratified water column of the open ocean. (After Falkowski and Raven, 1997. Reprinted by permission of Blackwell Science, Inc.)

ing light and increasing nutrients in a more stable environment (Fig. 22–8). Polar oceans mix year-round and provide a consistent level of nutrients to sustain phytoplankton growth (Fig. 22–5). In the Southern Ocean the haptophyte *Phaeocystis antarctica* dominates in deeply mixed waters whereas diatoms dominate where waters are more highly stratified. Diatoms are less effective than *Phaeocystis* in $CO_2$ drawdown (Chapter 2) and transport to the deep oceans. Hence oceanographers are concerned that global warming, which is predicted to increase upper-ocean stratification, may result in a dramatic change in the biological pump (transfer of carbon to deep oceans) (Arrigo, et al., 1999).

## Turbulence

Oceans and lakes are turbulent environments. The interplay of wind action and solar heating with tides and the rotation of the earth creates many different types of water motions. Texts on limnology and oceanography are a good source for detailed descriptions of these various motions. Water motions may affect populations of phytoplankton by concentrating or dispersing patches of phytoplankton. In addition, there is evidence that species of algae differ in their tolerance of turbulence (Fogg, 1991; Willen, 1991), and these differences may affect competitive interactions and the formation of blooms. Here we will focus on a few types of water motions that significantly affect the ecology of phytoplankton.

Convection cells, or Langmuir cells, are elongate, wind-driven surface rotations in lakes marked by con-

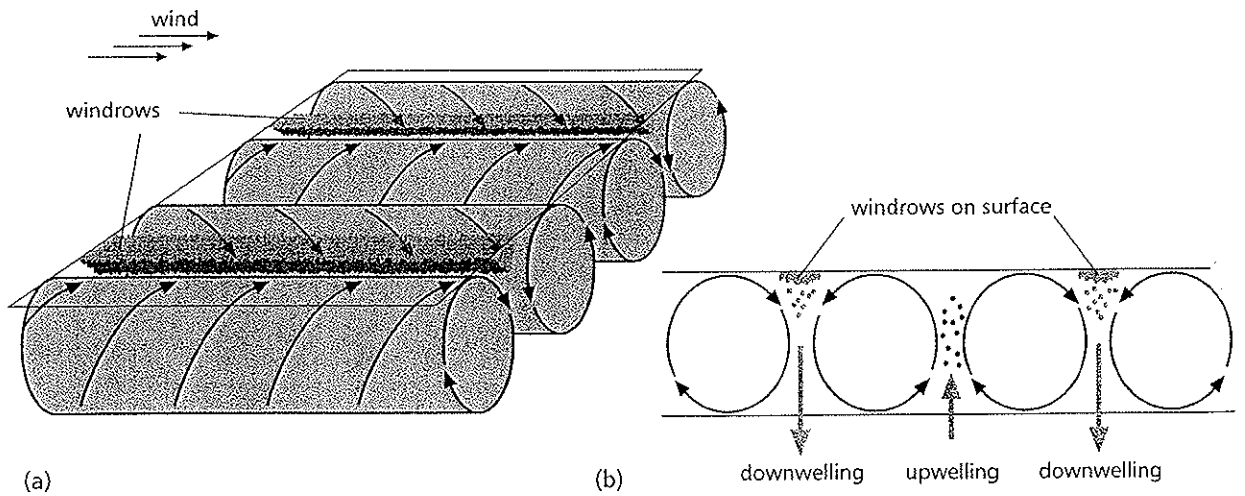


**Figure 22–9** The formation of Langmuir cells in a lake is marked by windrows on the surface (a). Water in each cell follows a spiral path through the water in the direction of the wind. Adjacent cells, seen in cross section in (b), rotate in opposite directions, creating regions of downwelling (where the windrows occur) and upwelling. Foam and buoyant algae (gray circles) accumulate in the downwelling regions where currents converge. Negatively buoyant algae (black circles) accumulate in the upwelling zones beneath the surface.

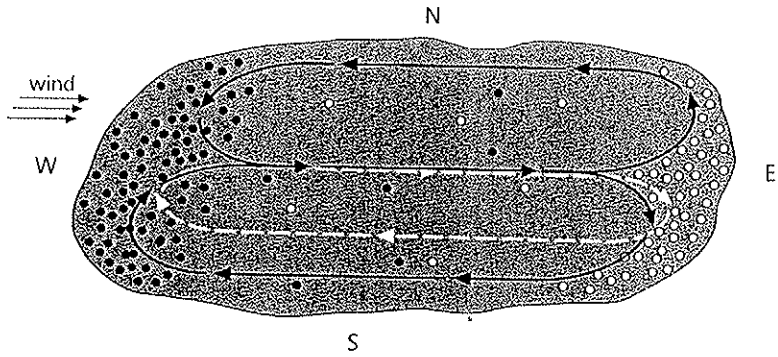


**Figure 22–10** Diagrammatic representation of a lake under a steady westerly wind. Return currents flow back toward the west along the north and south shores. Internally, there is also a return flow (dashed white lines), which acts much like a conveyor belt on suspended phytoplankton. Buoyant phytoplankton (white circles) build up on the eastern (downwind) shore. Phytoplankton that avoid the surface waters (black circles) may accumulate along the western shore to which they are carried by the subsurface return flow. (Based on diagrams in Verhagen, 1994; George and Edwards, 1976. Reprinted by permission of Blackwell Science, Ltd.)

spicuous lines of foam called windrows (Fig 22–9a). A minimum wind speed of about 11 km $hr^{-1}$ is necessary for their formation. Within each Langmuir cell, water moves in the direction of the wind but in a spiral pattern. Adjacent convection cells rotate in opposite directions, creating alternating zones of upwelling and downwelling between them. The foam streaks on the surface occur in the zones of downwelling where buoyant phytoplankton and bubbles accumulate. Between the rotating cells in the zones of upwelling, negatively buoyant particles and algal cells also concentrate (Fig. 22–9b). In both cases phytoplankton are moved across the lake in the direction of the wind.

Imagine a steady wind blowing from the west across a lake for an extended period of time. Such a wind transmits about 3% of its energy to the water surface (Goldman and Horne, 1983) and generates normal surface waves. The same kind of normal waves occur on the surface of the oceans, but on a much larger scale. When that flow of water reaches the eastern shore of the lake, waves, of course, crash

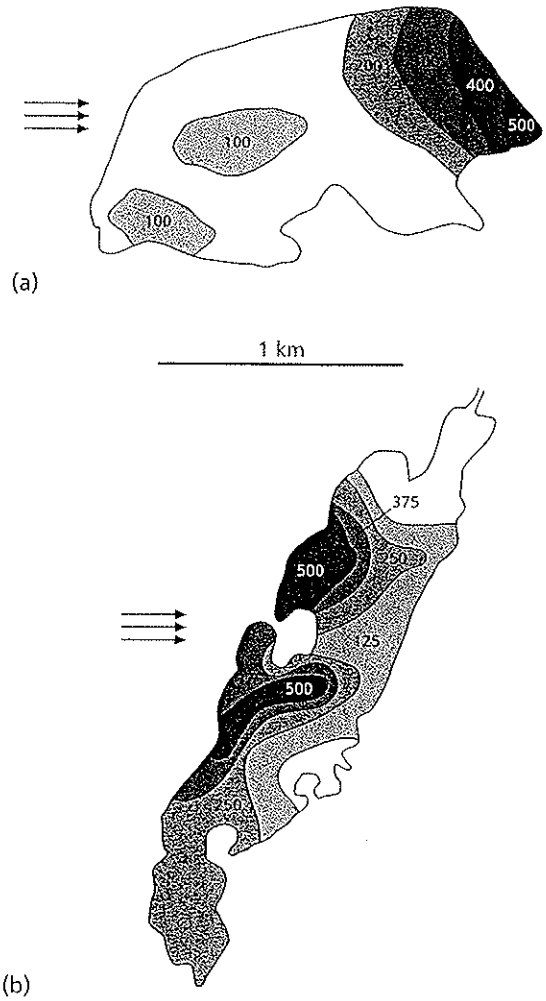


**Figure 22–11** Horizontal patches of phytoplankton due to westerly winds. (a) buoyant *Microcystis aeruginosa* builds up on the downwind (eastern) shore in Eglwys Nynydd, South Wales, reservoir. Isopleths in $\mu$mol chl *a* $l^{-1}$ (b) *Ceratium hirundinella* favors deeper strata in Esthwaite Water, Lake District, England, and is carried back toward the western shore by subsurface return currents. Isopleths are cells $ml^{-1}$ (a: After George and Edwards, 1976. Reprinted by permission of Blackwell Science, Ltd.; b: After Heany, 1976)

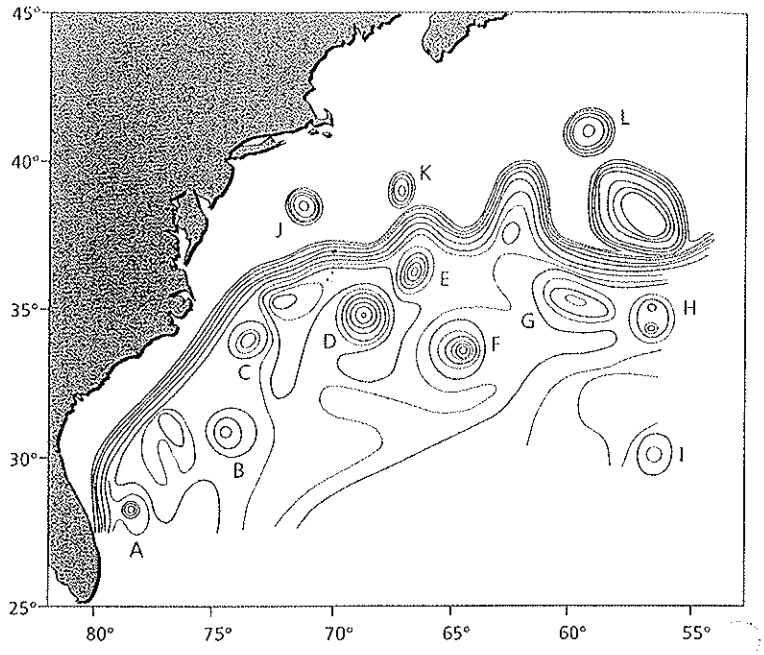


**Figure 22–12** Gulf stream rings in the western North Atlantic (A–L) from bathythermograph and infrared satellite imagery. Rings J, K, L are warm core rings north of Gulf Stream. Rings A–I are cold core rings. Warm core rings are headed northeasterly, while cold core rings flow southwesterly. (After Richardson, P. L., R. E. Cheney, and L. V. Worthington. *Journal of Geophysical Research* 83:6136–6144 ©American Geophysical Union)

on the beach, but also a surface current will move north and south along the shore, returning to the west along the north and south shores (Fig. 22–10). Internally there will also be an east-to-west return flow under the surface. This return flow acts like a conveyor belt, and it can have a substantial effect on the distribution of phytoplankton. If the phytoplankton are buoyant near the surface, then the surface flow of the conveyor tends to pile them up on the downwind (eastern) shore. Figure 22–11a shows an example where *Microcystis aeruginosa*, a buoyant cyanobacterium, piled up on the downwind shore in Eglwys Nynydd, South Wales (U.K.) (George and Edwards, 1976). *Ceratium hirundinella* maintains its position at a lower level in the water column. In Esthwaite Water, English Lake District (U.K.), westerly winds caused this dinoflagellate to accumulate on the western shore of the lake due to the action of the subsurface return currents (Fig. 22–11b) (Heaney, 1976). Clearly, winds can affect the distribution of phytoplankton patches. If sampling were done at a single fixed station, these types of large-scale population movements could result in widely varying population estimates.

In the oceans water movements occur on much larger scales than in lakes and largely without the edge effects of closed basins. Patch sizes are much larger, and phytoplankton are often monitored by remote sensing (see Text Box 22–1). While phytoplankton patches may extend for hundreds of meters in large lakes, they may extend for hundreds of kilometers in oceans. Two types of currents are of special importance to phytoplankton dynamics in the seas. A major ocean current like the Gulf Stream wanders north and south as it makes its way across the North Atlantic (see Fig. 23–18). As it wanders, it forms eddies or loops that become pinched off as rings varying in diameter from 100 km to over 250 km (Fig. 22–12). These rings rotate and move across the ocean carrying whole ecosystems as discrete parcels, which maintain their structure for up to two years. Warm core rings move northward into European coastal waters, and cold core rings may push south into the Sargasso Sea (Harris, 1986).

The second important type of current is that responsible for upwelling zones (Fig. 22–13). The most famous of these currents is the Peruvian upwelling. Off the coast of Peru, cold nutrient-rich water rises up from great depth to create an abundant growth of phytoplankton. Zooplankton graze on the phytoplankton and in turn support a rich fishery. An El Niño event occurs when warm Pacific water floods over the cold water and closes it off. The phytoplankton and then the fishery collapse. Moreover, the global climate is altered as storms become more severe on the west coast of North America. Why this occurs is not yet clear, but the strength of the southeast trade winds in the central Pacific is involved.

## Text Box 22–1 Remote sensing of phytoplankton

Phytoplankton pigments interact with light in ways that can be detected from space by means of satellite-borne sensors (radiometers). Sensor data can be used to construct global to local views of phytoplankton distribution patterns. Images can be used to study changes through time or to compare phytoplankton of different regions. For example, the lightest areas of the adjacent global map (a composite image, from September 1997 through July 1998) indicate regions of high chlorophyll concentrations/algal populations, most notably along the coasts of North America, northern Europe, northern Asia, Indonesia, southeastern South America, and southwestern southern Africa. More diffuse phytoplankton populations are indicated by bads extending through the northern and southern oceans; these contrast with mid-ocean regions where phytoplankton populations are low. A more localized example (left) reveals the extent of a phytoplankton (coccolithophorids) bloom in the Bering Strait. The bloom—showing up as the lighter gray areas off the Alaskan coast—imparted an aqua coloration to these normally dark waters.

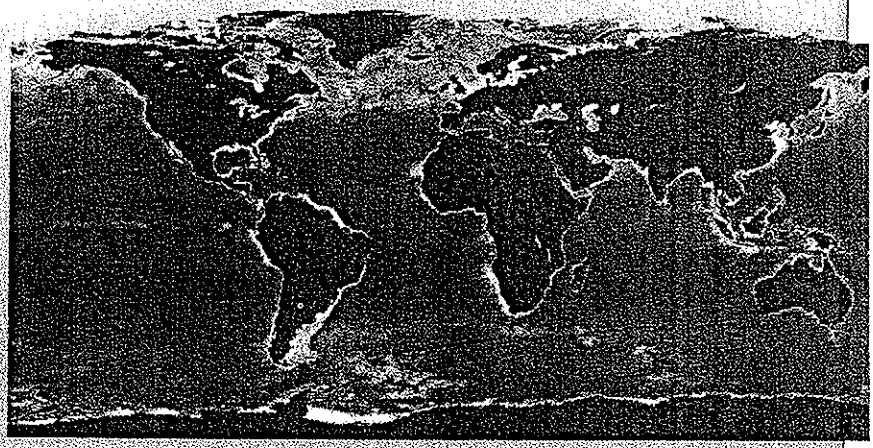

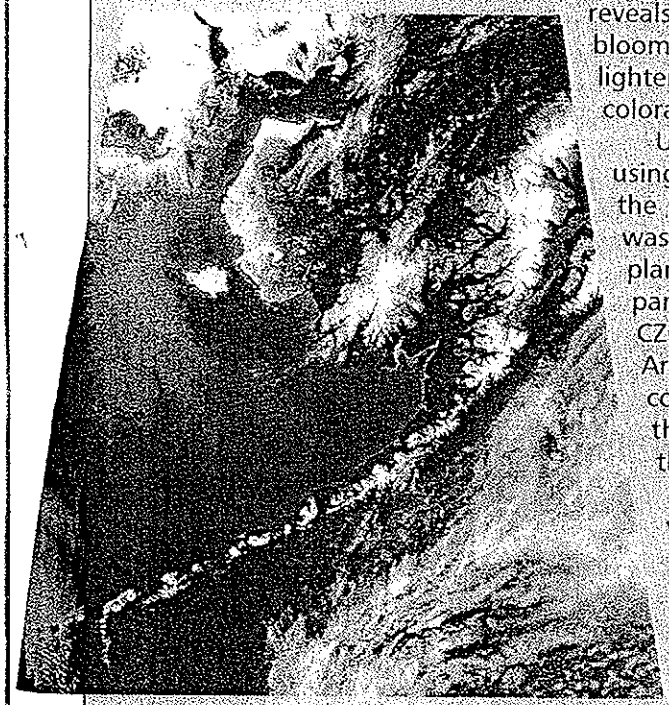

Until mid-1986, eight years of such records were made using the Coastal Zone Color Scanner (CZCS) operated on the Nimbus-7 environmental satellite mission. The CZCS was the first source of remote sensing data on phytoplankton, but was not continuously operational, so only partial data bases are available. The data obtained by the CZCS are maintained at the Goddard Distributed Active Archive Center (DAAC), which also collects all of the ocean color data from NASA satellite missions. These data (and those described below) are available free of charge through the World Wide Web and by other means.

Currently operating is the Sea-viewing Wide Field-of-view Sensor (SeaWiFS). It observes more than 90% of the oceans every two days, with a resolution of 4.5 km. This technology has allowed improved measurement of phytoplankton pigment concentration in both open ocean and turbid nearshore areas. The Goddard DAAC also archives SeaWiFS images.

In 1999 and 2000 a new imaging system will be orbited: this is the Moderate Resolution Imaging Spectroradiometer (MODIS). The new system will provide higher quality images as well as new capabilities. It will be possible to monitor chlorophyll fluorescence (an indicator of the physiological condition of phytoplankton), atmospheric levels of marine aerosols, detached coccolith concentrations, and other features.

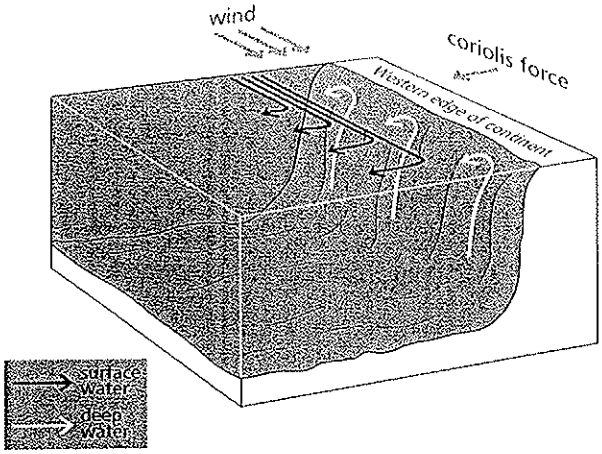


**Figure 22–13** Coastal upwelling. The combined action of wind and the Coriolis force of Earth's rotation move surface waters offshore along the western margins of continents (black arrows). This water is replaced by deep water rising to the surface (white arrows), which brings nutrients for phytoplankton growth. (After MARINE BIOLOGY 2nd. Edition, by J. W. Nybakken. ©1987 by HARPER COLLINS PUBLISHERS. Reprinted by permission of Addison-Wesley Educational Publishers)

All of these large-scale water movements affect the growth and distribution of phytoplankton populations. But what effect does turbulence have on the cells of individual species of phytoplankton? It has long been known that certain species of algae, including many dinoflagellates (White, 1976, Pollingher and Zemel, 1981), will not grow if stirred or aerated in small culture flasks. Cell division is inhibited at low rates of turbulence, and at high rates, cells disintegrate. Among marine red-tide dinoflagellates, *Prorocentrum micans* was more tolerant of turbulence than either *Gonyaulax polyedra* or *Gymnodinium sanguineum* (Thomas and Gibson, 1990, 1992; Thomas, et al., 1997). Dinoflagellate red tides are associated with extended periods of relatively calm seas. Thus red tides may be disrupted by turbulence, which damages dinoflagellate cells.

Turbulence has the opposite effect on diatoms. In the oceans, blooms of *Chaetoceros armatum* and *Asterionella socialis* occur in the surf zone of beaches in Washington State and New Zealand (Lewin and Norris, 1970). In cultures, the diatoms *Skeletonema costatum* and *Asterionella glacialis* grew better when subjected to turbulence than in controls in stationary culture (Thomas, et al., 1997). These preliminary results suggest that in the marine environment turbulence may act as a selective agent in determining competitive dominance. Turbulence and tolerance among freshwater forms has been discussed in reviews by Fogg (1991) and Willen (1991).

## The Chemical Environment

### Dominant Ions of Lakes and Oceans

Oceans contain about 34.8 g of dissolved salts per kg of seawater. Of this amount, sodium accounts for 10.77 g and chloride for 19.35 g. Oceans are dominated by sodium and chloride followed by magnesium (1.29 g $kg^{-1}$) and sulfate (2.71 g $kg^{-1}$). Lakes are dominated by calcium and bicarbonate, and their concentrations may vary greatly. Major ions in oceans vary by only a few percent from place to place, and turnover times are extremely long. Exceptions are aluminum and iron, which turn over at scales of $10^2$ years. Major ions in lakes have turnover times of weeks to at least one hundred years.

Phytoplankton have little use for sodium. In saline lakes, the high levels of sodium actually restrict the diversity of algae. Chloride is used in some biochemical transformations such as photolysis of water and ATP production. Calcium is necessary in small amounts for growth and cell wall integrity. Magnesium is needed by all cells for energy metabolism in converting ATP to ADP. It is also the central metal in the chlorophyll molecule. Sulfur as sulfate ($SO_4^{2-}$) is important in disulfide bonds, which stabilize the structure of enzymes and other proteins. Most of the major ions in freshwaters and the oceans are only needed by phytoplankton in small quantities and therefore rarely limit growth. Because their turnover times are relatively long, they are considered conservative substances in aquatic systems. Carbonate is the exception. As the principle source of carbon in aquatic systems, it is needed in large quantities.

Carbon is rarely limiting in aquatic systems because carbon dioxide—although relatively scarce in the atmosphere—is highly soluble in water. The form that carbon takes in water depends on the pH of that water. Most lakes have a pH of 6 to 9, where pH=7 is considered neutral. Acid waters may have a pH as low as 2, while some alkaline lakes may have a pH>10. Seawater is slightly alkaline, ranging from pH 7.5 to 8.4. Below pH 6, the bulk of $CO_2$ dissolved in water is present as soluble carbon dioxide or undissociated carbonic acid ($H_2CO_3$) (Fig. 22–14). Above

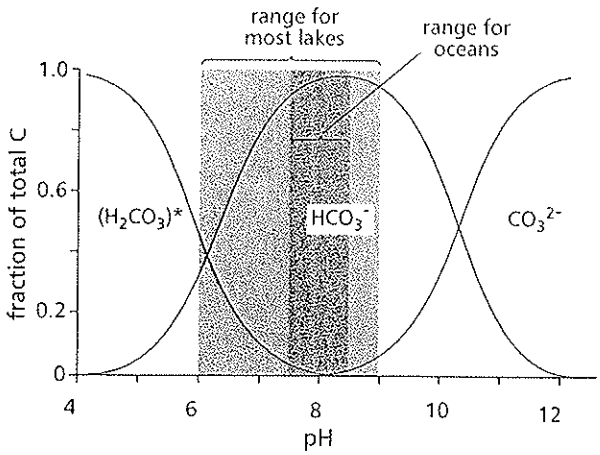


**Figure 22–14** Forms of inorganic carbon as a function of pH in lakes and oceans. Most lakes and all oceans are bicarbonate ($HCO_3^-$) solutions. $(H_2CO_3)^* = H_2O + CO_2$. (After Goldman, C. R., and A. J. Horne. 1983. *Limnology*. McGraw-Hill. Reproduced with permission of the McGraw-Hill Companies)

pH 6, bicarbonate ion ($HCO_3^-$) becomes increasingly important. Note that the normal range of pH for seawater spans the maximum for bicarbonate. Above pH 10, carbonate becomes increasingly important. Most lakes and all oceans are predominantly bicarbonate solutions, and phytoplankton acquire their carbon by taking up bicarbonate or converting it to $CO_2$ for uptake. In acidic lakes, carbon can occasionally become limiting to growth since green algae respond positively to additions of $CO_2$ or bicarbonate (Fairchild and Sherman, 1993). For more detail, see Chapter 2. The carbonate–bicarbonate–$CO_2$ equilibrium plays a major role in the buffering capacity of lakes. If a lake has abundant calcium, it will have abundant carbonate. When acid is added to such a lake in the form of protons ($H^+$), the protons combine with carbonate ($CO_3^{2-}$) to form bicarbonate ($HCO_3^-$), and the pH is stable. Calcium-rich lakes are generally well buffered. Calcium-poor lakes, such as are found in Scandinavia, the northeastern United States, and eastern Canada, have little buffering capacity and are thus susceptible to acidification by nitric and sulfuric acids in acid rain.

Dynamics of phytoplankton are primarily correlated with spatial and temporal fluxes of major nutrient ions such as N, P, and Si. Redfield (1958) determined that marine phytoplankton growing at their maximum growth rate possessed a characteristic ratio of major nutrient ions of 106 C : 16 N : 1 P. Diatoms, and perhaps other algae that require silica, should have an ion ratio of 106 C : 16 Si : 16 N : 1 P. Phytoplankton should show the Redfield ratio when growing close to their maximum growth rate, at which they are unlikely to be nutrient limited. In the remainder of this section we will consider the roles of nitrogen, phosphorus, and silicon as important limiting nutrients.

## Nitrogen

Nitrogen is present in waters primarily as dissolved dinitrogen gas ($N_2$). Ionic forms include the ammonium ion ($NH_4^+$), nitrite ion ($NO_2^-$), and nitrate ion ($NO_3^-$). In oceans, 95% of nitrogen occurs as $N_2$. About two thirds of the remainder is nitrate ion, which turns over very rapidly and is often so scarce in ocean waters as to be undetectable, especially in tropical and subtropical waters. In tropical oceans, the filamentous, nitrogen-fixing cyanobacterium *Trichodesmium* is fairly common. For a discussion of nitrogen fixation, refer to Chapters 2 and 6. Cells of the common marine diatom *Rhizosolenia* typically contain two filaments of the nitrogen-fixing cyanobacterium *Richelia*, which effectively acts as a nitrogen-fixing organelle (see Chapter 7). Nitrate only appears in quantity in zones of coastal upwelling or pollution.

The main source of nitrate in lakes is stream and river discharge. In most temperate oligotrophic and mesotrophic freshwaters, nitrate is present in relative excess and exceeds the supply of phosphorus. Nitrogen fixation plays a relatively minor role in such low-nutrient freshwaters. But in some western U.S. lakes whose basins are predominately volcanic rock, nitrogen is the limiting nutrient (Reuter and Axler, 1992). In tropical lakes, nitrogen may be in low supply due to low levels in the surrounding soils of the watershed. In oligotrophic freshwaters nitrate is the major form of dissolved inorganic nitrogen (DIN) while in eutrophic waters, $NH_4^+$ and $NO_2^-$ may be present at depth if oxygen is reduced. Nitrite is normally present in insignificant amounts, although in eutrophic lakes a narrow layer in the thermocline may contain elevated levels of nitrite (Fig. 22–15). If oxygen is present, $NO_2^-$ is converted to $NO_3^-$, whereas in anoxic waters, it is reduced to ammonia. The supply of phosphorus may exceed the supply of nitrogen in eutrophic waters. Under these circumstances nitrogen-fixing cyanobacteria such as *Anabaena*, *Aphanizomenon*, and *Gloeotrichia* may generate nuisance blooms. Such

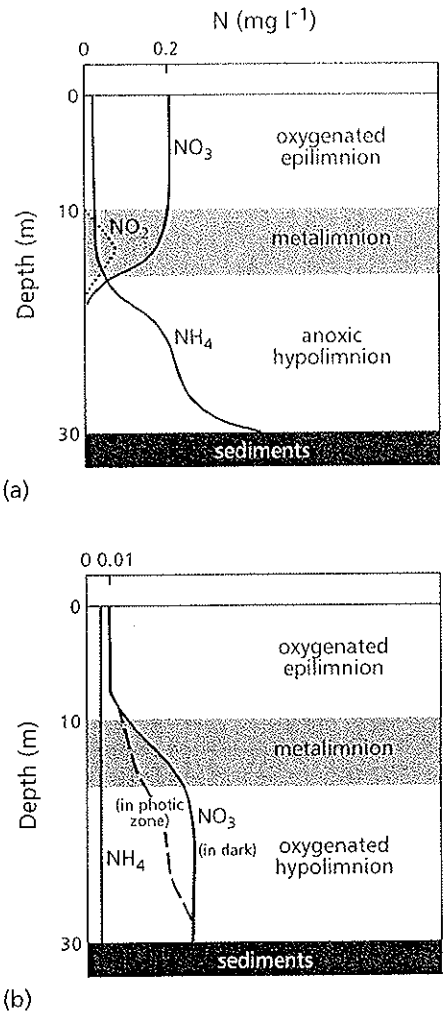


**Figure 22–15** Generalized distribution of nitrate, nitrite, and ammonia with depth in a eutrophic (a) and an oligotrophic stratified lake (b) in midsummer. (After Goldman, C. R., and A. J. Horne. 1983. *Limnology*. McGraw-Hill. Reproduced with permission of the McGraw-Hill Companies)

nitrogen-fixing cyanobacteria are common in freshwaters even when not at bloom levels (Chapter 6).

## Phosphorus

As indicated by the Redfield ratio, phytoplankton need phosphorus in relatively small amounts compared to carbon, nitrogen, and silicon. It is frequently growth-limiting, however, because it is often in short supply in many watersheds. Most of the total phosphorus (TP) in waters is in the form of living or dead particulates. Dissolved phosphorus occurs as either inorganic phosphates (DIP) or dissolved organic phosphorus (DOP). Most dissolved phosphorus is DOP. DIP is primarily orthophosphate ($PO_4^{3-}$) with much lower amounts of monophosphate ($HPO_4^{2-}$) and dihydrogen phosphate ($H_2PO_4^-$). Phytoplankton can only use dissolved inorganic phosphate, which is termed soluble reactive phosphate (SRP). When the supply of SRP is exhausted, phytoplankton can release alkaline phosphatases, which are extracellular enzymes capable of freeing phosphate bound to organic substances. In addition, when brief pulses of SRP do occur, many phytoplankton can take up and store excess phosphate as polyphosphate bodies within the cell. This so-called luxury consumption is an important mechanism for dealing with phosphate shortages. During nutrient pulses, an algal cell may be able to store enough phosphate to provide for as many as 20 cell divisions. Finally, many phytoplankton can take up phosphate at extremely low ambient levels, well below the level of detection (see below).

In many lakes the amount of phosphorus present in late winter determines the size of the phytoplankton populations that can develop in the summer. In winter, DIP turnover is relatively slow in all freshwaters—on the order of hours to days—as a result of low populations of algae with low growth rates. DIP represents less than 10% of TP in oligotrophic freshwaters, where, during summer, the demand for DIP is high, and the DIP pool may become unmeasurable. Phytoplankton depend on DIP recycling. Using the radioisotopes $^{32}PO_4$ and $^{33}PO_4$, Hudson and Taylor (1996) measured the rate of regeneration of phosphate (during summer) in two oligotrophic lakes. Measured rates ranged from 15 to 205 ng P $l^{-1}$ $hr^{-1}$. Grazers smaller than 40 $\mu$m accounted for 77% of the measured regeneration. Many marine waters are similar to oligotrophic freshwaters with respect to phosphate dynamics. In coastal marine waters, DIP builds up during the periods of vertical mixing. If the ocean stratifies, the DIP pool is depleted and phytoplankton depend on phosphorus recycling, as in oligotrophic freshwaters. DIP may approach 100% of TP in eutrophic freshwaters. The DIP pool may exhibit slow turnover due to the fact that DIP input may exceed algal growth requirements and thus build up to high levels.

## Silicon

Silicon can be a limiting nutrient for the growth of diatoms in lakes during summer stratification when

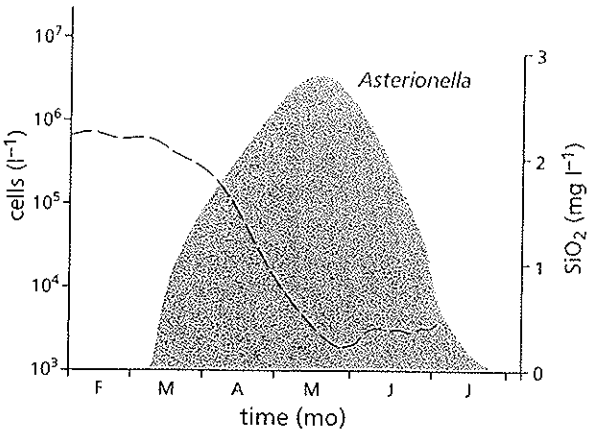


**Figure 22–16** The spring bloom of the diatom *Asterionella* in the north basin of Windemere, Lake District, England, and the depletion of the limiting nutrient silica (dashed line). (After Goldman, C. R., and A. J. Horne. 1983. *Limnology*. McGraw-Hill. Reproduced with permission of the McGraw-Hill Companies, based on data in Lund, 1964)

the pool of silica ($SiO_2$) falls to unmeasurable levels. The decline of silica is certainly one major factor in bringing about the decline of the spring diatom bloom in many lakes (Fig. 22–16). Since polymerized silica is dense (2.6 g $cm^{-3}$), it adds considerably to the density of diatoms, which consequently suffer population losses due to sedimentation. Polymerized silica decomposes slowly (on the order of 50 days) into soluble orthosilicic acid ($H_2SiO_4$) or soluble reactive silicate. It does not dissolve during gut passage through herbivorous zooplankton. Thus there is essentially no rapid recycling of silica in the epilimnion. Dissolved silica is only restored to surface waters by external inputs and the turnover of the water column at spring and fall mixing.

## Growth Processes of Phytoplankton Populations

Populations take up space, show various levels of mobility, and are distributed in a variety of patterns in time and space. Populations are characterized by the fact that they grow, that is, they change in size (numbers) and density (number per unit area or volume). The concept of growth rate is essential for describing population dynamics. In field research, growth rate usually means the net rate of change in numbers or biomass and represents the balance between additions due to reproduction and losses due to various sources of mortality or export. In culture studies, however, phytoplankton essentially grow without losses, and so growth rate is equivalent to the rate of reproduction or the "birth rate" in field research. These ideas can be expressed mathematically as:

$$\frac{dN}{dt} = rN \qquad (2)$$

In this equation, dN/dt represents the change in numbers or biomass during a unit of time (such as one day). Sometimes dN/dt is referred to as the growth rate, when it is actually the population growth rate or the change in population size in a unit of time. This change in population size is equal to r, the net growth rate (with units of reciprocal time or, in this case, $day^{-1}$) multiplied by N, the number of individuals in the population or its biomass. If we isolate r on the right side of the equation by dividing both sides by N, we can see that r is the change in the population size per individual in that population N or the net per capita growth rate. Since the net growth rate is equal to the rate of reproduction minus any losses due to death, the net growth rate is equivalent to:

$$r = \mu - \lambda \quad (3)$$

where $\mu$ is the gross growth rate, rate of reproduction, or the birth rate, and $\lambda$ is the death rate or the loss rate. The net growth rate may be positive or negative. If positive, then the population will increase in numbers or biomass. If negative, the population will decrease in numbers or biomass over time. Note that a population could have a high rate of gross growth ($\mu$) but show no net growth at all. This situation can arise anytime the gross growth rate ($\mu$) is roughly balanced by the loss rate ($\lambda$). In that situation ($r = 0$), a phytoplankton population could be photosynthesizing, taking up nutrients, and dividing at a significant rate, but repeated sampling would show no net change in numbers because losses balance production. Failure to understand the difference between gross growth and net growth has led to a great deal of confusion in the literature. Lack of evidence of net growth (r) among phytoplankton does not mean there is no gross growth or that the phytoplankton are not physiologically active.

Equation (2) (above) is an example of a differential equation because of the presence of the term dN/dt.

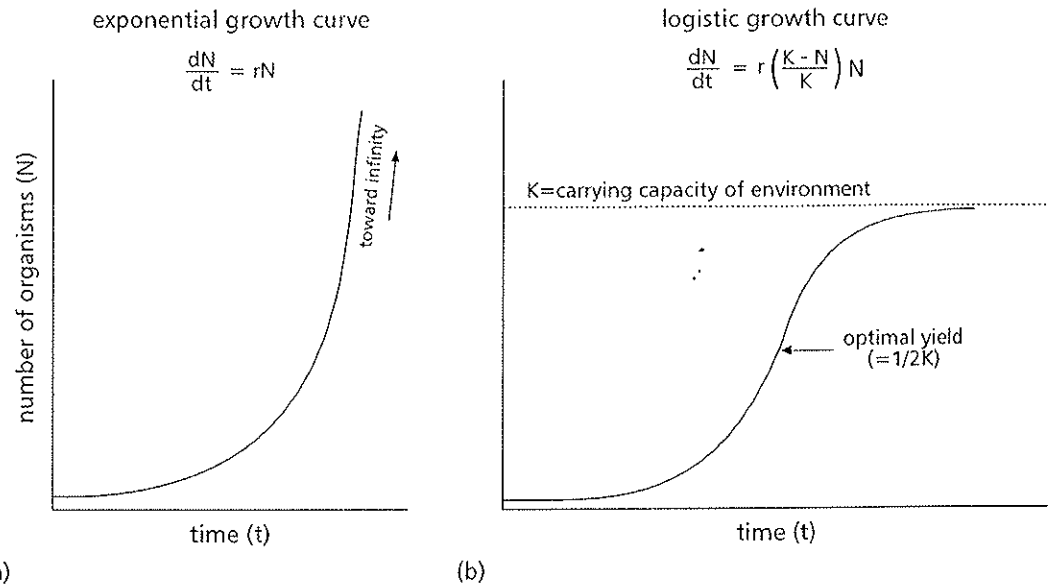


**Figure 22–17** Two basic models of population growth: (a) exponential and (b) logistic. (After Wilson and Bossert, 1971)

If equation (2) is solved explicitly to remove the differential term dN/dt, the result can be expressed as:

$$N = N_o e^{rt} \quad (4)$$

A population of phytoplankton growing according to equation (4) will increase exponentially without an upper limit (Fig. 22–17a). If the natural logarithms of both sides of equation (4) are taken, the equation becomes that of a straight line whose slope is the net growth rate (r):

$$\ln N = rt + \ln N_o \quad (5)$$

Thus, the net growth rate can be estimated from the natural logarithms of the population sizes. Equation (5) can also be used to calculate the doubling time of the population ($t_d$). If N is taken as twice the value of $N_o$, then equation (5) can be rearranged into the form:

$$\ln N - \ln N_o = \ln\frac{N}{N_o} = rt \quad (6)$$

Now, when N=2 ($N_o$), ln ($N/N_o$) = ln 2 or 0.69, and we get $t_d = \ln 2/r$. If the net growth rate were 0.69 $day^{-1}$, then the doubling time would be 0.69/0.69 $day^{-1}$ or 1.0 day. Therefore, an r of 0.69 $day^{-1}$ corresponds to one doubling per day. If the net growth rate were –0.69 $day^{-1}$, the population would decrease by 50% per day.

No population of phytoplankton can continue to grow indefinitely at an exponential rate as described by equation (4). Even a slow-growing population would soon overflow its habitat. There must be some sort of upper limit to population density due to limits in available resources such as nutrients. This upper limit is called the **carrying capacity** of a population. The first widely used expression that included a carrying capacity was the logistic equation:

$$\frac{dN}{dt} = rN\frac{(K-N)}{K} \quad (7)$$

In the logistic equation, the carrying capacity is represented by the parameter K, which has the same units as N (cells $ml^{-1}$ or mg $ml^{-1}$). Initially, when N is small, (K–N)/K is close to 1, and the population grows at nearly an exponential rate. As N approaches K, (K–N)/K approaches zero, and the population ceases to grow when at its carrying capacity (Fig. 22–17b). The logistic equation makes no explicit reference to the cause of the carrying capacity, that is, there is no term in the equation for the consumption of some resource that determines the magnitude of the final population size. For some practice in working with the exponential and logistic equations, refer to Question Box 22–1.

## Question Box 22–1 Working with the exponential and logistic equations

*Sample calculation.* The table and figure to the right present the results from a batch culture experiment in which the cyanobacterium *Anabaena flos-aquae* grew for 120 hours. Use these data to estimate the parameters r and K in the logistic growth equation (7).

| time (hr) | population (cells ml$^{-1}$) |
|---|---|
| 0 | 2,360,742 |
| 6 | 3,335,056 |
| 12 | 5,025,320 |
| 15 | 5,498,578 |
| 24 | 9,478,620 |
| 35 | 13,660,240 |
| 48 | 17,979,420 |
| 71 | 23,399,540 |
| 96 | 23,431,136 |
| 120 | 22,698,608 |

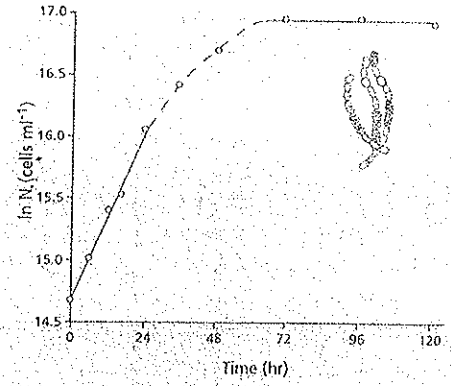


*Solution.* As shown in equation 5, we can determine the net growth rate (r) of *Anabaena* by taking the natural logarithms of the population sizes. We plot the natural logs against time, as shown in the graph. The first five points make a straight line. Using a calculator, you can run the linear regression of ln (N) on t for these five points. The resulting equation is $Y = 0.0578\ (X) + 14.68$, and the correlation coefficient is 0.99. The slope of this line is the net growth rate, $r = 0.0578\ hr^{-1}$. Multiplying this by 24 hr day$^{-1}$, r becomes 1.38 day$^{-1}$. The doubling time is given by $t_d = \ln (2)/r$. For *Anabaena*, $t_d = 0.69/1.38\ day^{-1}$, which equals 0.5 days. Determining the value of K is much simpler. The values of ln (N) for 71, 96, and 120 hours are roughly the same, and K can be taken as their average. Therefore K = 16.96 or 23,207,820 cells ml$^{-1}$.

*Practice problems.* Work the following problems with a pocket scientific calculator. You will find it essential to plot the data in order to decide which are to be used in making the estimates. Answers are given at the end of the chapter.

1. The following data give the results of three replicated batch cultures of *Chlamydomonas reinhardtii*. Calculate the net growth rate r for each batch culture. Take the average of the three as the net growth rate of *Chlamydomonas* in this study.

| | (cells ml$^{-1}$) | | |
|---|---|---|---|
| time (hr) | culture #1 | culture #2 | culture #3 |
| 0 | 9,280 | 13,890 | 7,860 |
| 24 | 38,550 | 42,490 | 24,300 |
| 48 | 100,680 | 143,480 | 129,620 |
| 71 | 249,250 | 355,780 | 321,440 |
| 95 | 946,230 | 1,283,390 | 1,131,070 |

2. The euglenoid flagellate *Euglena gracilis* grows in a culture medium containing acetate. While *Euglena* can photosynthesize, it can also grow in the dark by using acetate as an energy source. The table below contains data on growth of *E. gracilis* in the light and dark. Calculate r for each growth experiment. How much did photosynthesis increase the growth rate of *Euglena* over the rate in the dark? By how much did photosynthesis reduce the doubling time?

| dark-grown | | light-grown | |
|---|---|---|---|
| time (hr) | cells ml$^{-1}$ | time (hr) | cells ml$^{-1}$ |
| 0 | 915 | 0 | 2,830 |
| 24 | 1,605 | 24 | 4,695 |
| 48 | 2,590 | 46 | 14,910 |
| 147 | 56,454 | 72 | 31,120 |
| 219 | 360,464 | | |

*continued→*

## Question Box 22–1 *continued*

3. Growth of *Chlorella pyrenoidosa* was followed in batch culture for 24 days. Use the following table of population counts (cells $ml^{-1}$) to estimate the logistic parameters r and K.

| day | cells $ml^{-1}$ | day | cells $ml^{-1}$ |
|---|---|---|---|
| 1 | 45,740 | 10 | 3,710,040 |
| 2 | 71,904 | 13 | 5,266,840 |
| 3 | 85,740 | 14 | 8,326,400 |
| 4 | 229,640 | 15 | 8,753,200 |
| 5 | 517,580 | 17 | 7,576,200 |
| 6 | 570,640 | 20 | 10,357,000 |
| 7 | 1,189,320 | 24 | 9,341,700 |
| 9 | 2,112,780 | | |

An alternative way to write the logistic equation is to remove the parentheses:

$$\frac{dN}{dt} = rN - \frac{rN^2}{K} \qquad (8)$$

In this form, the logistic equation embodies much of the controversy and theory that prevails in plankton ecology. The first term to the right of the equal sign is the familiar exponential growth term. If populations of phytoplankton fundamentally show exponential growth, then some external forces such as water turbulence, washout, or high temperatures must occur frequently enough to keep the phytoplankton below their carrying capacity. Such external forces occur independently of whatever density the algal population may have reached at the time they occur. Hence they are density-independent, and the population may be said to be under density-independent control. Algal populations under density-independent control are regulated by external, abiotic (physical and chemical forces) in the environment. Such algal populations would likely show wide fluctuations in abundance because external disturbances would occur randomly.

On the other hand, if the second term on the right of the equal sign also is important, then phytoplankton are limited by density-dependent factors. As the population approaches its carrying capacity, resources are depleted, reproduction rates decrease, and/or rates of mortality increase. In either case the controlling factors are biological and density-dependent. Algal populations under density-dependent control would probably show fairly stable levels of abundance. Furthermore, if many phytoplankton species were all close to their carrying capacities at the same time, then they would likely be in competition with each other for one or more resources. Thus, if phytoplankton are regulated by density-dependent factors, competition and other biotic interactions are more likely to control the structure of phytoplankton communities than would physical and chemical factors.

Are phytoplankton communities made up largely of species subject to density-independent control or are many of the planktonic algae at or close to their carrying capacities and subject to density-dependent control? The answer is more than just of academic interest because the way we view the structure of planktonic communities affects the kinds of management plans that are employed on lakes and in the oceans. Those plans in turn affect the quality and use of aquatic resources.

Yet another way to gain insight into ecological theory from the logistic equation in (8) is the concept of r and K-strategists, where r and K are the parameters in the logistic equation (MacArthur and Wilson, 1967). It is a readily demonstrated fact that phytoplankton differ with respect to their gross growth rates or rates of reproduction. There is also a good correlation between cell size and growth rate (Table 22–2). Small cells have faster growth rates than large cells and larger surface to volume ratios (Table 22–1). This has led to the idea that there are r-strategists and K-strategists in phytoplankton communities. R-strategists are small and can grow exponentially to exploit temporarily favorable conditions. Being small, they are readily eaten by grazers. They are opportunistic species. At the opposite end of the spectrum are K-

strategists, which are large and grow relatively slowly. These are largely immune to predation and grow close to their carrying capacity. They are considered to be good competitors.

Today, r and K-strategists are not thought of as two opposite poles but as a continuum. Species are thought to have characteristics selected to exploit certain environmental conditions. An r-strategist can exploit a temporary pulse of nutrients washed in by a storm and rapidly build up its population. The resulting bloom can just as quickly be dispersed by turbulence in the water. A K-strategist grows slowly but can survive between pulses of nutrients by living off stored nutrients. K-strategists maintain more constant population levels. The set of characteristics that constitute an r-strategy may be best suited to the highly mixed and turbulent waters of spring and fall, while those of a K-strategy may be appropriate for the stable, stratified waters of summer. Between extreme r and K strategists are the large number of phytoplankton of intermediate size with a range of growth rates and nutrient storage capacities that may be adapted to intermediate disturbances of nutrients and turbulence. Phytoplankton communities are mixtures of species with various combinations of the characteristics of these strategies.

## Growth and Light

In the previous section we described the general process of phytoplankton growth without regard to the specific resources that might be directing that growth. In the following sections we will discuss growth as a function of specific factors such as light and nutrients.

The most fundamental aspect of phytoplankton ecology is the conversion of light energy into biomass through photosynthesis. Photosynthesis is the biochemical process by which light energy is used to transform inorganic molecules into organic matter. Details of the biochemistry are beyond the scope of this chapter. Excellent recent treatments are available in Geider and Osborne (1992) and Falkowski and Raven (1997). The process of photosynthesis can be summarized by the familiar equation:

$$6CO_2 + 6H_2O \rightarrow C_6H_{12}O_6 + 6O_2 \quad (9)$$

Light energy is used to strip protons and electrons from water molecules with the resulting production of oxygen. Those protons and electrons are used to reduce $CO_2$ to an organic carbon molecule such as glucose, as shown in equation (9). A significant fraction of carbon metabolism may be coupled to nitrate assimilation with the final production of amino acids and proteins (Turpin, 1991).

Plant physiologists quantify photosynthesis in two ways. Gross photosynthesis ($P_g$) is the light-dependent rate of electron flow from water to $CO_2$ in the absence of respiratory losses (Lawlor, 1993). Respiration ($R_l$) is the flow of electrons from organic carbon to $O_2$ with the production of $CO_2$. Photosynthesis only occurs in the light, and respiratory losses in the light reduce the level of gross photosynthesis. The difference between gross photosynthesis and respiration is called net photosynthesis ($P_n$). Therefore:

$$P_n = P_g - R_l \text{ or } P_g = P_n + R_l \quad (10)$$

All three terms are rates and therefore time-dependent.

Equation (9) indicates two ways to measure photosynthesis: by carbon uptake and by oxygen evolution. In the past, the most commonly used method was the uptake rate of $^{14}C$ (usually as $H^{14}CO_3^-$) into organic matter. The resulting rates may be expressed as mg C g $hr^{-1}$, mg C $cell^{-1}$ $hr^{-1}$ or mg C (mg chl *a*)$^{-1}$ $hr^{-1}$. Their interpretation is complicated by the fact that it is not clear whether gross or net photosynthesis is being measured. If short incubation times are used, the $^{14}C$ uptake method should approximate gross photosynthesis. If incubation runs to equilibrium, the rates may approach net photosynthesis (Falkowski and Raven, 1997). Radiocarbon techniques provide no information about respiration.

Interpretation is more straightforward if oxygen evolution techniques are used. If photosynthesis is measured with an oxygen electrode, the data represent net photosynthesis since respiration removes oxygen. Oxygen methods allow direct measurement of respiration. If a chamber containing algae is covered immediately after net photosynthesis measurements with a light-tight bag, the consumption of oxygen gives a good approximation for $R_l$, the respiration rate in the light. Furthermore, if the chamber remains in the dark for several hours, the dark or basal rate of respiration can also be obtained. Both methods share the problem of requiring confined spaces. If natural phytoplankton assemblages are used, bacteria and microzooplankton may alter the observed rates through their own metabolic activities.

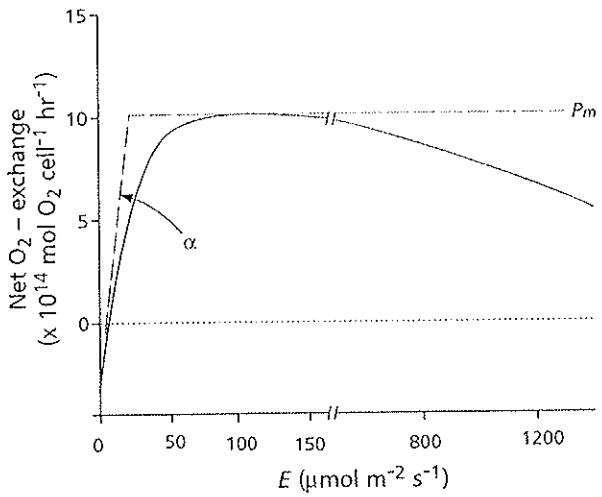


**Figure 22–18** Relationship between irradiance E and photosynthesis in *Chlamydomonas reinhardtii*. $P_m$ is the maximum rate of light-saturated photosynthesis, and α is the initial slope of the curve. The compensation point lies at the intersection of the P-curve and the zero net-$O_2$ exchange line (dashed). (Based on Neale, 1987, in Geider and Osborne, 1992 with kind permission of Kluwer Academic Publishers)

Phytoplankton show a characteristic response curve to increasing light intensity (Fig. 22–18). At some low light level, the rate of net photosynthesis ($P_n$) will just balance the rate of respiration (R). This light level is called the **compensation point**. For any light level greater than the compensation point, the alga will make a net gain in photosynthesis over losses due to respiration. If algal cells are exposed to low light levels for several hours, they will adapt physiologically by increasing their chlorophyll content. Initially, when light is limiting, there is a linear increase in photosynthesis with increasing light. The slope of this linear increase is termed α, a parameter used in modeling. As light levels continue to increase, the rate of increase in photosynthesis declines and the photosynthesis-versus-light curve bends over and levels off at a maximum value ($P_m$). Different phytoplankton appear to be adapted to different optimal light levels. Diatoms are especially efficient at photosynthesis under the low light levels and photoperiods that prevail in spring when the water column is mixing and the elevation of the sun is low. Thus diatoms are numerically abundant in temperate lakes and oceans in spring and fall and during most of the ice-free season in polar latitudes. The red-pigmented cyanobacterium *Planktothrix* is adapted to very low light levels in European lakes (Mur and Bejsdorf, 1978).

At high light levels approaching that of full sunlight, many phytoplankton species show **photoinhibition**, a decline in photosynthesis with increasing light. In this case, respiration increases with light while photosynthesis remains constant such that the photosynthesis versus light curve declines with increasing light (Fig. 22–18). Phytoplankton will exhibit decreased levels of chlorophyll in their cells at these high levels. Prolonged exposure to such light levels can result in damage to the photosynthetic apparatus in the cell. Kromkamp (1990) has examined photoinhibition in *Anabaena flos-aquae*.

Surface waters are a turbulent environment, however, and vertical mixing can carry the phytoplankton from the surface down to 10 m depth and back again in as little as 30 minutes to a few hours. Thus, within as little as 30 minutes an individual algal cell could experience light levels ranging from photoinhibiti[illegible]o below the compensation point and back again.

A large number of models have been proposed for gross photosynthesis as a function of light (Geider and Osborne, 1992). Two of the most widely tested and successful are the exponential function (equation 11) and the hyperbolic tangent function (equation 12):

$$P = P_m\left[1 - \exp\left(\frac{\alpha E}{P_m}\right)\right] \qquad (11)$$

$$P = P_m \tanh\left(\frac{\alpha E}{P_m}\right) \qquad (12)$$

These models were reformulated by Jassby and Platt (1976) to express them using the same two parameters. $P_m$ is the maximum rate of gross photosynthesis, and E is the light intensity expressed as μmol quanta m$^{-2}$ s$^{-1}$. The parameter α is the slope of the initial increase in gross photosynthesis with light. [illegible]an be estimated by the same process as the net growth rate in equation (5). The above models have been successful in the study of coral reefs, phytoplankton, and macroalgae.

## Growth and Nutrient Uptake

As phytoplankton grow, they consume mineral resources such as C, N, P, S, and Si. Earlier it was noted that C and S are rarely limiting in natural aquatic systems. This leaves N and P (plus Si for

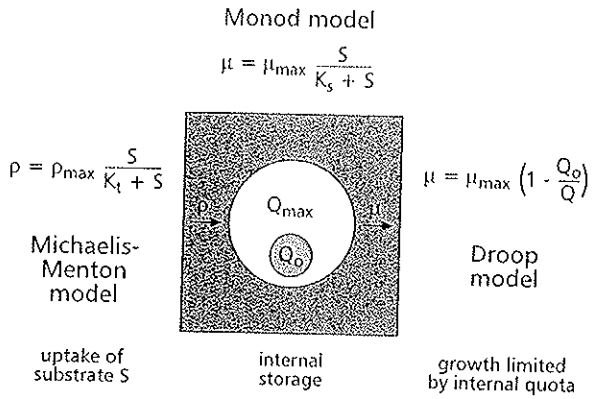


**Figure 22–19** Relationships among the various nutrient-based models of phytoplankton growth. The Michaelis-Menten model describes the process of nutrient uptake from the environment. The Droop model describes growth as a function of internal nutrient stores, while the Monod model defines growth in terms of external nutrient supply.

diatoms) as essential macronutrients that must be taken up from the environment for growth to occur. Other (micro)nutrients are essential but seldom limiting because they are needed in such small amounts.

## Nutrient Uptake

The process by which nutrients are taken up from the environment and transported into the algal cell has been described by the Michaelis-Menten model, which is based on the kinetics of enzyme function. Authors differ somewhat in their choice of variables, but the following equation is widely used to describe nutrient transport into algal cells:

$$\rho = \rho_{max}\left(\frac{S}{K_t + S}\right) \qquad (13)$$

In this formulation, $\rho$ is the velocity of the nutrient transporter or the nutrient transport rate in units of $\mu$mol of nutrient per cell per minute. If the cell is not the chosen unit for the algal population but some measure of biomass, then the units could be $\mu$mol mg$^{-1}$ min$^{-1}$. Refer to the diagram of nutrient-based models of growth (Fig. 22–19). The term $\rho_{max}$ is the maximum velocity of the nutrient transporter; $\rho$ approaches $\rho_{max}$ when the level of the external nutrient—the substrate concentration S—is high and the internal store of that same nutrient (Q) is low. $K_t$ is the half-saturation constant, which equals the value of S where $\rho = 1/2\ \rho_{max}$; that is, where the enzyme-based nutrient transporter is half-saturated with the substrate S. S and $K_t$ have the same units of concentration ($\mu$mol l$^{-1}$). Figure 22–20 illustrates the relationships between $\rho$, $\rho_{max}$, $K_t$ and S for *Anabaena* taking up phosphorus. Note that as the concentration of phosphorus (S) increases, the measured level of nutrient uptake, $\rho$, first increases rapidly and essentially linearly. The curve of $\rho$ then bends over to a plateau as $\rho$ approaches $\rho_{max}$. The point where $\rho$ reaches 1/2 $\rho_{max}$ defines the phosphorus concentration, which is $K_t$. For some measured values of $K_t$ and $\rho_{max}$, refer to Table 22–3, which is taken from Sandgren (1988). In this table, $\rho_{max}$ is referred to as $V_{max}$. In some papers, $V_{max}$ has a different meaning and has units of $t^{-1}$ (min$^{-1}$ or hr$^{-1}$). In this context, $V_{max}$ is the maximum specific uptake rate and:

$$V_{max} = \frac{\rho_{max}}{Q} \qquad (14)$$

## Internal Nutrient Stores

For the next steps in nutrient dynamics, refer again to the diagram (Fig. 22–19). As the nutrient transporter pumps nutrients like P or N into the cells, they go into an internal pool Q with units of $\mu$mol cell$^{-1}$. Q varies between two fixed levels, which are set by natural selection and vary with cell size. $Q_o$ is the minimum cell quota or minimum stored nutrient supply, and $Q_{max}$ is the maximum internal quota of nutrient. The alga draws off the internal storage pool as it grows.

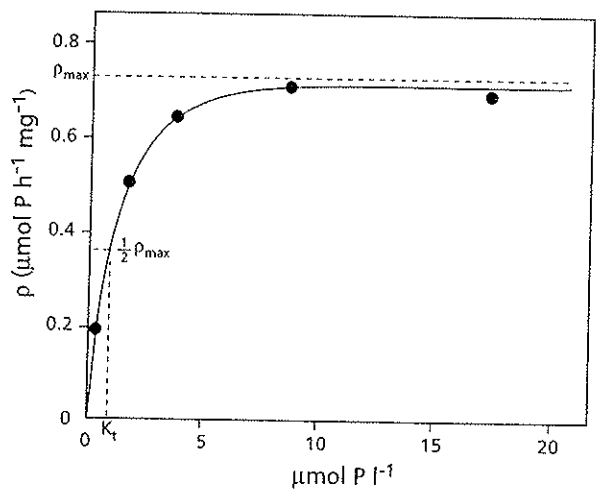


**Figure 22–20** Phosphorus transport in *Anabaena*. (Based on Lampert and Sommer, 1997 ©Georg Thieme Verlag)

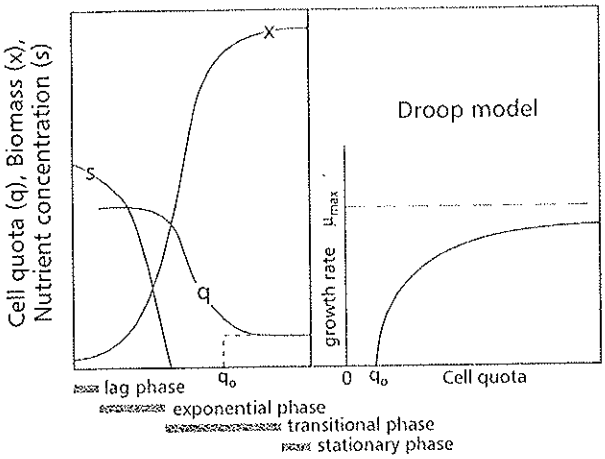


**Figure 22–21** Droop model (right) and batch growth of organism X on substrate S (left). (After Lampert and Sommer, 1997 ©Georg Thieme Verlag)

Droop (1983) advanced the following equation for the relationship between growth rate and internal nutrient quota:

$$\mu = \mu_{max}\frac{(1 - Q_o)}{Q} \qquad (15)$$

Here $\mu$ is the gross growth rate or rate of reproduction with units of $t^{-1}$ ($day^{-1}$ or $hr^{-1}$). The maximum rate of reproduction is $\mu_{max}$. Note when Q approaches $Q_o$, then $\mu$ is zero. When Q reaches $Q_{max}$, $\mu$ is approximately $\mu_{max}$. Figure 22–21 presents graphs of the Droop model $\mu$ versus Q in the right-hand graph and in the left-hand graph changes in biomass of a hypothetical organism X as substrate S is consumed and internal cell quota Q is depleted to $Q_o$ (or $q_o$). In the right-hand figure, $\mu$ does not begin until Q is greater than $q_o$. The value of $\mu$ then increases rapidly and levels off as Q approaches $Q_{max}$ and $\mu$ approaches $\mu_{max}$. In the left-hand graph, S drops away rapidly as it is entirely picked up by the nutrient transporter and joins the internal quota. Growth of X then continues as long as Q is greater than $Q_o$. As Q approaches $Q_o$, growth stops and X reaches its carrying capacity.

For actual values of $Q_o$ and $Q_{max}$ refer to Table 22–3 from Sandgren (1988) for chrysophycean flagellates. Measured $Q_{max}$ values are considerably larger than $Q_o$. In fact, the ratio of $Q_o/Q_{max}$ varies from about 3% to 9.5%. Larger volume cells have higher values of $Q_{max}$ than do small cells, presumably because they have more room inside for storage of polyphosphate. Values of $\mu_{max}$ vary over a rather narrow range. The $K_s$ values are quite low for phosphorus among these algae.

## Growth and External Nutrient Supply

Our final consideration is the process of population growth as a function of nutrient concentration in the surrounding environment. Here we must consider two types of culture: the batch culture and the continuous culture or chemostat. In the batch culture there is a fixed initial amount of nutrient or substrate S. The organism X is introduced and grows at the expense of S. In Figure 22–21, the left-hand graph shows a batch growth process for X growing on S and storing S as Q. The process of depletion of S and growth of X can be described by a Monod (1950) equation, which is similar to a Michaelis-Menten equation:

$$\mu = \mu_{max}\frac{S}{K_s + S} \qquad (16)$$

Here $\mu$, $\mu_{max}$, and S have been defined previously. $K_s$ is the half-saturation constant for growth as a function of substrate S and is that value of S at which $\mu = 1/2\ \mu_{max}$. When S is very large relative to $K_s$, then $S/(K_s + S)$ is close to 1 and $\mu$ equals $\mu_{max}$. To describe the batch growth process, we write equations for the use of S and the growth of X as follows:

$$\frac{dS}{dt} = -\mu_{max}\left(\frac{S}{K_S + S}\right)\frac{X}{Y} \qquad (17)$$

$$\frac{dX}{dt} = \mu_{max}\left(\frac{S}{K_S + S}\right)X \qquad (18)$$

In words, equation (17) says the change in S in the batch culture is equal to the consumption of S by the growth of alga X. The parameter Y is the yield coefficient for conversion of S into X. If X were expressed as cells $ml^{-1}$ and S in $\mu mol\ l^{-1}$, then Y would have units of cells $ml^{-1}/\mu mol\ l^{-1}$. Equation (18) then says X grows as a function of S. For some practice working with the Michaelis-Menten and Monod models, refer to Question Box 22–2.

In continuous cultures, nutrients are continuously being added to a culture vessel and unconsumed nutrients and organisms continuously being washed out at a dilution rate D with units of $t^{-1}$. In continuous cul-

**Table 22–3 Values of parameters in models of growth and phosphorus uptake for P-limited chrysophyte flagellates (from Sandgren, 1988)**

| species | clone | mean cell volume ($\mu m^3$) | $\mu_{max}$ ($day^{-1}$) | $K_S$ ($\mu M$) | $V_{max}$ ($10^{-9}$ µmol $cell^{-1}$ $min^{-1}$) | $K_t$ ($\mu M$) | $Q_{max}$ ($10^{-9}$ µmol $cell^{-1}$) | $Q_o$ ($10^{-9}$ µmol $cell^{-1}$) |
|---|---|---|---|---|---|---|---|---|
| *Dinobryon cylindricum* | 1 | — | 0.90 | — | — | — | — | 2.40 |
| | 5 | 272 | 0.51 | 0.014 | — | — | 18.5 | 1.77 |
| | 7 | — | 0.58 | — | — | — | — | 2.15 |
| | 13 | 290 | 0.75 | 0.021 | — | — | 21.0 | 1.87 |
| *Dinobryon bavaricum* | | 80 | — | — | 0.34 | 0.72 | — | — |
| | | | | | 0.10 | 0.11 | — | — |
| *Dinobryon sociale* | | — | — | — | 0.22 | 0.01 | — | |
| *Dinobryon divergens* | | — | — | — | 2.32 | 0.39 | — | — |
| *Synura petersenii* | 2b | 374 | 0.51 | 0.003 | 5.1 | 0.10-0.27 | | — |
| | 7c | 431 | 0.76 | 0.001 | 21.8 | 1.19 | 90.0 | 3.04 |
| *Mallomonas cratis* | UW-126 | 1516 | 0.55 | 0.001 | 14.2 | 1.35 | 55.2 | 1.96 |
| *Mallomonas caudata* | 2j | 10,625 | 0.30 | — | — | 0.36 | 152.0 | 7.90 |
| | | | | | | — | — | — |

ture, D represents a loss rate like λ, which we discussed previously with exponential growth. The equations for the same substrate and organism in continuous culture as in equations (17) and (18) are:

$$\frac{dS}{dt} = D\,(S_o - S) - \mu_{max}\left(\frac{S}{K_S + S}\right)\frac{X}{Y} \qquad (19)$$

$$\frac{dX}{dt} = \mu_{max}\left(\frac{S}{K_S + S}\right)X - DX \qquad (20)$$

In words, equation (19) says that the change in substrate concentration in the continuous culture vessel is equal to the amount delivered ($DS_o$), minus any residual that is carried out in the overflow (–DS), minus the amount consumed by growth of alga X. Equation (20) then says the change in population of X is equal to growth ($\mu X$), minus loss due to washout (–DX). While the equations may look formidable, they can be solved because in continuous culture, a steady state or equilibrium can be reached where growth equals losses and thus both dS/dt and dX/dt = 0.

If we set equation (20) equal to zero and substitute $\mu$ for $\mu_{max}\,[S/(K_s + S)]$, we get:

$$0 = \mu X - DX \quad (21)$$

And consequently:

$$\mu = D \quad (22)$$

This means that at steady state, the growth of X equals the loss rate or dilution rate, D. If we now set equation (19) equal to zero we get:

$$0 = D\,(S_o - S) - \mu\left(\frac{X}{Y}\right) \qquad (23)$$

Since $\mu$ = D at steady state, we can substitute D for $\mu$ in (23) above:

$$0 = D\,(S_o - S) - \left(\frac{DX}{Y}\right) \qquad (24)$$

And:

$$X = Y\,(S_o - S) \quad (25)$$

which in words means the steady state concentration of X equals the amount of substrate consumed times the yield coefficient, which converts the amount of S used into units of alga X. If D is greater than $\mu_{max}$, the population of algae cannot maintain itself against this loss rate and will wash out of the continuous culture vessel.

Continuous cultures have been a major research tool for the study of phytoplankton populations in culture because the cultures can be studied for long time periods. Single species of phytoplankton and mixtures of species in competitive and predation interactions have been examined. The equations describing species interactions in continuous culture can be

## Question Box 22–2 Working with the Michaelis-Menten and Monod models of nutrient uptake and growth

*Sample calculations.*

1. Tilman (1976) calculated the following growth parameters for the diatoms *Asterionella formosa* and *Cyclotella meneghiniana* under both $PO_4$ limitation and $SiO_2$ limitation.

| | $SiO_2$ limitation | | $PO_4$ limitation | |
|---|---|---|---|---|
| | $\mu_{max}$ ($day^{-1}$) | $K_s$ ($\mu M$ $SiO_2$) | $\mu_{max}$ ($day^{-1}$) | $K_s$ ($\mu M$ $PO_4$) |
| *Asterionella formosa* | 1.59 | 3.9 | 0.76 | 0.04 |
| *Cyclotella meneghiniana* | 1.74 | 1.4 | 0.76 | 0.25 |

Use these data in the Monod equation (16) to plot the growth rates of each alga as a function of the concentration of $SiO_2$ and separately as a function of the concentration of $PO_4$. Which alga will dominate under $PO_4$ limitation? Which will dominate under $SiO_2$ limitation? These results will be useful in a later section on nutrient competition.

*Solution.* We choose a convenient range of values of the nutrient concentration of 0 to 10 $\mu$M. The Monod equations are:

| | $SiO_2$ | $PO_4$ |
|---|---|---|
| *A. formosa* | $\mu = 1.59\,[S/(3.9 + S)]$ | $\mu = 0.76\,[S/(0.04 + S)]$ |
| *C. meneghiniana* | $\mu = 1.74\,[S/(1.4 + S)]$ | $\mu = 0.76\,[S/(0.25 + S)]$ |

From the graphs below, it is clear that if $SiO_2$ is limiting, *C. meneghiniana* will dominate over *A. formosa*. At every concentration of $SiO_2$ its growth rate $\mu$ is higher, and because its $K_s$ value is lower, it can reduce $SiO_2$ to levels where *A. formosa* cannot grow. Conversely, if $PO_4$ is limiting, *A. formosa* dominates *C. meneghiniana* at all levels of $PO_4$. *Asterionella formosa* can reduce the levels of $PO_4$ to exclude *C. meneghiniana* because its $K_s$ value is so much smaller. Note that as $K_s$ values become smaller, the growth curves rise more rapidly toward $\mu_{max}$ and appear more angular. These results give us an important insight into nutrient competition among phytoplankton—if two species are competing for a single nutrient such as silicate, the one with the lower $K_s$ value will always win because it can reduce that nutrient's level to the point where the other species cannot grow.

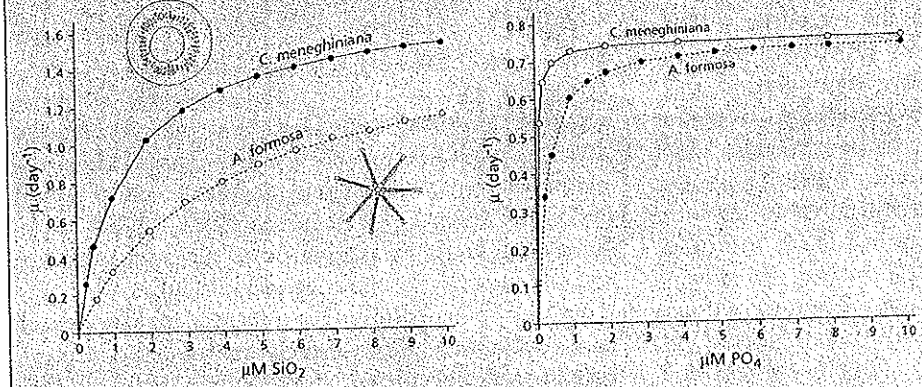


Redrawn with permission from Tilman, D. Ecological competition between algae: Experimental confirmation of resource-based competition theory. *Science* 192:463–465 ©1976 American Association for the Advancement of Science

2. The following data show the process of phosphorus uptake by *Cyclotella meneghiniana* as a function of phosphate concentration (adapted from Tilman and Kilham, 1976).

## Question Box 22–2 *continued*

| S (μM $PO_4$) | ρ (μM $PO_4$ $cell^{-1}$ $hr^{-1}$ x $10^{-9}$) |
|---|---|
| 1.00 | 2.87 |
| 1.38 | 3.40 |
| 2.08 | 5.21 |
| 2.86 | 3.30 |
| 4.00 | 4.65 |
| 4.76 | 4.48 |
| 6.66 | 5.05 |

Determine the parameters $K_t$ and $\rho_{max}$ in the Michaelis-Menten equation (13) for this set of data. Values of S represent the initial phosphate concentrations. Uptake rates were measured by following the removal of $PO_4$ and the increase in cell numbers over several hours.

*Solution.* In research applications, the final parameters are determined by nonlinear regression techniques on a computer. You can, however, obtain good estimates of the parameters by a linear transformation of the Michaelis-Menten equation, where ρ and S are the variables and $\rho_{max}$ and $K_t$ are constants. We use the algebraic axiom that if $x = y$ then it is also true that $1/x = 1/y$. The first step is to invert equation 13 to yield:

$$\frac{1}{\rho} = \frac{K_t + S}{\rho_{max} S}$$

We can now separate the two terms on the right-hand side to give us:

$$\frac{1}{\rho} = \frac{K_t}{\rho_{max}}\left(\frac{1}{S}\right) + \frac{S}{\rho_{max} S}$$

Canceling out the S in the far-right term we finally derive:

$$\frac{1}{\rho} = \frac{K_t}{\rho_{max}}\left(\frac{1}{S}\right) + \frac{1}{\rho_{max}}$$

This is the equation of a straight line of the form $y = mx + b$, where $y = 1/\rho$, $x = 1/S$, the slope $m = K_t/\rho_{max}$ and the intercept $b = 1/\rho_{max}$. To derive this equation for our example, we have only to take the inverses of the values of S and ρ, plot them on graph paper, and take the linear regression of $1/\rho$ on $1/S$. The intercept will be the inverse of $\rho_{max}$, and the slope will give us $K_t$. The inverses are:

| x = 1/S | y = 1/ρ |
|---|---|
| 1.00 | 0.348 |
| 0.72 | 0.294 |
| 0.48 | 0.192 |
| 0.35 | 0.303 |
| 0.25 | 0.215 |
| 0.21 | 0.223 |
| 0.15 | 0.198 |

If we use all seven points, the resulting linear equation is $Y = 0.1529\ (X) + 0.1842$ with a correlation coefficient of 0.78 (refer to the plot below). The maximum uptake rate $\rho_{max}$ is the inverse of 0.1842 or $5.4 \times 10^{-9}$ μM $PO_4$ $cell^{-1}$ $hr^{-1}$. $K_t = 0.1529\ \rho_{max}$, so $K_t = 0.83$ μM $PO_4$. These values are quite close to those reported by Tilman and Kilham (1976) from nonlinear regression ($\rho_{max} = 5.1 \times 10^{-9}$ and $K_t = 0.8$). In most cases real data are much noisier than this set, and linear regression can at most provide a starting point for a nonlinear regression routine.

*continued*→

## Question Box 22–2 *continued*

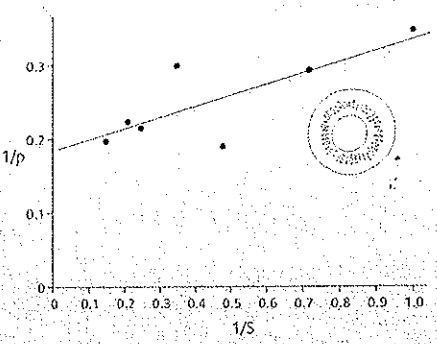


*Problems.*

1. Tilman and Kilham (1976) measured the uptake of $SiO_2$ by the diatom *Cyclotella meneghiniana*. Use the following data adapted from their paper to estimate the uptake parameters $\rho_{max}$ and $K_t$. How do the dynamics of $SiO_2$ uptake compare to those of $PO_4$ calculated in the above sample problem?

| $SiO_2$ (μM) | ρ μM cell$^{-1}$ hr$^{-1}$ (×10$^9$) |
|---|---|
| 0.893 | 1.66 |
| 2.270 | 4.29 |
| 3.860 | 5.77 |
| 7.270 | 6.72 |
| 15.000 | 8.93 |
| 27.300 | 12.56 |

2. Tilman, et al. (1981) examined silicate and phosphate growth kinetics of four Lake Michigan diatoms to test his resource competition theory. The following parameters were obtained for *Fragilaria crotonensis* and *Synedra filiformis* under silicate-limiting conditions.

| | $\mu_{max}$ (day$^{-1}$) | $K_s$ (μmol l$^{-1}$) |
|---|---|---|
| *Fragilaria* | 0.62 | 1.5 |
| *Synedra* | 1.11 | 19.7 |

Plot the curves of the Monod growth model (16) for each species. Based on these graphs, what $SiO_2$ conditions would favor growth of each species?

3. Tilman and Kilham (1976) also measured the growth of *Asterionella formosa* as a function of $SiO_2$ concentration. Use the following data adapted from their paper to estimate the growth parameters $\rho_{max}$ and $K_s$ in the Monod equation (16). *Hint*: the same procedure can be used as with the Michaelis-Menten model of uptake dynamics.

| $SiO_2$ (μM) | μ (doublings day$^{-1}$) |
|---|---|
| 3.5 | 0.508 |
| 3.7 | 0.515 |
| 6.5 | 0.690 |
| 7.0 | 0.700 |
| 10.2 | 0.783 |
| 13.2 | 0.813 |
| 18.6 | 0.833 |
| 22.0 | 0.933 |

*Note*: in the actual data set, the values of $\mu$ at low $SiO_2$ levels are prone to large variation. Therefore the values of $1/\mu$ are also subject to high variation and were not used in the regression. Answers are found at the end of the chapter.

solved for steady-state equilibrium values, and the solutions of the equations can be compared to observations. Unfortunately, this research also has led to the assumption that steady-state equilibrium models can be applied to natural aquatic systems. No matter how attractive the equations may be, however, this does not mean steady-state models work in the real world.

## Growth and Uptake of Organic Carbon

The previous two sections have covered autotrophic processes of growth, that is, processes by which algae generate their own food through photosynthesis coupled with uptake of inorganic nutrients. But phytoplankton also exhibit two common heterotrophic processes of growth, consumption of particulate organic matter and uptake of dissolved organic carbon (DOC). Such versatile organisms are called mixotrophic because they have the capability for a mixture of feeding processes. The chrysophycean *Ochromonas* is a good example of a mixotrophic flagellate. For more details refer to Chapters 1 and 13 in the section on variations in algal nutrition. Some DOC-users have chlorophyll (*Euglena*) and others not (*Prototheca*). For more information concerning DOC use by algae, refer to Chapter 2.

## Loss Processes

What are loss processes? Recall our earlier discussion of net growth rate being equal to the gross growth rate or rate of reproduction minus the death rate or the sum of all loss processes (equation 3). Loss processes are all those factors that remove or displace phytoplankton in the aquatic environment. Following the formulation of Lampert and Sommer (1997), loss processes can be described by the expression:

$$\lambda = \gamma + \sigma + \chi + \delta + \pi + \omega \quad (26)$$

Here the Greek letter $\lambda$ stands for losses and the remaining Greek letters for specific types of loss processes. Greek gamma ($\gamma$) stands for grazing—the loss of algal cells to herbivores such as ciliates, rotifers, and crustaceans (see Chapter 3). The letter sigma ($\sigma$) stands for sedimentation—the sinking of nonmotile algal cells out of the euphotic zone. Losses due to competition are represented by the letter chi ($\chi$). Delta ($\delta$) stands for death or physiological mortality, and pi ($\pi$) is parasitism. The final symbol, omega ($\omega$), represents loss due to washout.

## Perennation

We will discuss each of these processes, but first we need to mention an adaptation used by many groups of phytoplankton to reduce losses altogether, namely **perennation**. Perennation is the formation of some sort of resting stage that allows the algal population to avoid a period of adverse environmental conditions. Many cyanobacteria form akinetes, a type of asexual spore that develops from vegetative cells (Chapter 6). Akinetes may be resuspended into the

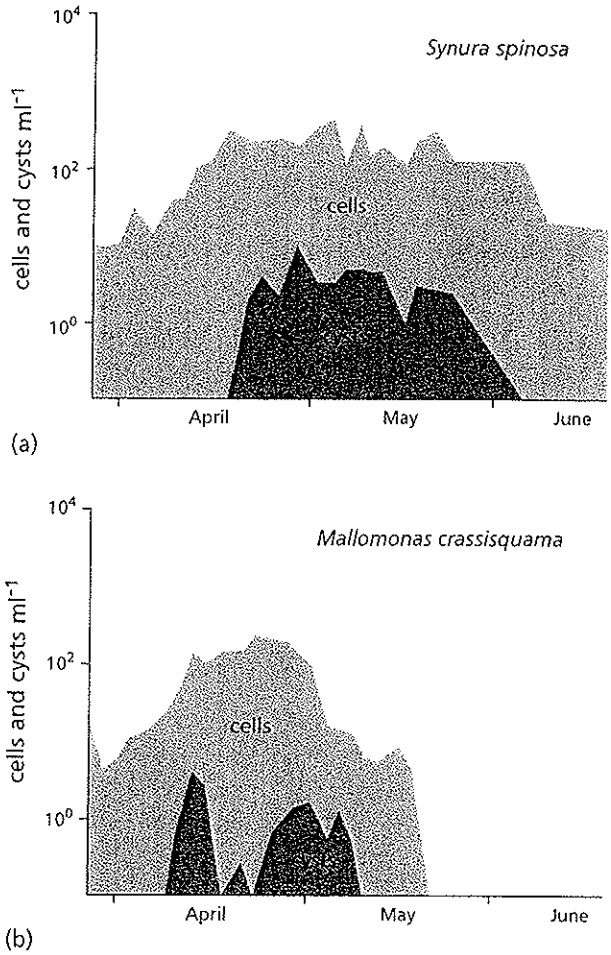


**Figure 22–22** Cells and cysts per ml of two planktonic chrysophyceans from Egg Lake, Washington, U.S.A., in spring 1976. (After Sandgren, 1988)

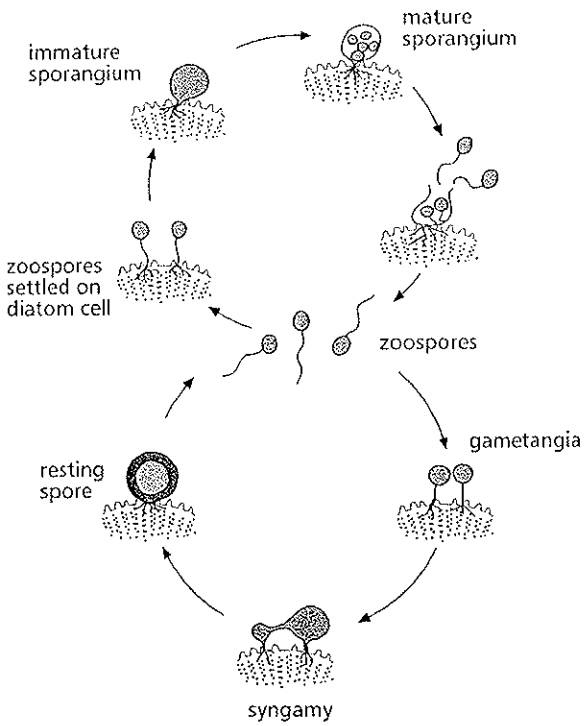


Figure 22–23 Life cycle of the chytrid *Zygorhizidium planktonicum*. (Adapted from van Donk and Ringelberg, 1983 by permission of Blackwell Science, Ltd.)

water column where they will germinate (Reynolds, 1972). One study found that akinetes could survive and germinate after more than 60 years buried in sediments (Livingstone and Jaworski, 1980). *Microcystis*, however, can survive as vegetative cells on sediment surfaces with neither light nor oxygen for several years (Reynolds, et al., 1981). Some centric diatoms such as *Melosira* and *Stephanodiscus* form a resting vegetative cell in which the protoplast contracts into a ball within the frustule; these resting cells can survive on the sediments for several months to a year (see also Chapter 12).

Green algae often produce resting zygotes (Chapters 20 and 21), and dinoflagellates form cysts (Chapter 11). The dinoflagellate *Ceratium hirundinella* forms cysts in response to declining nutrients; this is an example of control by an external factor or exogenous control. Chrysophyceans, on the other hand, produce a resting spore or stomatocyst whose formation is under endogenous (internal) control. The production of stomatocysts is directly dependent on the cell density (Fig. 22–22). Most chrysophyceans are only present in the plankton for a few weeks per year and produce their resting cysts when the population is most abundant.

Perennation stages play important roles in both the freshwater and marine environments. In oceans, however, if perennation stages sink, they would need to do so over shallow continental shelves to have a chance for survival. A cyst sinking into the abyssal depths of the open oceans is a lost cyst.

## Mortality and Washout

A few of the loss terms can be dealt with very briefly. Physiological mortality ($\delta$) can only be determined if "bodies," such as diatom frustules can be recovered. Most algal cells are either eaten or sink out of the mixing layer. Similarly, washout ($\omega$) is not often a significant factor for phytoplankton. Most algal populations are sufficiently numerous and dispersed that washout due to a flood event is unlikely to reduce the population significantly.

## Parasitism

Parasitism ($\pi$) upon phytoplankton populations has been relatively little studied. Viruses have been recovered from cyanobacteria and have been shown to lyse them in lab cultures. Van Etten, et al. (1991) surveyed viruses and viruslike particles in eukaryotic algae, especially in symbiotic *Chlorella* species. In the marine environment, Sieburth, et al. (1988) reported viruses in the pelagophycean picoplankter *Aureococcus anophagefferens*, and Suttle, et al. (1990) showed that viruses could reduce primary productivity in marine waters.

Fungal parasites of algae are better known. Most belong to the phylum Chytridiomycota. Free-swimming uniflagellate zoospores seek out and attach to host cells (Fig. 22–23) A mycelial thread penetrates the host cell and supplies nutrients to the enlarging zoospore, which becomes a sporangium. Zoospores are released from the sporangium to complete the cycle. The host cell is killed by the infection. Van Donk (1989) followed the populations of *Asterionella formosa* and their infection with the chytrid *Zygorhizidium planktonicum* in Lake Maarsseveen (Netherlands) during the spring from 1978 to 1982 (Fig. 22–24). Heavy infection of *A. formosa* allowed the diatoms *Fragilaria crotonensis*, *Stephanodiscus astraea*, and *S. hantzschii* to become abundant. Some small protozoa are known to attack large colonial green algae as parasites causing heavy mortality (Canter, 1979). Little is

known about the dynamics of most parasites acting on planktonic algae or the impact they may have on phytoplankton communities. This is one area of aquatic ecology in which it is not a cliché to say that more research is needed. For additional information, refer to Chapter 3.

## Sedimentation (σ)

If an algal cell sinks below the euphotic zone, it will be lost unless it functions as a perennation stage. Many phytoplankton, however, can minimize sedimentation losses by controlling their position in the water column.

### Swimming and buoyancy

Flagellates can swim at speeds sufficient to maintain their position in the water column. The average swimming speeds of flagellated phytoplankton are about ten times greater than the average sinking rate, which is on the order of 0.5 m day$^{-1}$ (Sournia, 1982). Flagellates may perform extensive daily vertical migrations, often moving from upper waters by day to deeper waters at night. *Peridinium cinctum* migrates 8–10 m daily in Lake Kinneret, Israel (Berman and Rodhe, 1971), and *Cryptomonas ovata* carries out a daily migration of 5 to 7.5 m in Finstertaler See, Austria (Tilzer, 1973). In the oceans, dinoflagellates may migrate to depths of 10–20 m daily (Eppley, et al., 1968). The largest migration in freshwaters has been reported from Lake Cahora Bassa, Mozambique. There *Volvox* sp. migrates as much as 20 m into the deeper strata at descent rates of 1.8 to 3.6 m hr$^{-1}$ and returns every day. *Volvox* require high levels of phosphorus for growth. Its half-saturation constant ($K_s$) for P-limited growth is on the order of 19 to 59 $\mu$g P l$^{-1}$ (Senft, et al., 1981). In the euphotic zone of Lake Cahora Bassa, P-levels are undetectable (Fig. 22–25). Thus *Volvox* may be migrating down to a depth of 20 or more meters to take up phosphorus at night and then return to upper waters for photosynthesis and growth in the day (Sommer and Gliwicz, 1986).

Many cyanobacteria also control their position in the water column by adjusting the formation of intracellular gas vacuoles and regulating cellular ballast. See Chapter 6 for a discussion of buoyancy regulation in cyanobacteria. Genera that generate nuisance blooms, such as *Microcystis*, *Anabaena*, and *Aphanizomenon*, use such buoyancy mechanisms to adjust their vertical position. During windless periods, daily rhythms of vertical migration have been observed (Reynolds, et al., 1987). Vertical migration rates can be high. In Lake George, Uganda, *Microcystis aeruginosa* migrated at speeds greater than 3 m hr$^{-1}$ (Ganf, 1975). *Aphanizomenon flos-aquae* reached speeds of 40 cm hr$^{-1}$ to 2.75 m hr$^{-1}$ in the Chowan River of North Carolina (Paerl and Ustach, 1982). *Oscillatoria* also uses the same buoyancy control mechanisms to maintain stable

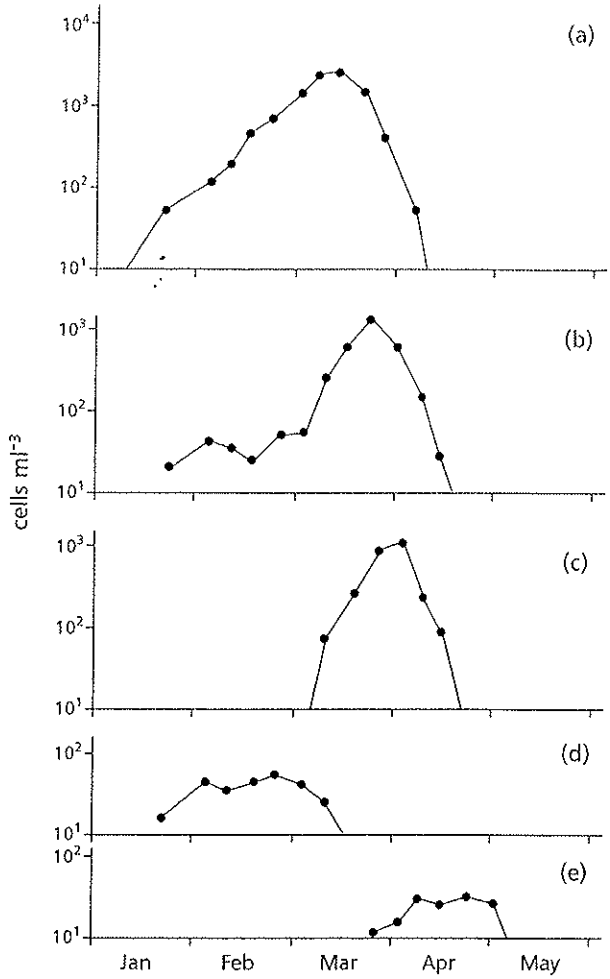


**Figure 22–24** Population of *Asterionella formosa* in spring of 1982 in the surface waters of Lake Maarsseveen, Netherlands, divided into five categories. (a) uninfected *A. formosa* cells, (b) cells with zoospores of *Zygorhizidium planktonicum*, (c) *A. formosa* infected with sporangia, (d) cells infected with thick-walled spores, (e) cells with resting spores of *Z. planktonicum*. Most of the *A. formosa* population was infected by late March (After van Donk, 1989 ©Springer-Verlag)

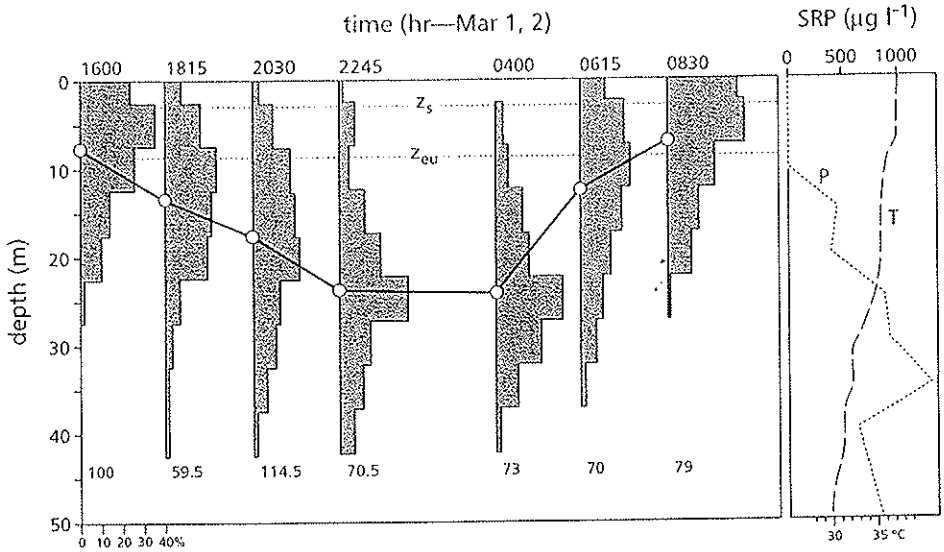


**Figure 22–25** Evening descent and morning ascent of *Volvox* in Lake Cahora Bassa on March 1–2, 1983. The upper horizontal axis gives 24-hour time. The column diagrams show the depth distribution of *Volvox* in percent of total population. The numbers at the bottoms of the column diagrams give the areal population density in units of $10^3$ colonies $m^{-2}$. The solid lines track the median depth. $Z_s$ marks Secchi-disk transparency in m, and $Z_{eu}$ the depth of the euphotic zone. Note soluble reactive phosphorus (P) is unmeasureable within the euphotic zone. The lake is quite hot by comparison to north temperate lakes (> 30° C). (From Sommer and Gliwicz, 1986)

populations in the metalimnion of lakes for periods of weeks (Fig. 22–7).

Buoyancy regulation and vertical positioning work best under stable water conditions. Turbulent mixing causes cyanobacteria to circulate along with other phytoplankton. Prolonged turbulent mixing can shift dominance away from cyanobacteria and toward other algae such as greens (Harris, et al., 1980).

## Sinking

Phytoplankton that can neither swim by flagella nor regulate their buoyancy with gas vacuoles are subject to sinking through the water column. Most phytoplankton are only slightly more dense than water at 1.02 to 1.05 g $ml^{-1}$, but diatoms have densities around 1.3 g $ml^{-1}$. The silicate making up their frustules is very dense at about 2.6 g $ml^{-1}$. Only a few substances within algal cells are less dense than water—lipids have densities around 0.86 g $ml^{-1}$ and the gas vacuoles of cyanobacteria have values around 0.12 g $ml^{-1}$.

The sinking velocity of a falling sphere was originally described by Stokes' law. Since phytoplankton are living rather than inert and are often shaped other than as spheres, Ostwald's modification of Stokes' law was formulated to adjust sinking rates for the form resistance of nonspherical phytoplankton cells. The modified Stokes' law has the form:

$$v_s = \left(\frac{2}{9}\right) g\, r_s^2\, (q' - q)\, \upsilon^{-1}\, \phi^{-1} \qquad (27)$$

Here, $v_s$ is the sinking velocity in m $s^{-1}$, g is the gravitational acceleration of the earth (9.8 m $s^{-2}$), and $r_s$ is the radius (in meters) of a sphere of volume equivalent to that of the algal cell. The term q' is the density of the algal cell expressed in kg $m^{-3}$, and q is the density of the fluid medium. For water, q has the value 1000 kg $m^{-3}$. Thus, (q' – q) is the difference between the density of the algal cell and the surrounding water. This difference is positive for most algae, which are more dense than water, but it may be negative for cyanobacteria with gas vacuoles or an alga with a high intracellular concentration of lipids. The term $\upsilon$ (Greek upsilon) is the viscosity of water, which is expressed in units of kg $m^{-1}$ $s^{-1}$. Water is more viscous at lower temperatures, and thus $\upsilon = 1 \times 10^{-3}$ kg $m^{-1}$ $s^{-1}$ at 20° C but $1.8 \times 10^{-3}$ kg $m^{-1}$ $s^{-1}$ at 0° C (Lampert and Sommer, 1997). The final term $\phi$ (Greek phi) stands for form resistance and is dimensionless. Form resistance accounts for the fact that most algae have nonspherical shapes and may possess horns and spines.

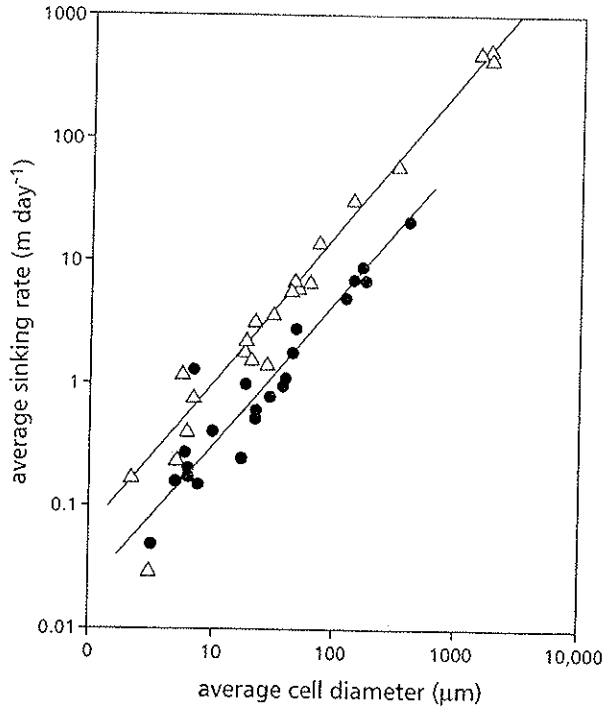


**Figure 22–26** Data for sinking rates of phytoplankton. Triangles represent senescent cells, closed circles, actively growing cells. (Based on Smayda, 1970, in Harris, 1986 with kind permission of Kluwer Academic Publishers)

In words, equation (27) says that the sinking velocity of an algal cell is proportional to the gravitational force of the earth times a measure of the size of the cell (the radius squared) times the difference between the densities of the cell and its fluid medium. According to the equation, larger cells or colonies or more dense cells such as diatoms should sink more rapidly. Conversely, the more viscous the water and the greater the form resistance of the algal cell, the slower the sinking velocity. Some representative data and a sample calculation are presented in Question Box 22–3 together with a few practice problems.

Observed sinking rates of living algal cells and colonies frequently do not correlate well with the predictions of the Ostwald modification of Stokes' law. Living cells do not sink as rapidly as dead or senescent cells of the same species (Fig. 22–26). Reynolds (1984) found that the observed sinking velocity of killed cells of *Stephanodiscus astraea* was highly correlated ($r = 0.98$) with the radius of a sphere having a volume identical to that of the killed cells ($r_s$), the parameter used in the Stokes' equation. There was no correlation between $r_s$ and the observed sinking rates of living cells of *S. astraea*. Thus living cells do not behave in a water column as the inert spheres of Stokes' Law but dead cells do, with allowance for form resistance.

Phytoplankton that sink rapidly require more rapid vertical mixing to remain in the water column than do cells that sink slowly. In part this fact may account for the seasonal occurrence of large diatoms and desmids during periods of strong vertical mixing.

Phytoplankton have a number of adaptations to reduce sinking rates. Small cell size is the most obvious one. Large cells are not simply bigger small cells. Larger diatom species have a reduced surface-to-volume ratio compared to small diatoms. This means they have proportionally less siliceous frustule material and are thus less dense than small diatoms. Some large marine diatoms such as species of *Rhizosolenia* and *Ethmodiscus* are actually positively buoyant. Among *Rhizosolenia* spp., the rate of ascent was highly correlated with cell diameter (Fig. 22–27). The mechanism of this positive buoyancy is still unclear, but the ascent rates can be quite rapid with upper limits approaching 7–8 m hr$^{-1}$.

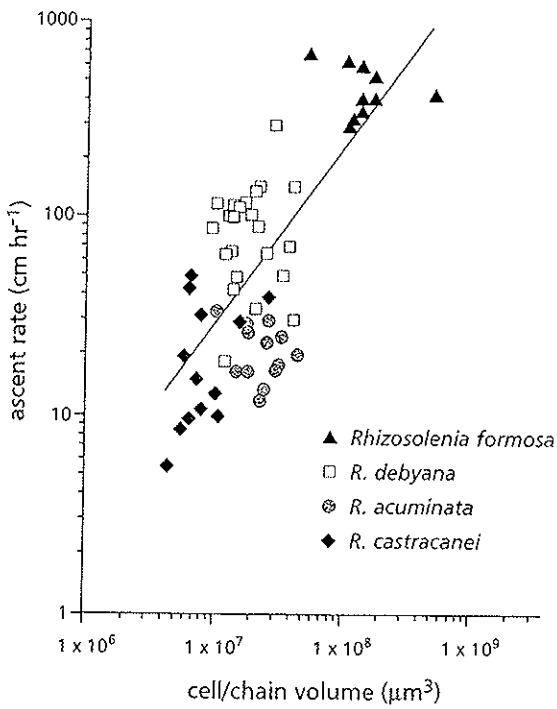


**Figure 22–27** *Rhizosolenia* spp. can ascend through the water column. Larger forms rise faster than smaller forms. (After Moore and Villareal, 1996)

## Question Box 22–3 Working with the Ostwald modification of Stokes' law

The table below shows some representative algal species, their cell or colony volumes, the radius of a sphere with a volume equal to that of the algal cell or colony, and the algal density.

| Algal species | volume ($\mu m^3$) | radius ($\mu m$) | density ($kg\ m^{-3}$) |
|---|---|---|---|
| *Stephanodiscus astraea* | 5,930[a] | 11.23 | 1091[a] |
| *Asterionella formosa* | 5,160[a] | 10.72 | 1130[a] |
| *Chorella vulgaris* | 30[b] | 1.9 | 1095[c] |
| *Microcystis aeruginosa* | $4.2 \times 10^6$ [a] | 100.1 | 999.4[d] |

[a] Reynolds, 1984
[b] Bellinger, 1974
[c] Oliver, et al., 1981
[d] Reynolds, et al., 1981

*Sample calculation for* Stephanodiscus astraea *at 20° C.* From the text, $g = 9.8\ m\ s^{-2}$, $\rho = 1000\ kg\ m^{-3}$, and $\upsilon^{-1} = 10^3\ m\ s\ kg^{-1}$, the inverse of $\upsilon$. The value of q' is given in the above table. Convert the table values of radius in $\mu m$ to meters by multiplying by $10^{-6}\ m\ \mu m^{-1}$. For the moment we do not concern ourselves with $\phi$. Then:

$$v_s = \left(\frac{2}{9}\right) 9.8\ m\ s^{-2} (11.23 \times 10^{-6}\ m)^2 (1091 - 1000\ kg\ m^{-3})\ 10^3\ m\ s\ kg^{-1}\ \phi^{-1}$$

Which becomes:

$$v_s = 2.177\ m\ s^{-2} (126.1 \times 10^{-12}\ m^2) (91\ kg\ m^{-3})\ 10^3\ m\ s\ kg^{-1}\ \phi^{-1}$$

And finally:

$$v_s = 24.98 \times 10^{-6}\ m\ s^{-1}\ \phi^{-1}$$

If we multiply this result by $3600\ s\ hr^{-1}$, we find that *S. astraea* is predicted to sink at the rate of $0.09\ m\ hr^{-1}$. If we multiply the result in (30) by $10^6\ \mu m\ m^{-1}$ instead, we get $v_s = 24.98\ \mu m\ s^{-1}$. Reynolds (1984) reported that the actual sinking rate of killed *S. astraea* cells was $27.62\ \mu m\ s^{-1}$. Thus, $\phi$ is 24.98/27.62 or 0.904.

*Practice calculations.* Work the following problems with a pocket scientific calculator. Answers are given at the end of the chapter.

1. Calculate the predicted sinking velocity of an 8-celled colony of *Asterionella formosa* according to the Ostwald modification of Stokes' law. Reynolds (1984) reports that the actual sinking velocity of this algal colony is $7.33\ \mu m\ s^{-1}$. What therefore must be the value of $\phi$?

2. Calculate the sinking velocity of *Chlorella vulgaris* using equation (27). Assume for this spherical alga a $\phi$ of 1.0. What does this tell you about the effect of size on sinking rate?

3. Calculate the ascending velocity of a large buoyant colony of *Microcystis aeruginosa* from the data in the table. Assume the colonies are essentially spherical, so $\phi = 1.0$. How does this rate compare to some of the upward migration rates reported in the text for cyanobacteria?

4. In an earlier section on algae in space research (Chapter 4), it was suggested that algae may one day be introduced to Mars as part of a terraforming effort. If *Stephanodiscus astraea* were introduced to a reformed Martian lake, how fast might it sink through a Martian lake's water column? *Hint*: the gravitation force of Mars is 0.38 of that of Earth.

Many large phytoplankton cells and colonies, including the desmid *Staurastrum* and cyanobacteria such as *Coelosphaerium* and *Microcystis*, possess a mucilaginous sheath or matrix in which the cells are embedded. Since the density of mucilage is close to that of water, a mucilaginous sheath can reduce the overall cell or colony density to levels closer to that of water, but it cannot make a cell or colony buoyant. At the same time, adding mucilage can increase cell or colony diameter, which should (according to Stokes' law) increase sinking rate. Reynolds (1984) has shown that there is a trade-off of effects such that adding mucilage decreases sinking up to a point, after which further additions cause sinking rate to rise again. Mucilage may serve other purposes than decreasing sinking rates, as will be discussed later.

A further adaptation of phytoplankton to sinking is contained in the Ostwald modification of Stokes' law as the parameter $\phi$ for form resistance. According to the original Stokes' equation, larger cells should sink more rapidly. But if larger cells or colonies depart from a spherical shape, they acquire a form resistance, which slows their sinking rates. Thus many large desmids like *Staurastrum* have long arms extending out from the cell, and dinoflagellates such as *Ceratium* have long, straight or curved horns (Fig. 22–1). Conway and Trainor (1972) showed that spine-bearing *Scenedesmus* spp. sink less rapidly than species without spines. Walsby and Xypolyta (1977) removed chitinous fibers from the marine diatom *Thalassiosira weissflogii* with the enzyme chitinase and observed that fiberless cells sank twice as fast as cells with fibers, although the fibers were more dense than the cells. According to Stokes' law, colonies should sink faster because they have larger equivalent spherical volumes than their component cells. As cells are added to colonies, the predicted sinking rate $v_s$ from Stokes' law should increase nearly exponentially. Reynolds (1984) showed, however, that many diatom colonies increase their form resistance by adding cells to such an extent that their actual sinking rates approach a constant rate. In *Asterionella formosa*, the sinking velocity increased to a constant at 6–8 $\mu$m $s^{-1}$ as the number of cells reached eight to nine cells per colony. Beyond this number, additional cells filled in the colony, decreased the form resistance, and increased the sinking rate. Thus an eight to nine cell colony appears to be optimal to maximize size and minimize sinking rate (Reynolds, 1984).

Recently form resistant shapes have been interpreted as a response to grazing pressure. Spined *Scenedesmus* are less taken by certain grazers than non-spiny species of the same size. In nearshore marine waters, long-spined *Thalassiosira* are not consumed by microzooplankton including ciliates, while non-spiny *Thalassiosira* are readily eaten. The long-spined diatoms can be taken by crustacean zooplankton (Gifford, et al., 1981). Phytoplankton with mucilaginous sheaths may be rejected by grazers because they are too big to be eaten. Porter (1977) has shown that some algae with mucilaginous sheaths may pass through the guts of grazers unharmed. These species may even benefit from the gut passage by acquiring nutrients during the process. There seems to be little reason to claim that features such as horns, arms, spines, or mucilaginous sheaths are either flotation devices or defense mechanisms exclusively. They may well have arisen in diverse forms because they serve more than one useful function simultaneously.

## Competition

No subject in phytoplankton ecology generates as much controversy and passionate rhetoric as the concept of competition. The idea that competition plays a central role in phytoplankton ecology derives from early ecological theory. Darwin's theory of natural selection proposed that natural populations deplete their resources and press against their carrying capacity. The research of Gause in the 1930s later showed that if two species were grown together in the laboratory, the natural outcome would be depletion of resources and competition in which one of the two species would eventually be eliminated. Gause's work then led to the competitive exclusion principle and niche theory, and their application as the dominant paradigm in the natural world. But the application of this paradigm to phytoplankton communities led to a paradox, as recognized by Hutchinson (1961). If phytoplankton species were all at or near their carrying capacity and competition were a major force in community structure, how could one explain the coexistence of 50 to 100 species in a milliliter of water under the same apparent conditions? That paradox has led to a great deal of research in an effort to circumvent the competitive exclusion principle and allow coexistence of so many species in an homogeneous environment.

### Lotka-Volterra model

The first attempt to formulate mathematically the process of competition between two species was made by Volterra in 1926 and by Lotka in 1932. Their efforts have come down to us as the Lotka-Volterra

competition equations. They are structurally very similar to the logistic growth equation presented earlier:

$$\frac{dN_1}{dt} = \frac{r_1 N_1 (K_1 - N_1 - \alpha N_1)}{K_1} \quad (28)$$

$$\frac{dN_2}{dt} = \frac{r_2 N_2 (K_2 - N_2 - \beta N_2)}{K_2} \quad (29)$$

As in the logistic equation, $N_1$ and $N_2$ are the population densities of species 1 and species 2 in units such as cells $ml^{-1}$ or mg $ml^{-1}$. $K_1$ and $K_2$ are the carrying capacities of the two species expressed in the same units, and $r_1$ and $r_2$ represent the net per capita growth rates of the two species with units of $days^{-1}$ or $hr^{-1}$. The only new elements are the terms $\alpha N_2$ and $\beta N_1$, which represent the competitive interactions between species 1 and species 2. In the logistic equation, as species 1 grows, the increasing density of its own population slows down its population growth rate as $N_1$ approaches $K_1$. How does competition by species 2 affect species 1? Species 2 acts as if it were additional members of species 1 and thus slows down the population growth rate of species 1 faster than species 1 would alone. If $\alpha$ were equal to 1, species 2 would act exactly like additional members of species 1. If $\alpha$ is less than 1, then species 2 has less impact on species 1 than members of species 1 have on each other. If $\alpha$ is greater than 1, individuals of species 2 have a more severe impact on species 1 than does its own population. The same arguments apply to $\beta$ and species 1 impacting species 2. The parameters $\alpha$ and $\beta$ are the competition coefficients. Alpha ($\alpha$) translates units of species 2 into equivalent units of species 1, while beta ($\beta$) translates species 1 into units of species 2. Another way to look at these equations is that species 2 acts on species 1 as a loss process; any growth of species 2 results in a reduction in growth of species 1 by the amount $\alpha N_2$.

The outcome of competition between the two species is determined by the values of the carrying capacities and competition coefficients. If we set both equations equal to zero such that $dN_1/dt = dN_2/dt = 0$, the net growth rates and the carrying capacity terms in the denominators disappear, leaving:

$$N_1 = K_1 - \alpha N_2 \quad (30)$$

$$N_2 = K_2 - \beta N_1 \quad (31)$$

These equations represent two straight lines of slopes $\alpha$ and $\beta$. If the x-axis represents $N_1$ and the y-axis $N_2$, then equation (33) intercepts the x-axis (when $N_2 = 0$) at $N_1 = K_1$ and the y-axis (when $N_1 = 0$) at $N_2 = K_1/\alpha$. Equation (34) intercepts the x-axis at $N_1 = K_2/\beta$ and the y-axis at $N_2 = K_2$. These lines are known as zero growth isoclines. We will have further use for zero growth isoclines in the following section on mechanistic models of competition.

Four possible arrangements of these two lines are shown in Figure 22–28. These graphs represent four possible types of competitive interaction between two species. The arrows in the figures indicate the direction in which the populations of each species will move over time. In Figure 22–28a, species $N_1$ wins in competition against species $N_2$. In the region between the two isoclines, species 1 increases but species 2 decreases in population size. The arrows point downward to the right, and they terminate when species 1 reaches $K_1$.

The case where species 2 displaces species 1 is shown in Figure 22–28b. Here the zero growth isocline for species 2 is above that of species 1. Thus in the region between the two isoclines, species 2 can still increase but species 1 will decrease in population size. The arrows now point upward and to the left and will end at $K_2$, the carrying capacity for species 2, which is the stable equilibrium point.

The third case shown in Figure 22–28c is somewhat unusual. The two zero growth isoclines intersect, and the point of intersection is an equilibrium point. But the equilibrium is unstable. Any perturbation will drive the system away from equilibrium.

The last case in Figure 22–28d is of more interest. Here again the two zero growth isoclines intersect, but in this case the intersection is a stable equilibrium. As indicated by the directions of the arrows, any perturbation that moves the populations of both species away from the equilibrium point, causes changes in the populations so as to drive the species back to that equilibrium.

How well do these equations represent real interactions between organisms? The Russian microbiologist G. F. Gause (1934) was the first to investigate the Lotka-Volterra equations experimentally using microbial systems. The single set of experiments for which Gause is most famous are the competition experiments with the ciliate protozoans *Paramecium caudatum* and *Paramecium aurelia*, which can be easily distinguished under a microscope by the differences in their lengths. Gause grew these ciliates in 5 ml volumes of physiological salt solution with bacteria as food. Every day, he withdrew 0.5 ml for counting and replaced it with

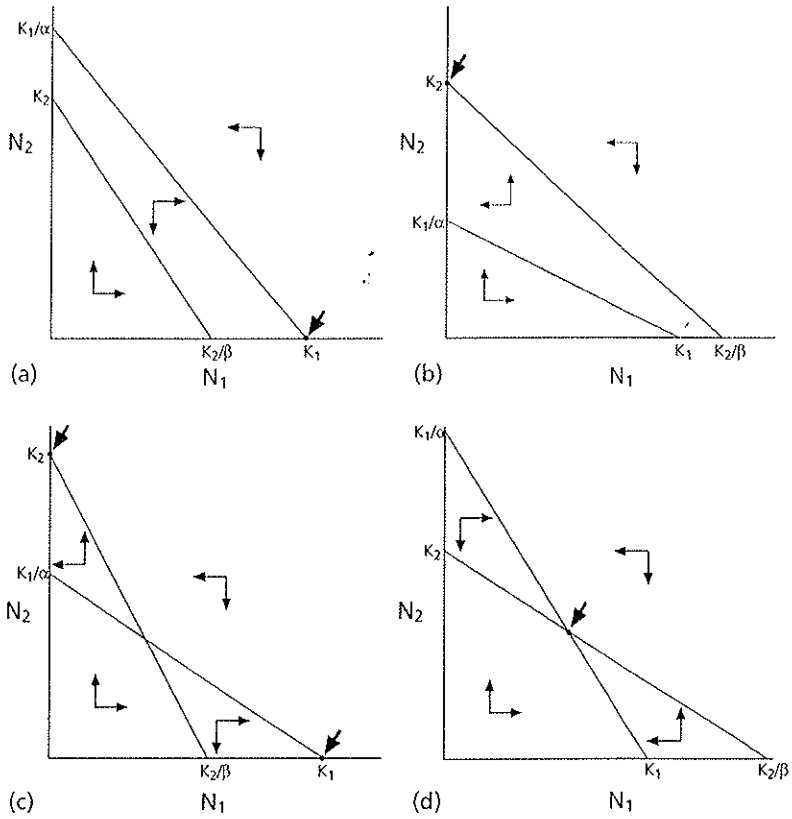


**Figure 22–28** Zero growth isocline analysis of the Lotka-Volterra model of competition between two species. The outcome depends on the relative values of $K_1$, $K_2$, $K_1/\alpha$, and $K_2/\beta$. Large arrows indicate final equilibrium. (a) Species 1 wins at $K_1$, (b) Species 2 wins at $K_2$, (c) unstable equilibrium where either species 1 or 2 may win, (d) stable equilibrium with species 1 and 2 coexisting.

fresh solution. The results of one such experiment, which was run for 16 days, is shown in Figure 22–29. In every experimental run, *P. aurelia* always drove down the population of *P. caudatum*. But note that *P. aurelia* had not eliminated *P. caudatum* after 16 days. These observations became the key data in the establishment of the competitive exclusion principle and niche theory, and their application to all of ecological theory. In fact, these were the only solid data for a competitive exclusion principle.

Despite the historical significance of the Lotka-Volterrra equations, they have a serious drawback. They cannot be used to make predictions about the outcome of competition. A researcher must actually perform a competition experiment, derive values for the competition coefficients and then fit the Lotka-Volterra equations to the data. The Lotka-Volterra equations say nothing about the mechanism of competition—that is, for what are the two species competing?

## Tilman's mechanistic model

Tilman (1976) was the first to address this problem directly by adapting the Monod equation for nutrient-limited growth to the two species competi-

$$\frac{dS}{dt} = D\,(S_o - S) - \mu_{m1}\left(\frac{S}{K_{S1} + S}\right)\left(\frac{N_1}{Y_1}\right) - \mu_{m2}\left(\frac{S}{K_{S2} + S}\right)\left(\frac{N_2}{Y_2}\right) \qquad (32)$$

$$\frac{dN_1}{dt} = \mu_{m1}\left(\frac{S}{K_{S1} + S}\right)N_1 - DN_1 \qquad (33)$$

$$\frac{dN_2}{dt} = \mu_{m2}\left(\frac{S}{K_{S2} + S}\right)N_2 - DN_2 \qquad (34)$$

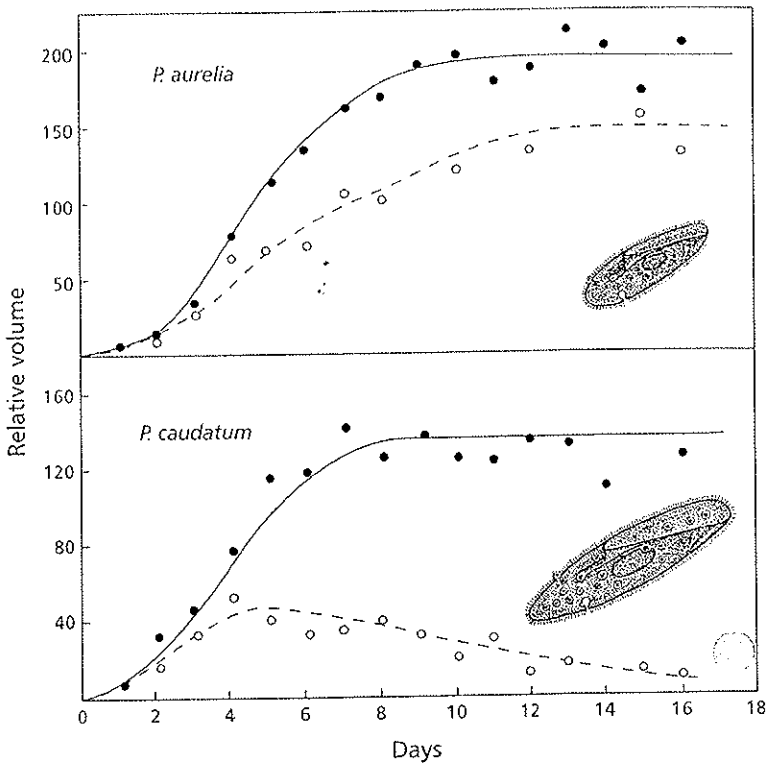


**Figure 22–29** Growth of *Paramecium caudatum* and *P. aurelia* in separate and mixed culture with bacteria as food. Sample removal and replacement effectively provided a dilution rate of D = 0.1 day$^{-1}$. Solid lines—growth in separate culture. Dashed lines—growth in mixed culture. Cells counted in 0.5 ml samples. Relative volume calculated by assuming volume of *P. caudatum* equal to 1.0, and *P. aurelia* equal to 0.43 of volume of *P. caudatum*. (After Gause, 1934. Drawings from Jahn, T. L., E. C. Bovee, and F. F. Jahn. 1979. *How to Know the Freshwater Protozoa*. McGraw-Hill. Reproduced with permission of the McGraw-Hill Companies)

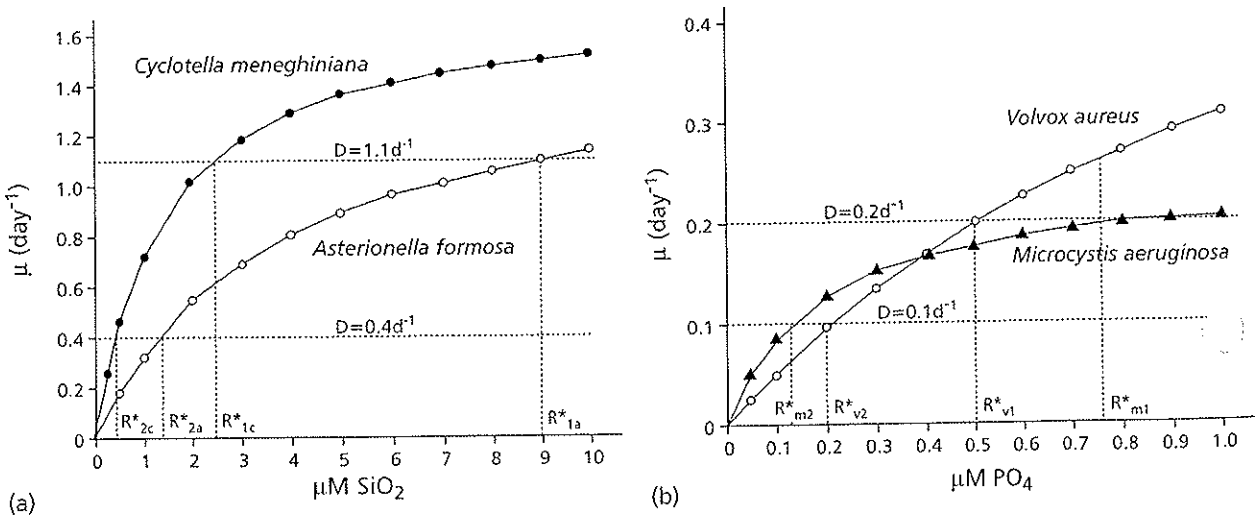


**Figure 22–30** (a) Competition between *Cyclotella meneghiniana* and *Asterionella formosa* for silicate in continuous culture. *Cyclotella meneghiniana* always displaces *A. formosa* because it can reduce the level of silicate below that at which *Asterionella* can grow, at any dilution rate ($R^*_c$ always < $R^*_a$). (b) Competition between *Volvox aureus* and *Microcystis aeruginosa* for phosphate in continuous culture. *Volvox* wins above the point of intersection of the curves, *Microcystis* wins below the intersection. (a: Parameters from Tilman, 1976; b: Kinetic constants from Holm and Armstrong., 1981; Senft, et al., 1981)

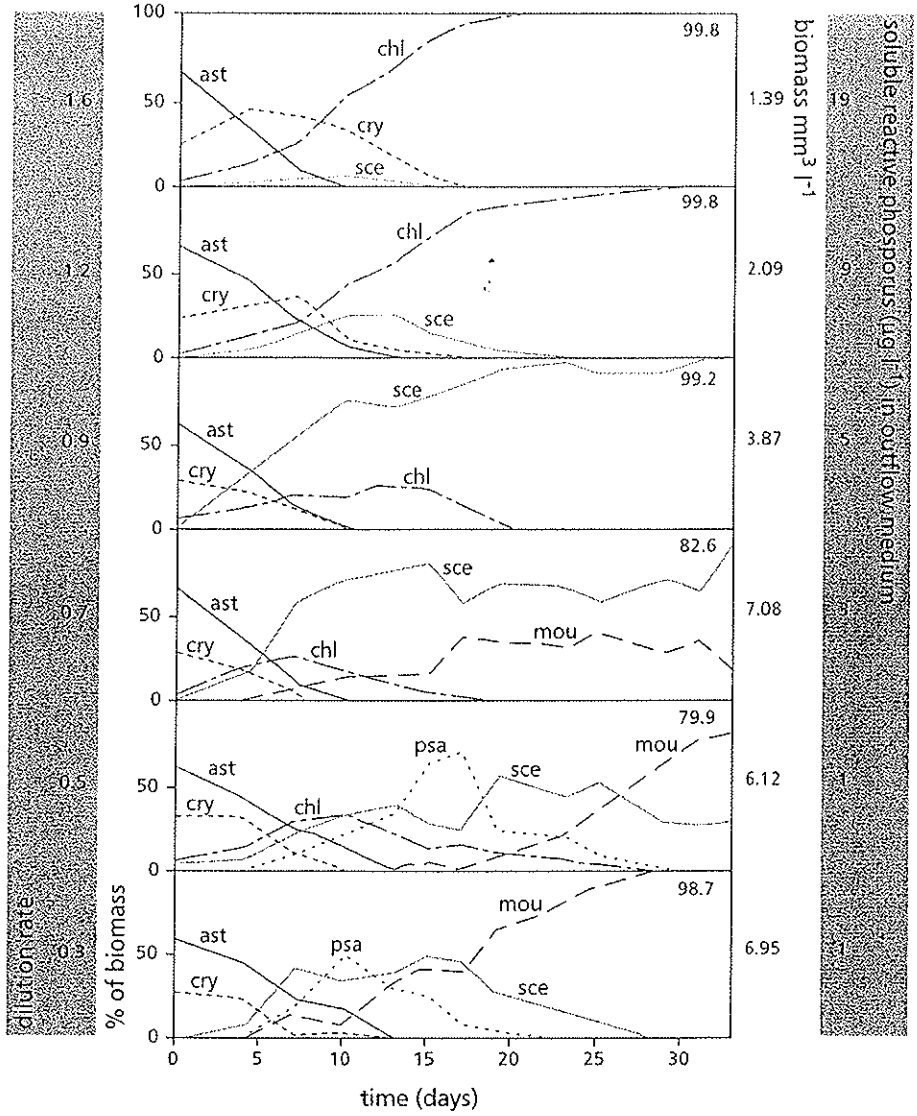


**Figure 22–31** Chemostat competition experiments with culture medium lacking silicate and inoculum consisting of natural phytoplankton from Lake Constance in May. Left axes: dilution rates and percentage of total biovolume. Right axes: biomass ($mm^3\ l^{-1}$) and soluble reactive phosphorus ($\mu g\ l^{-1}$) in the outflow medium (S). In all six experiments, the initial phosphate level was 1 $\mu$M in the inflow medium ($S_o$). Abbreviations for algal species: ast—*Asterionella formosa*, chl—*Chlorella minutissima*, cry—*Cryptomonas ovata*, mou—*Mougeotia thylespora*, psa—*Pseudanabaena catenata*, sce—*Scenedesmus acutus*. (After Sommer, 1986a ©Springer-Verlag)

tion problem for algae. In the simplest case, assume that two species are competing for a single nutrient in a continuous culture. Figure 22–30a (from Tilman, 1976) shows the growth curves for the diatoms *Cyclotella meneghiniana* and *Asterionella formosa* in continuous culture under silicate-limited conditions. The equations for the growth of these two species and the consumption of the limiting nutrient ($SiO_2$) in chemostat culture are given in equations 32 through 34 below. These equations are simply an extension of the equations presented earlier for growth of a single species in continuous culture. In words, these equations state that the concentration of nutrient in the chemostat equals the amount flowing in ($DS_o$) minus the unused nutrient flowing out (– DS) minus the consumption of limiting nutrient by the growth of each species. The growth of each species occurs according to the Monod model of nutrient-limited growth ($\mu$N) minus the loss of cells due to washout (– DN). At equilibrium, D = $\mu$, and *C. meneghiniana* always wins in competition for silicate with *A. formosa* over the entire range of dilution rates because it can always reduce the nutrient level below that at which its competitor can grow (Fig. 22–30a). $R^*_c$ is always less than $R^*_a$ at any D. Their Monod growth curves never cross.

In Figure 22–30b, however, the growth curves for *Volvox aureus* and *Microcystis aeruginosa* in continuous culture do cross. Now if the dilution rate is high (D = 0.2 $day^{-1}$), *V. aureus* has a higher growth rate

**Table 22–4 Values of R* for *A. formosa* and *C. meneghiniana***

| | nutrient required at D = 0.25 day$^{-1}$ (R*) | |
|---|---|---|
| | $PO_4$ (μM) | $SiO_2$ (μM) |
| *A. formosa* | 0.01 | 1.9 |
| *C. meneghiniana* | 0.20 | 0.6 |

than *M. aeruginosa* and can reduce the level of phosphate to $R^*_{v1}$. *Microcystis aeruginosa* will wash out because it needs at least $R^*_{m1}$ to grow at a dilution rate of 0.2 day$^{-1}$. If the dilution rate is lower (D = 0.1 day$^{-1}$), however, *M. aeruginosa* now has a higher growth rate and can reduce the nutrient level to $R^*_{m2}$, a level where *V. aureus* cannot grow and washes out of the chemostat. In each case, the species that wins in competition is the one that can grow and reduce the nutrient level to the lowest level.

Sommer (1986a) tested this idea by inoculating natural phytoplankton from Lake Constance, on the German/Swiss/Austrian border, into a chemostat with a culture medium lacking silicate. After several weeks only one species of green alga remained. At the lowest dilution rate only *Mougeotia thylespora* was present. At intermediate dilutions, *Scenedesmus acutus* dominated, and at the highest dilution rate, *Chlorella minutissima* took over the culture vessel (Fig. 22–31). Despite uncertainties in the estimation of the half-saturation constants ($K_s$), these results were in accord with the predictions of Monod kinetics. Thus, unlike the Lotka-Volterra equations, the Monod-based model of competition is predictive.

When many species compete for a single limiting nutrient under steady-state conditions, the mechanistic model predicts that only one species—the one with the lowest value of $K_s$ for that nutrient—can persist. But what happens when there is more than one nutrient limiting growth? Tilman (1976, 1977) developed a Monod-based model to predict the outcome of competition between two species of diatom for two limiting nutrients, silicate and phosphate. Because of the importance of this model in phytoplankton ecology, we will devote some space to the development of these ideas. In an earlier section on growth and nutrient uptake, we presented Tilman's results for growth of the diatoms *Asterionella formosa* and *Cyclotella meneghiniana* under both phosphate and silicate limitation (Question Box 22–2). Under phosphate limitation, *A. formosa* always wins because its $K_s$ for $PO_4$ (0.04 μM) is lower than that of *C. meneghiniana* (0.25 μM). Under silicate limitation, however, *C. meneghiniana* dominates because its $K_s$ for silicate (1.4 μM) is lower than that of *A. formosa* (3.9 μM).

The Monod growth curves for each diatom species growing separately in continuous culture limited by silicate and phosphate are shown again in Fig. 22–32. Assume each continuous culture is operating at a dilution rate of 0.25 day$^{-1}$. At steady state in a chemostat, D = μ. The dilution rate is represented in each graph by a straight line parallel to the x-axis (y = 0.25). The intersection of this line with the Monod growth curve gives us the minimum amount of $PO_4$ or $SiO_2$ (R*) that each diatom needs to grow at the dilution rate D = 0.25 day$^{-1}$. For a mathematical formula to calculate R*, refer to Question Box 22–4: Working with the Mechanistic Model of Competition. The values of R* are given in Table 22–4. Consider a resource plane in which the concentrations of $PO_4$ are plotted on the y-axis and those of $SiO_2$ on the x-axis (Tilman, 1982). *Asterionella formosa* cannot grow in continuous culture at D = 0.25 day$^{-1}$ and washes out if [$PO_4$] < 0.01 μM or [$SiO_2$] < 1.9 μM. These conditions define two lines in the resource plane (x = 1.9 μM $SiO_2$ and y = 0.01 μM $PO_4$. In the rectangular area above these lines, *A. formosa* can grow, but below them it washes out (Fig. 22–33a). The lines are zero net growth isoclines, just as we used in the Lotka-Volterra model. On these lines, growth of *A. formosa* just balances losses due to washout so dN/dt = 0.

Similarly, *C. meneghiniana* cannot grow at D = 0.25 day$^{-1}$ if [$PO_4$] < 0.2 μM or [$SiO_2$] < 0.6 μM. These values define the zero net growth isoclines for *C. meneghiniana* as x = 0.6 μM $SiO_2$ and y = 0.2 μM $PO_4$ (Fig. 22–33b). *Cyclotella meneghiniana* shows positive net growth in the region above these lines and washes out below them.

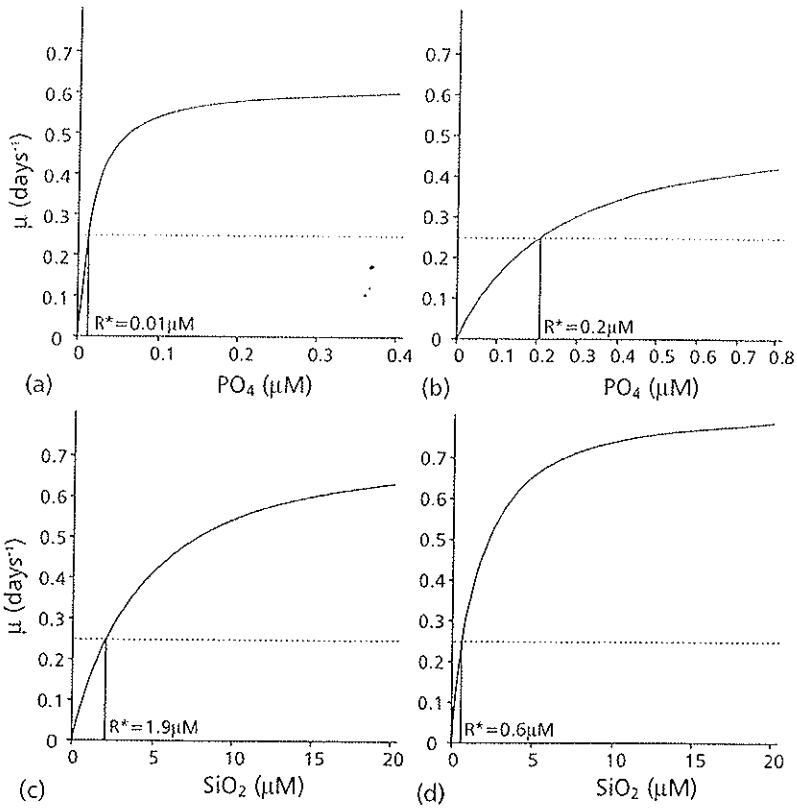


**Figure 22–32** Tilman's (1977) mechanistic model of competition. Monod growth curves for *Asterionella formosa* and *Cyclotella meneghiniana* as functions of $[PO_4]$ (a and b) and $[SiO_2]$ (c and d). (After Lampert and Sommer, 1997 ©Georg Thieme Verlag)

If we now plot both sets of zero growth isoclines on the same resource plane, the rectangular areas intersect and define four regions (Fig. 22–33c). Both diatoms will wash out in region 1. In region 2 defined by x = 0.6 and x = 1.9 $\mu$M $SiO_2$ and above y = 0.2 $\mu$M $PO_4$, only *C. meneghiniana* can grow. *Asterionella formosa* would wash out because $[SiO_2] < 1.9$ $\mu$M. Region 3 is defined by x > 1.9 $\mu$M $SiO_2$ and y between y = 0.01 $\mu$M and 0.2 $\mu$M $PO_4$; *A. formosa* can grow there, but *C meneghiniana* cannot because the level of $PO_4$ is too low. Finally, in region 4 where x > 1.9 uM $SiO_2$ and y > 0.2 uM $PO_4$, both diatoms will be able to grow separately.

What happens in region 4 if both diatoms are in continuous culture together? Three outcomes are possible: *C. meneghiniana* displaces *A. formosa*, both diatoms coexist in a stable equilibrium, or *A. formosa* displaces *C. meneghiniana*. What determines the areas within region 4 where these three outcomes may occur? At the intersection of the two rectangles in Fig. 22–33c, there is a point of stable coexistence where *A. formosa* is limited by $SiO_2$ and *C. meneghiniana* is limited by $PO_4$. What happens in region 4 above this point depends on the relative amounts of $PO_4$ and $SiO_2$ delivered to the continuous culture compared to the half-saturation constants of the two diatoms for each nutrient. To make this clearer, refer to Table 22–5, where we list the values for the half-saturation constants for each nutrient and diatom and the ratio of these constants.

From the information in Table 22–5 we can then derive the information given in Table 22–6, which defines the nutrient supply ratios that determine whether $PO_4$ or $SiO_2$ is limiting growth of each diatom.

If the ratio of supply of phosphate to silicate is less than 0.0103, both diatoms are limited by $PO_4$. *Asterionella formosa* wins in competition by virtue of having the lower value of $K_s$ for $PO_4$. If the ratio of supply is greater than 0.1786, both diatoms are limited by $SiO_2$, and *C. meneghiniana* will displace *A. formosa* because it has the lower $K_s$ value for silicate and can therefore reduce silicate to a level where its competitor cannot grow. If the supply ratio is greater than 0.0103 but less than 0.1786, *A. formosa* is limited by silicate and *C. meneghiniana* is limited by phosphate. Note each diatom is limited by the nutrient that it is least effective at acquiring. Under these conditions each diatom species has more effect on itself than do

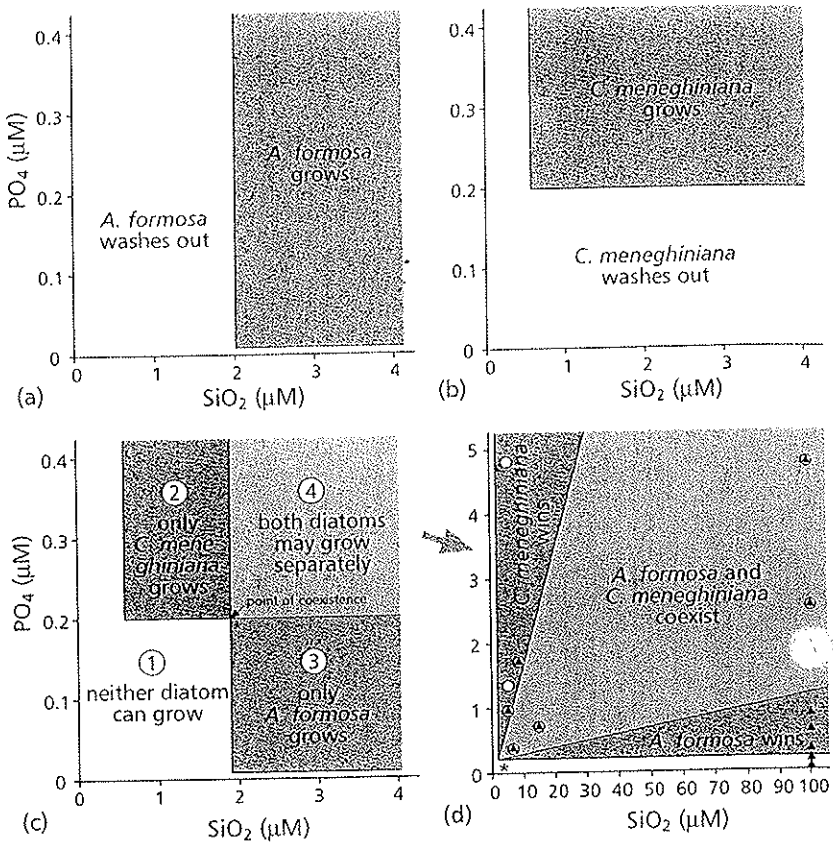


**Figure 22–33** Zero growth isoclines for *A. formosa* and *C. meneghiniana* as functions of $PO_4$ and $SiO_2$ at D = 0.25 $day^{-1}$. (a) zero growth isoclines for *A. formosa*, (b) zero growth isoclines for *C. meneghiniana*, (c) combined zero growth isoclines for both diatoms, (d) region 4 of (c) expanded with consumption vectors added. Symbols indicate experimental results. open circle—*A. formosa* only, black triangle—*C. meneghiniana* only, circled triangles—both diatoms coexisted. (d: After Lampert and Sommer, 1997 ©Georg Thieme Verlag)

members of the other species. This is the zone of stable coexistence under steady-state chemostat conditions.

How do we put this information into our nutrient resource plane to define the zones of competitive displacement and coexistence? We treat the above ratios of nutrient supply as the slopes of consumption lines or vectors originating at the point where the two rectangles intersect, namely the point x = 1.9 $\mu$M $SiO_2$, y = 0.2 $\mu$M $PO_4$, which is a point of stable coexistence. We wish to construct two straight lines starting at x = 1.9, y = 0.2 with slopes m = 0.0103 for *A. formosa* and m = 0.1786 for *C. meneghiniana*. The following algebraic formula will generate the equations of the straight lines.

$$m = \frac{y - y_1}{x - x_1} \qquad (35)$$

where m is the required slope (the ratio of half-saturation constants) and $(x_1, y_1)$ is the origin (1.9, 0.2). Thus, 0.0103 = (y – 0.2)/(x – 1.9) yields y = 0.0103x + 0.1805 for *A. formosa*, and 0.1786 = (y – 0.2)/(x – 1.9) gives y = 0.1786x – 0.1393 for *C. meneghiniana*. These equations are the consumption vectors that divide region 4 into areas of competitive displacement or coexistence. We have added these lines in Figure 22–33d. Above the upper consumption vector, *C. meneghiniana* displaces *A. formosa*. Below the lower consumption vector, *A. formosa* out competes *C. meneghiniana*. The region between the two consumption vectors is the zone of coexistence where the two diatoms are limited by different nutrients. The results of Tilman's competition experiments have been placed on the figure to show the excellent agreen between prediction and observation. Refer to Question Box 22–4—Working with the Mechanistic Model of Competition—to try a similar analysis on data for *Fragilaria crotonensis* and *Synedra filiformis*.

Tilman's research on competition between *A. formosa* and *C. meneghiniana* is presented in several papers including Tilman (1976, 1977) and Tilman and Kilham (1976). His mechanistic theory of competition is developed fully in Tilman (1982) and Tilman, et al. (1982), which also contains a table of Monod kinetic constants for a variety of phytoplankton. Tilman then

**Table 22–5 Values of $K_s$ and ratios of $K_s$ values for *A. formosa* and *C. meneghiniana***

| | $K_s$ (μM $PO_4$) | $K_s$ (μM $SiO_2$) | $K_s$ ($PO_4$)/$K_s$ ($SiO_2$) |
|---|---|---|---|
| *A. formosa* | 0.04 | 3.9 | 0.01026 |
| *C. meneghiniana* | 0.25 | 1.4 | 0.17857 |

extended his studies to four species of Lake Michigan diatoms including *A. formosa*, *Fragilaria crotonensis*, *Synedra filiformis*, and *Tabellaria flocculosa*. He found that *A. formosa* and *F. crotonensis* were competitively equal; they coexisted at all ratios of silicate to phosphate because they appear to have similar resource requirements. This result suggests a novel way species diversity may increase. Even if two phytoplankton species are morphologically distinct, they can coexist if they are physiologically very similar. It is not known how common this phenomenon might be.

Temperature was later found to be capable of altering the outcome of competitive interactions (Tilman, et al., 1981, Mechling and Kilham, 1982). Monod kinetic constants changed as a function of temperature. In one set of experiments, *A. formosa* displaced *Synedra ulna* below 20° C, but *S. ulna* displaced *A. formosa* above 20° C.

While Tilman, the Kilhams, and their students have primarily focused on freshwater diatoms, and silicate and phosphate as limiting nutrients, they have extended their observations to green algae and cyanobacteria. Cyanobacteria studied include *Oscillatoria agardhii* (Ahlgren, 1978) and *Microcystis aeruginosa* (Holm and Armstrong, 1981). Among green algae, we have data on *Volvox aureus* and *V. globator* (Senft, et al., 1981), *Mougeotia thylespora*, *Scenedesmus acutus*, and *Chlorella minutissima* (Sommer, 1986a), and *Scenedesmus quadricauda*, *Oocystis pusilla*, and *Sphaerocystis schroeteri* (Grover, 1989). Work by Sandgren (1988) and Lehman (1976) has provided data on chrysophycean flagellates. Data on Monod kinetics for marine phytoplankton and for nitrogen as a limiting nutrient are available. In one marine study, Sommer (1986b) examined Tilman's mechanistic model of competition among five species of marine diatoms from Antarctic waters for limiting supplies of nitrate and silicate (see Question Box 22–4 problem 2). In general, the predictions of the mechanistic model and experimental observations of competition have been in excellent agreement. Despite some gaps in specific taxonomic groups, Tilman's model has been well verified in continuous cultures at steady state.

While the model successfully predicts coexistence between two species competing for two different limiting nutrients, there are a very limited number of potentially limiting nutrients. The list includes only sil-

**Table 22–6 Regions of nutrient limitation defined by the ratios of $K_s$ values**

| | limited by $PO_4$ | limited by $SiO_2$ |
|---|---|---|
| *A. formosa* | $\frac{[PO_4]}{[SiO_2]} < 0.01026$ | $0.01026 < \frac{[PO_4]}{[SiO_2]}$ |
| *C. meneghiniana* | $\frac{[PO_4]}{[SiO_2]} < 0.17857$ | $0.17857 < \frac{[PO_4]}{[SiO_2]}$ |

## Question Box 22–4 Working with the mechanistic model of competition

1. Tilman (1981) tested his resource competition theory on four species of Lake Michigan, U.S.A., diatoms. The Monod kinetic parameters $\mu_{max}$ ($day^{-1}$), $K_s$ ($\mu M$) and cell quotient Q ($\mu mol\ cell^{-1}$), the amount of nutrient necessary to produce one cell of a species, were determined. Q is the inverse of the yield coefficient. The kinetic parameters under phosphate and silicate limitation for two of the diatoms, *Fragilaria crotonensis* and *Synedra filiformis* are shown in the following table.

parameters under phosphate limitation

| | $\mu_{max}$ ($day^{-1}$) | $K_s$ ($\mu M$) | Q ($\mu mol\ cell^{-1}$) |
|---|---|---|---|
| *Fragilaria* | 0.80 | 0.011 | $4.7 \times 10^{-8}$ |
| *Synedra* | 0.65 | 0.003 | $1.1 \times 10^{-7}$ |

parameters under silicate limitation

| | $\mu_{max}$ ($day^{-1}$) | $K_s$ ($\mu M$) | Q ($\mu mol\ cell^{-1}$) |
|---|---|---|---|
| *Fragilaria* | 0.62 | 1.5 | $9.7 \times 10^{-7}$ |
| *Synedra* | 1.11 | 19.7 | $5.8 \times 10^{-5}$ |

The diatoms were all grown in continuous culture at $D = 0.25\ day^{-1}$, as were *A. formosa* and *C. meneghiniana* in the main text. To calculate the minimum concentration of each nutrient that just allows each diatom species to persist in continuous culture at $D = 0.25\ day^{-1}$, we rearrange the terms in the Monod growth equation and substitute in the parameter values from the table above. Thus:

$$\mu = \mu_{max}\left(\frac{S}{K_s + S}\right)$$

At equilibrium, $D = \mu = 0.25\ day^{-1}$ and $S = R^*$, the nutrient level that allows the diatom to remain in culture with $dN/dt = 0$. Then substituting in the Monod equation, we get:

$$D = \frac{\mu_{max} R^*}{K_s + R^*}$$

We now solve for $R^*$ by multiplying both sides by $(K_s + R^*)$:

$$D(K_s + R^*) = \mu_{max} R^*$$

Then a few algebraic manipulations to isolate $R^*$ gives us:

$$DK_s + DR^* = \mu_{max} R^*$$

$$\mu_{max} R^* - DR^* = DK_s$$

$$(\mu_{max} - D) R^* = DK_s$$

$$R^* = \frac{DK_s}{\mu_{max} - D}$$

## Question Box 22–4 *continued*

As a practice problem, graph the four Monod curves for *Fragilaria* and *Synedra*, each limited by phosphate and silicate. Use the above formula for R* to calculate the minimum levels of silicate and phosphate at which each diatom can just maintain a population in continuous culture at $D = 0.25\ day^{-1}$. Then plot the zero growth isoclines on a resource plane where $y = [PO_4]$ and $x = [SiO_2]$. (*Hint:* you will have to make the axis for $PO_4$ extend over a very small range, on the order of 0.05 $\mu$M). Tilman (1981) used the ratios of the nutrient quotients ($Q_p/Q_{si}$) as his slopes of the consumption vectors. If you use the ratios of the half-saturation constants, the final figure is not greatly changed. Finally, plot the consumption vectors in your resource plane.

2. Sommer (1986b) studied nitrate and silicate competition among marine diatoms from the frigid waters around Antarctica. He obtained the following values for Monod kinetic constants at 0° C for four species of marine diatoms:

| | $\mu_{max}$ ($day^{-1}$) | $K_n$ ($\mu$M) | $K_{Si}$ ($\mu$M) |
|---|---|---|---|
| *Corethron criophilum* | 0.39 | 0.3 | 60.1 |
| *Nitzschia kerguelensis* | 0.56 | 0.8 | 88.7 |
| *Thalassiosira subtilis* | 0.40 | 0.9 | 5.7 |
| *Nitzschia cylindrus* | 0.59 | 4.2 | 8.4 |

Sommer grew these diatoms in continuous culture at $D = \mu = 0.25\ day^{-1}$. Use the formula in problem 1 above to calculate the values of R* for each diatom and nutrient. Then use this information to plot the zero growth isoclines in a resource plane where $x = \mu M\ NO_3^-$ and $y = \mu M\ SiO_2$. You can then use the values of the half-saturation constants to calculate the slopes of the consumption vectors that extend from the intersection points of the zero growth isoclines. (The consumption vectors should be plotted on a separate graph where the axes cover a wider range than that used for the zero growth isoclines.) Answers are found in the section at the end of the chapter.

icon (for diatoms), nitrogen, phosphorus, carbon (possibly in some acidic waters), iron in oceans, and perhaps vitamins. Recent work by Huisman and Weissing (1994) has shown that light can act as a limiting nutrient. It is unlikely that many other items will be added to this list.

When more than two species compete for two limiting nutrients, the mechanistic model predicts that no more than two species can coexist stably at any given combination of those two nutrients. This result is usually presented as a model diagram such as Figure 22–34 from Lampert and Sommer (1997). Here, four species compete for two nutrients in a resource plane. Regions labeled with one number indicate dominance by that one species. Regions with two numbers indicate coexistence by those two species. For all four species to persist, the ratio at which both resources are supplied must move along a gradient through these

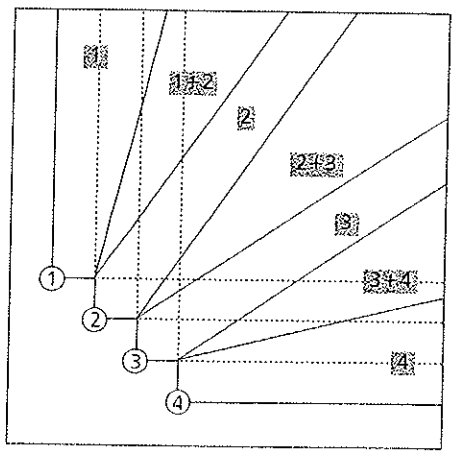


**Figure 22–34** Tilman's model for steady-state competition for two resources among four species of algae. Zero growth isoclines and consumption vectors are shown. Single numbers indicate regions where one species dominates, double numbers where two species coexist. (After Sommer, 1989 ©Springer-Verlag)

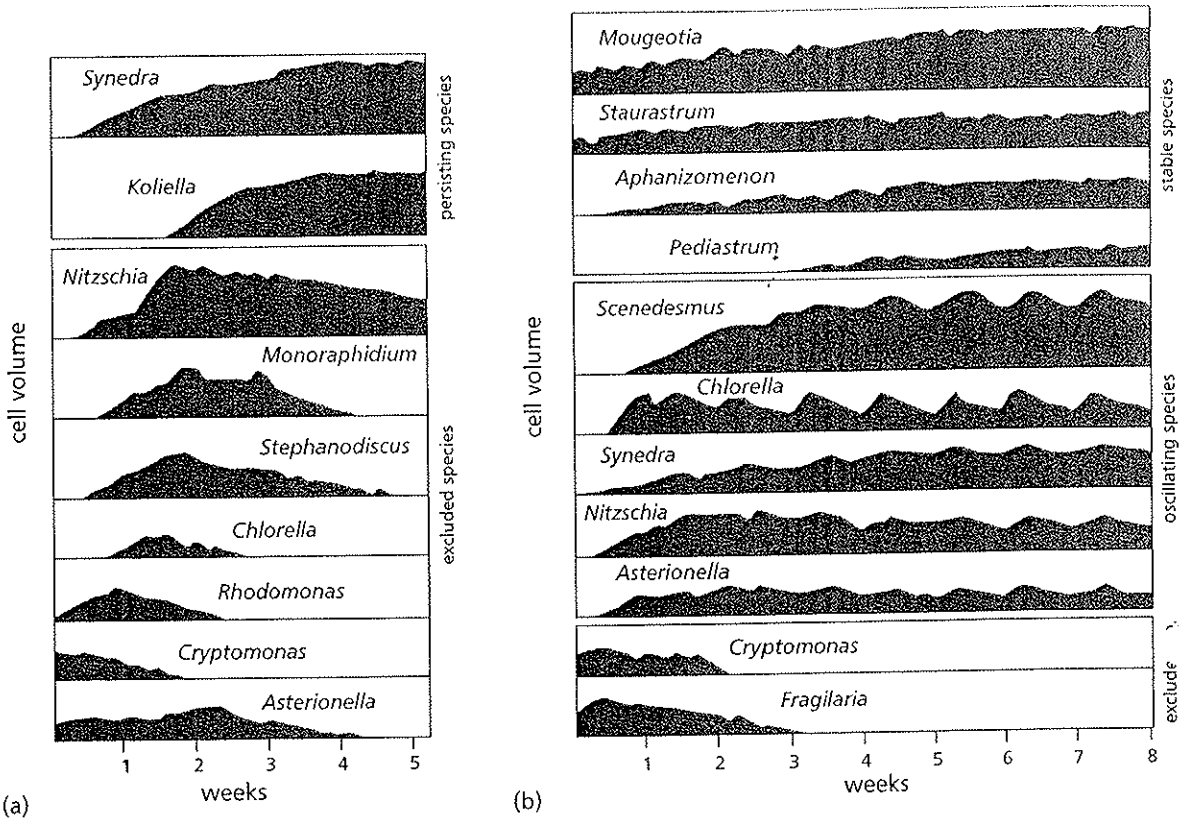


**Figure 22–35** (a) Chemostat competition experiment with natural phytoplankton from Lake Constance at Si:P = 20:1. (b) Pulsed P and Si (1 week intervals) competition experiment with the same phytoplankton inoculum at Si:P = 20:1. Biomass—$\log_{10}(\mu m^3\ ml^{-1})$—of all species that represent more than 5% of total biomass. Under continuous culture conditions, only two species persisted. Under weekly pulsed P and Si conditions, nine species persisted for over eight weeks. (After Sommer, 1985)

regions. Thus at one time species 1 and 2 may be coexisting while species 3 and 4 are in decline. The ratio of resources moves from the region where species 1 and 2 coexist to the region where species 2 and 3 coexist and then to the region of coexistence of species 3 and 4 before either is completely displaced. Then the ratio has to return to the original state before species 1 and 2 are displaced. If more than two species are to coexist on two limiting nutrients, the model must invoke not steady-state conditions but incorporate a cycle of steady states. Resources must change over time in a manner determined by the growth dynamics of the competing species if additional species are to persist. For an example of four marine diatoms involved in competition for two limiting nutrients, refer to the second problem in Question Box 22–4.

The mechanistic model of competition under steady state continuous culture conditions cannot account for more species than the number of potentially limiting nutrients, which is no more than about seven. Researchers have therefore turned to examining the role that perturbations in the supply of nutrients or non-steady–state conditions may have on competition and the number of coexisting species of phytoplankton. In these experiments, continuous culture results become a control to compare against the results of various severities and frequencies of disturbances.

In an early study of perturbations, Turpin and Harrison (1980) studied the marine diatoms *Chaetoceros* spp., *Skeletonema costatum*, and *Thalassiosira nordenskioldii* in natural and artificial assemblages, under both continuous and pulsed additions of ammonium. Continuous cultures were dominated by *Chaetoceros* spp. *Skeletonema costatum* dominated cultures receiving a spike of ammonium every third day. When the ammonium spike was delivered every seventh day, *T. nordenskioldii* dominated cultures. The authors noted that as nutrient addition became

**Table 22–7 Species number in chemostat and pulsed experiments as a function of the Si:P molar ratio. (adapted from Sommer, 1985)**

| | | Si:P (molar) | | | | | | | |
|---|---|---|---|---|---|---|---|---|---|
| | | 4:1 | 10:1 | 20:1 | 30:1 | 40:1 | 80:1 | 140:1 | ≥200:1 |
| # of species | chemostat | 1 | 2 | 2 | 3 | 2 | 1 | – | – |
| | pulsed P | 8 | – | 6 | – | 6 | – | 5 | 5 |
| | pulsed P + Si | 8 | 8 | 9 | – | 10 | 8 | 7 | 6 |

less frequent, the dominant diatom had a larger average cell size. Presumably this is because larger cells can store up more nutrient to survive the depleted conditions between additions.

Sommer (1985) took natural phytoplankton communities from Lake Constance and compared competition in chemostats to competition in cultures where either phosphate or both phosphate and silicate were added in pulses at one week intervals. Si:P ratios from 0:1 to 280:1 were tested. Pulsed additions of nutrients led to a marked increase in number of persisting species from 1–2 to 9–10 (Table 22–7). Continuous nutrient additions favored diatoms, while pulsed additions promoted greens (Fig. 22–35). These results applied to a single fixed interval of pulses of nutrients.

In a later study, Gaedeke and Sommer (1986) varied the frequency of pulses from 1 to 14 days. At one-day intervals, only one species dominated cultures—the cyanobacterium *Pseudanabaena catenata* in silicate-enriched systems and the green alga *Koliella spiculiformis* in silicate-free cultures. As the interval between nutrient additions reached three days, species diversity rose and reached a maximum at seven days. At greater intervals than seven days, diversity declined slowly (Fig. 22–36). Perturbations had to occur at an interval greater than the average generation time of the algae before they affected species diversity. Interestingly, the maximum diversity occurred at seven days, an interval roughly equal to that of the passage of weather events across bodies of water. Gaedeke and Sommer (1986) believe their results support the intermediate disturbance hypothesis of Connell (1978), which states that moderate levels of disturbance promote species diversity.

Perturbation studies have established that competitive exclusion can be circumvented by intermediate disturbances in the nutrient supplies. The mechanistic models assume that if nutrients are limiting, then competition will occur. Conversely, if nutrients are not limiting, competition will not occur. How often are various nutrients limiting? Sommer (1988a) tried to determine whether silicon, phosphorus, and nitrogen were limiting in Lake Constance by adding spikes of each nutrient to water samples from the lake at weekly intervals over a year. If the phytoplankton did not respond by growing, then the nutrient was not likely to have been limiting in the sample. Silicate was limiting for diatoms throughout the stratified period, but surprisingly nitrate and phosphate were limiting to growth in an intermittent manner. When they were limiting, that limitation was weak to moderate and

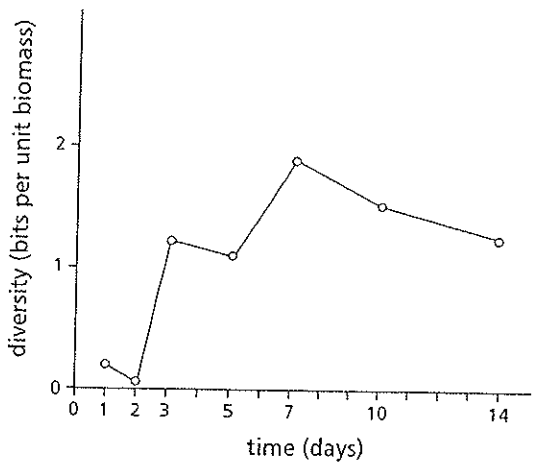


**Figure 22–36** Species diversity index (Shannon and Weaver, 1949) as a function of the interval between nutrient additions in semicontinuous competition experiments. Maximum diversity (the highest number of coexisting species) was reached when the interval between nutrient additions was seven days. (After Gaedeke and Sommer, 1986 ©Springer-Verlag)

rarely severe. These results indicate that in Lake Constance, diatoms are likely to be competing for silicate over the stratified period, but other phytoplankton may be competing only during brief, widely separated intervals. If these results are generally true (more research on lakes of various trophic state would be useful), then competition is a sporadic event, and many species may be able to coexist because they are not competing all the time. The diversity of phytoplankton is only a paradox if we assume competition is continuous. This viewpoint is very different from the old idea that all species are at their carrying capacity and in continuous competition, and suggests that competition is only one loss process among many that shape phytoplankton communities.

## Grazing

The most dramatic phytoplankton loss process is grazing loss. Grazing refers to predator-prey interactions where the prey are bacteria and algae, and the predators are rotifers and crustaceans. Some phytoplankton can ingest bacteria and even other algae. For examples, refer to Chapter 3. Protozoa may act both as predators on algae and bacteria as well as prey to crustaceans. Rotifers are mainly filter feeders, but a few specialists feed raptorially on large algae. Among crustaceans the lower boundary of phytoplankton cell sizes is determined by the mesh width of the filtering appendages, which range from 0.16 to 4.2 μm in cladocerans (Geller and Müller, 1981). Cladocerans with the finest mesh sizes (*Cydorus sphaericus*, *Daphnia magna*) can remove large bacteria, while those with the coarsest filters (*Sida cristallina*, *Holopedium gibberum*) miss picoplanktonic algae (0.5 to 2 μm). For copepods, which generally feed by raptorial capture, the upper limit of algal cell size is about 50 μm (Burns 1968). Thus cell or colony size in part determines the relative susceptibility of phytoplankton to grazing losses.

How important are losses due to grazing on phytoplankton? The significance of grazing losses is indicated by the existence of a clear-water phase in late spring and early summer in many mesotrophic and eutrophic lakes. The development of a clear-water phase is shown in Lake Schöhsee near Plön, Germany, in May 1983 (Fig. 22–37). As the dominant grazers (species of *Daphnia* and *Eudiaptomus*) increase in numbers, the smaller (<35 μm) algae decline, and Secchi disk transparency increases (Lampert, et al., 1986). For such a clear-water phase to occur, the loss rate due

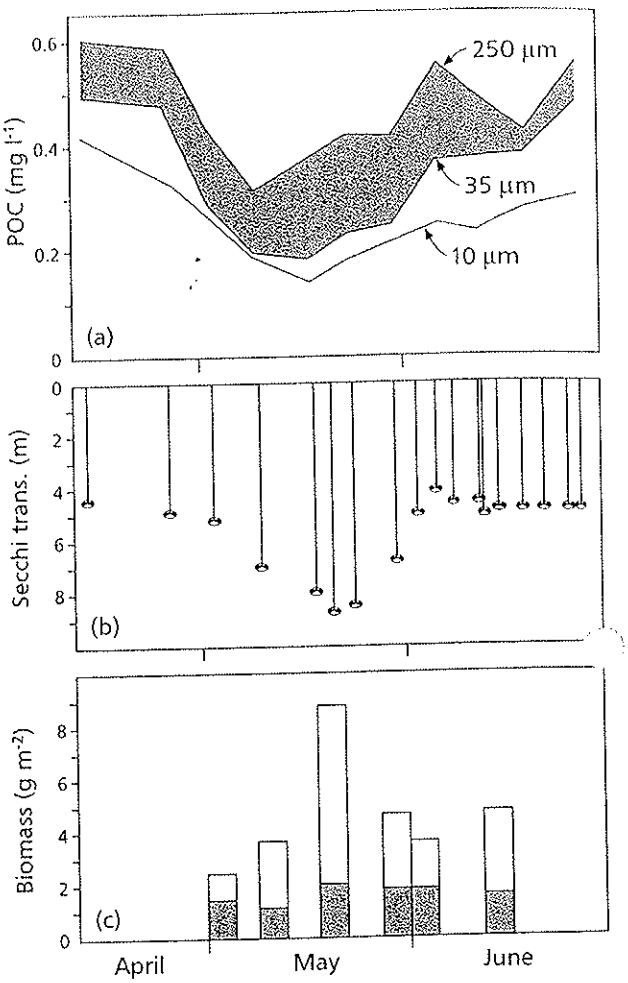


**Figure 22–37** Development of a clear-water phase in Lake Schöhsee, Germany, in 1983. (a) Particulate organic carbon (POC) separated by size (< 10 μm, < 35 μm, < 250 μm). (b) Secchi disk transparency (m). (c) Biomass (g $m^{-2}$) of *Daphnia* spp. (open bar) and *Eudiaptomus* spp. (shaded bars). (After Lampert, et al., 1986)

to grazing (γ) must exceed the phytoplankton production rate (r).

Cladocerans play a major role in the generation of these clear-water phases. *Daphnia*, in particular, has a strong impact on the structure of phytoplankton communities and on the microbial food web in general. Compare the two food webs in Figure 22–38. In Figure 22–38a, *Daphnia* dominates the system and suppresses all the protozoans and edible phytoplankton. The microbial food web consists of large, inedible, or grazing-resistant algae and small bacteria that escape the mesh size of *Daphnia* (Jürgens 1994). Phytoplankton are too large to be grazed or else survive gut

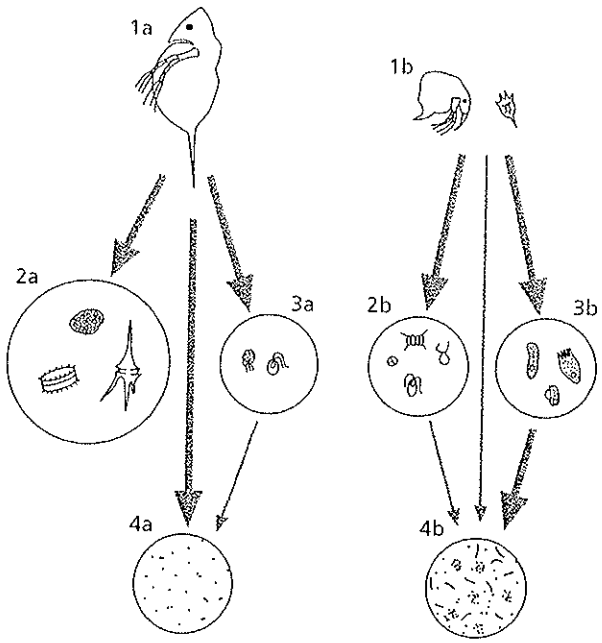


**Figure 22–38** Impact of different zooplankton assemblages on the microbial food web. (a) Domination by *Daphnia* leads to grazing resistant algae, small flagellates and small bacteria. (b) Domination by *Cydorus* and rotifers produces small edible algae, diverse protozoa and grazing resistant bacteria.

passage because of protective sheaths (Porter 1977). In contrast, Figure 22–38b shows a food web dominated by rotifers and *Cydorus*. Protozoa are numerous and diverse, while phytoplankton are small and mostly edible. The protozoa graze heavily on the bacteria, leaving grazing-resistant (filamentous and clumped) forms (Jürgens and Güde, 1994). Thus, the type of grazing pressure affects the composition of phytoplankton and microbial communities.

Grazing can also alter the outcome of competition between phytoplankton. Rothhaupt (1992) added the diatom *Synedra*, *Cryptomonas*, and bacteria to a chemostat. Both *Synedra* and bacteria had low half-saturation constants for phosphorus and grew rapidly. *Cryptomonas*, however, had a higher $K_s$ value for phosphorus and remained in culture only at low density (Fig. 22–39). *Synedra* reached a constant population level due to silica limitation. At week three, Rothhaupt introduced the heterotrophic flagellate *Spumella*, which grazed on the bacteria and released the bacterial phosphorus into the vessel. Since *Synedra* was silica limited, it could not use the added phosphorus, and *Cryptomonas* eventually became the dominant alga in the chemostat. Grazing pressure can thus alter competitive interactions. The dominance of grazing-resistant algae after the clear-water phase is in large part due to the release of nutrients from edible algae by grazers. Large phytoplankton, or those with protective sheaths, are generally poor nutrient competitors. Grazers act to shuttle nutrients from edible to inedible algae. This capacity of grazing pressure to change algal assemblages has led to a great deal of research on trophic dynamics and to the use of biomanipulations to affect changes in aquatic systems.

Before we consider trophic dynamics and biomanipulations, we need to ask first how grazing is measured. Terminology and mathematical expressions vary among authors, and definitions should be checked carefully in references. Here we define the feeding rate or ingestion rate as the number or mass of cells ingested per individual grazer in a unit of time. Thus:

$$I = C\ ind^{-1}\ t^{-1} \quad (36)$$

C is expressed in cells or some measure of biomass such as biovolume ($\mu m^3$), mg dry weight or mg C.

The filtering rate F of a zooplankton is the volume of water filtered by that herbivore to ingest C cells in time t, assuming 100% efficiency in filtration and retention. F has units of ml $ind^{-1}\ t^{-1}$. In practice, two formulas are used in the determination of a filtration rate, depending on the method of measurement. If cell counts are used, then Gauld's (1951) equation is used:

$$F = \frac{V\ (\ln C_o - \ln C_t)}{N_t} \quad (37)$$

The equation assumes an exponential decline in cells or biomass from $C_o$ to $C_t$ as a result of ingestion by N herbivores over time t. V is the volume of the container in ml. $C_o$ and $C_t$ are measured by direct cell counts or, more commonly now, by an electronic particle counter. Because t is necessarily fairly long (a few hours), correction must be made for any increase in number of algal cells. For additional precautions, refer to Peters (1984).

Alternatively, a radioisotope such as $^{32}P$ or $^{14}C$ may be used. Grazing animals ingest the labeled algal cells, and the activity of each is measured by liquid scintillation. The form of this equation is:

$$F = \frac{A_a\ 60}{A_s\ (N)\ t} \quad (38)$$

where $A_a$ is the activity in counts $min^{-1}$ of the N herbivores measured after t minutes of exposure to the

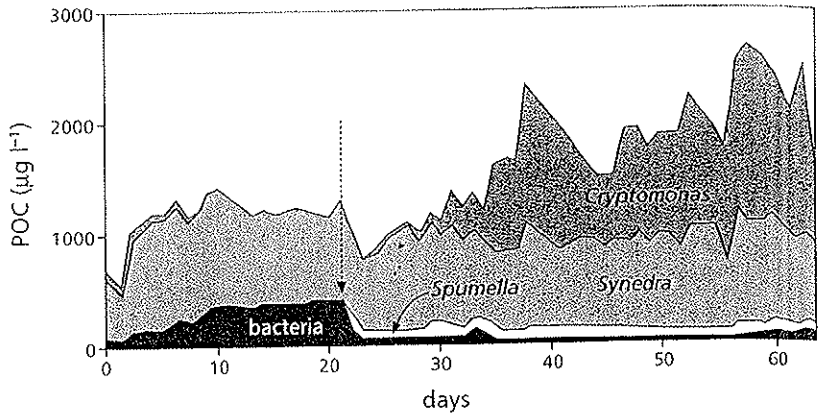


**Figure 22–39** Competition between *Synedra*, *Cryptomonas*, and bacteria for phosphorus in a chemostat. The addition of the heterotrophic flagellate *Spumella* on day 21 reduces the bacterial biomass and makes phosphorus available for growth of *Cryptomonas*. (After Rothhaupt, 1992)

labeled cells. $A_s$ is the activity of the labeled algae in counts $min^{-1}$ ml. The number 60 converts the minutes of exposure into the more useful units of ml $ind^{-1}$ $h^{-1}$. The equation assumes a linear uptake of cells over the short incubation time. The exposure period must be short because it must be less than the gut passage time of the herbivore. Otherwise, labeled cells will be ingested but not counted because they have been expelled. Gut passage times increase with body size; most are about 15 minutes or more. Peters (1984) provides an extensive table.

Filtration rates can be calculated for individual zooplankton species and for separate life cycle stages such as copepodids—the juvenile stages of copepods between the naupliar stage and the adult. Table 22–8 gives individual filtration rates for zooplankton in Blelham Tarn, Cumbria, U.K. (Thompson, et al., 1982).

If we multiply each of these filtration rates by the number of individuals of each species or stage in a liter, we get a new parameter, the community grazing rate:

$$G = \Sigma F_i N_i \quad (39)$$

G represents the losses due to grazing by the entire zooplankton community on the algae used as a tracer and all other phytoplankton with the same relative edibility as the tracer alga. Here it is the same as the $\gamma$ term in our loss equation (26). Thompson, et al. (1982) measured the community grazing rate (or index) by summing the individual filtration rates on *Chlorella* as tracer alga for all significant herbivores in Blelham Tarn enclosures multiplied by their respective population densities. G varied from 0.2% to 200% $day^{-1}$, meaning that on some occasions the entire volume of water in an enclosure was filtered twice in one day! Such a rate exceeds the growth rate of many phytoplankton.

Haney (1973) pioneered the direct measurement of G by radioactivity as:

$$G\ (day^{-1}) = A_a\ 60\left(\frac{24}{V}\right)A_s\ t \quad (40)$$

V is the volume of the chamber (Haney chamber) used in the field, in ml. $A_a$ is the radioactivity of all animals in the chamber, and $A_s$ is that of the tracer alga introduced to the chamber. The value of t is expressed in minutes, and (60 × 24) converts readings from minutes into days. In eutrophic Heart Lake, Ontario, Canada, Haney found that the summer value of G often exceeded 100% $day^{-1}$ with the average G from June through September being 62–80% $day^{-1}$. The net growth rate of the phytoplankton (r) was generally balanced by the community grazing rate G (or $\gamma$) in Heart Lake. In oligotrophic Hall's Lake, Ontario, Canada, however, r exceeded $\gamma$.

Because of the labor involved, relatively few researchers have followed the procedures of Haney (1973) or Thompson, et al. (1982). Furthermore, neither procedure takes into account the relative edibility or selectivity of different phytoplankton species. If we assume that our tracer alga is highly edible and defenseless, we can define its selectivity as $\omega = 1.0$. Relative to it, all other algae would have a selectivity $\omega$ of 1.0 or less. Figure 22–40 gives the relative selectivity coefficients for *Daphnia magna* feeding on a variety of phytoplankton (Sommer, 1988b). In this

**Table 22–8 Ranges and means of individual filtration rates for each category of zooplankton in enclosure A in Blelham Tarn, Cumbria, U.K., in 1978. (from Thompson, et al., 1982)**

| Species and stage | Filtration rates: range (mean) (ml $ind^{-1}$ $day^{-1}$) |
|---|---|
| *Daphnia hyalina* V | 42.1 – 62.6 (53.0) |
| *Daphnia hyalina* IV | 14.0 – 60.0 (28.4) |
| *Daphnia hyalina* III | 9.3 – 29.3 (19.8) |
| *Daphnia hyalina* II | 5.7 – 19.3 (11.8) |
| *Daphnia hyalina* I | 4.0 – 7.6 (6.8) |
| *Diaptomus gracilis*, adult + cop 5 | 0.5 – 10.2 (4.4) |
| *Diaptomus gracilis*, cops 1-4 | 0.5 – 6.7 (2.7) |
| *Cydorus sphaericus* | 0.6 – 2.6 (1.0) |

case, the loss rate due to grazing by *D. magna* on each of these algae is:

$$\gamma_i = G\, w_i \quad (41)$$

G is the grazing rate of *D. magna* on a tracer alga, and the $w_i$ are the selectivity coefficients of each of the other algae. To derive a community grazing index for all herbivores on all phytoplankton, one would need a similar table for each zooplankton species as well as for many life-cycle stages. For obvious reasons this has not been done. Lampert, et al. (1986) developed an interesting approach to this problem. They used two different tracer algae in a Haney chamber. *Scenedesmus acutus* labeled with $^{14}C$ had a diameter of 10 $\mu$m and was used to measure grazing on edible nanoplankton; $^{32}P$-labeled *Synechococcus elongatus* with a diameter of 1 $\mu$m was used to measure grazing on picoplankton. Grazing rates varied from 40% to 170% $day^{-1}$. In general, values of G in excess of 1.0 may persist in lakes for several months (Sterner 1989).

As grazing studies gradually accumulated, it was recognized that zooplankton could have significant impact on phytoplankton communities and even gen-

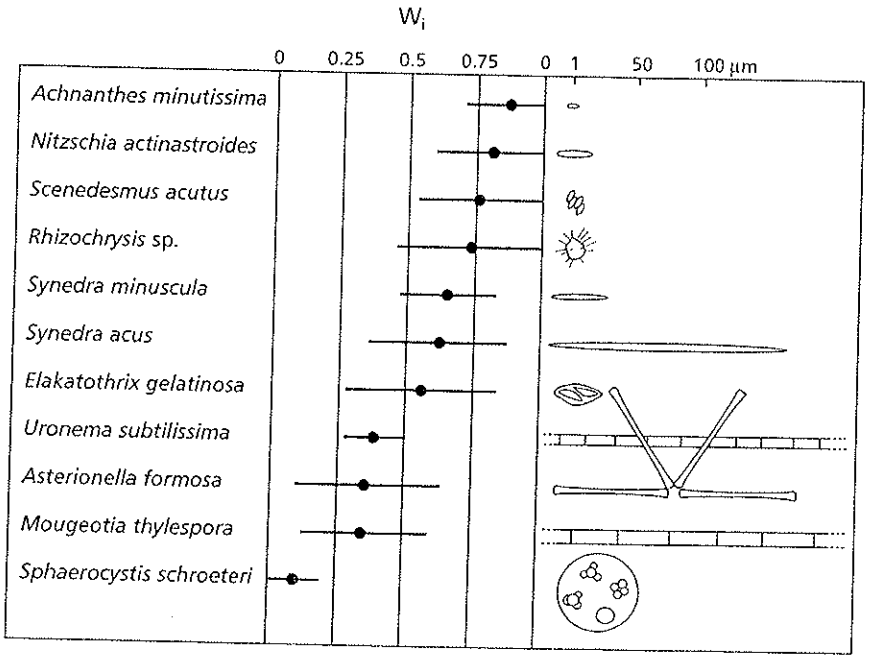


**Figure 22–40** Selectivity coefficients ($w_i$) for various phytoplankton fed on by *Daphnia magna*. Note that large species and those with gelatinous sheaths are not grazed upon well. (After Lampert and Sommer, 1997 ©Georg Thieme Verlag)

erate clear-water phases in some lakes (Porter, 1977; Bergquist, et al., 1985; Bergquist and Carpenter, 1986; Jürgens, 1994). At the same time, evidence was gathered indicating that other trophic levels in aquatic systems could have major impact on the levels below them (Carpenter, 1989). Piscivorous fish can shape the assemblage of planktivorous fish (Tonn and Magnuson, 1982). Planktivorous fish can, in turn, determine the species composition and size structure of zooplankton (Brooks and Dodson, 1965). All these studies led to the idea of a **trophic cascade** in which effects cascade from top to bottom down a chain of linked trophic levels (Carpenter, et al., 1985). The top predators—piscivorous fish—are seen as keystone species (Paine, 1969) with effects extending down many trophic levels below their own position in the food web. The keystone species concept led to the hypothesis that, in aquatic systems, control proceeds from the top of the food web downward. Thus, if one were to manipulate the top trophic levels, one might be able to alter the phytoplankton community to achieve a clear-water lake with enhanced aesthetic and recreational value.

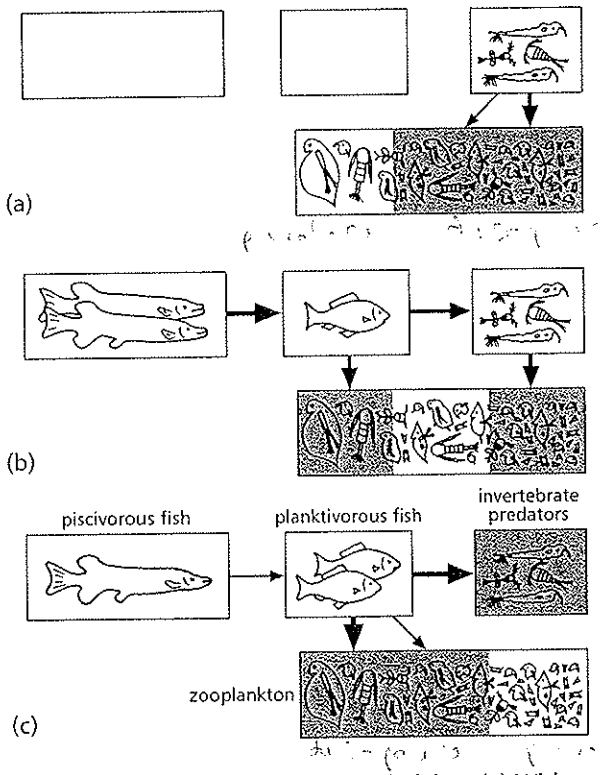


**Figure 22–41** The trophic cascade in lakes. (a) With only invertebrate predators, large zooplankton result. (b) Large populations of piscivorous fish suppress the planktivorous fish and lead to medium-sized zooplankton. (c) Having few piscivorous fish leads to many planktivorous fish and small zooplankton. (After Lampert, 1987 ©Springer-Verlag)

These trophic cascade concepts are diagrammed in Figure 22–41. The top diagram (a) shows a lake without fish; where the dominant herbivores are invertebrates like *Chaoborus*. *Chaoborus* prefers small zooplankton prey. Consequently, large *Daphnia* and copepods dominate and suppress the phytoplankton as in Figure 22–38a. Figure 22–41b shows a lake with large stocks of piscivorous fish that feed on the planktivorous fish. A mixed assemblage of various sizes of zooplankton results with strong grazing pressure on the phytoplankton. In Figure 22–41c, few piscivorous fish lead to numerous planktivorous fish and small zooplankton. The small zooplankton in turn lead to a microbial food web as in Figure 22–38b, with many small, edible algae and protozoa. Both Figures 22–41a and b represent biomanipulations.

The keystone species concept is often referred to as the "top-down" hypothesis of aquatic system control. In its simplest form, the top-down hypothesis predicts that adjacent trophic levels are negatively correlated. In other words, more piscivorous fish means fewer planktivorous fish, which leads to more and larger zooplankton and fewer algae. Conversely, more planktivorous fish would mean fewer zooplankton and more algae. The top-down hypothesis is often contrasted to the older, "bottom-up" hypothesis. The bottom-up hypothesis says that all trophic levels are positively correlated. Thus more nutrients means more phytoplankton and more zooplankton. Comparison across many lakes of different trophic status generally supports a bottom-up hypothesis. Figure 22–42 shows two significant cross-lake correlations between phosphorus and total phytoplankton chlorophyll *a* (a) and between phytoplankton and zooplankton (b). Biomanipulations within lakes and enclosures, however, often support the top-down hypothesis. Before we discuss these contrasting hypotheses further, we will present some of the top-down data.

Tests of the trophic cascade hypothesis are difficult to carry out because of the large workload. Many trophic levels must be monitored in both manipulated and co riod of time. Bioma ce manipula- tions latter being amena

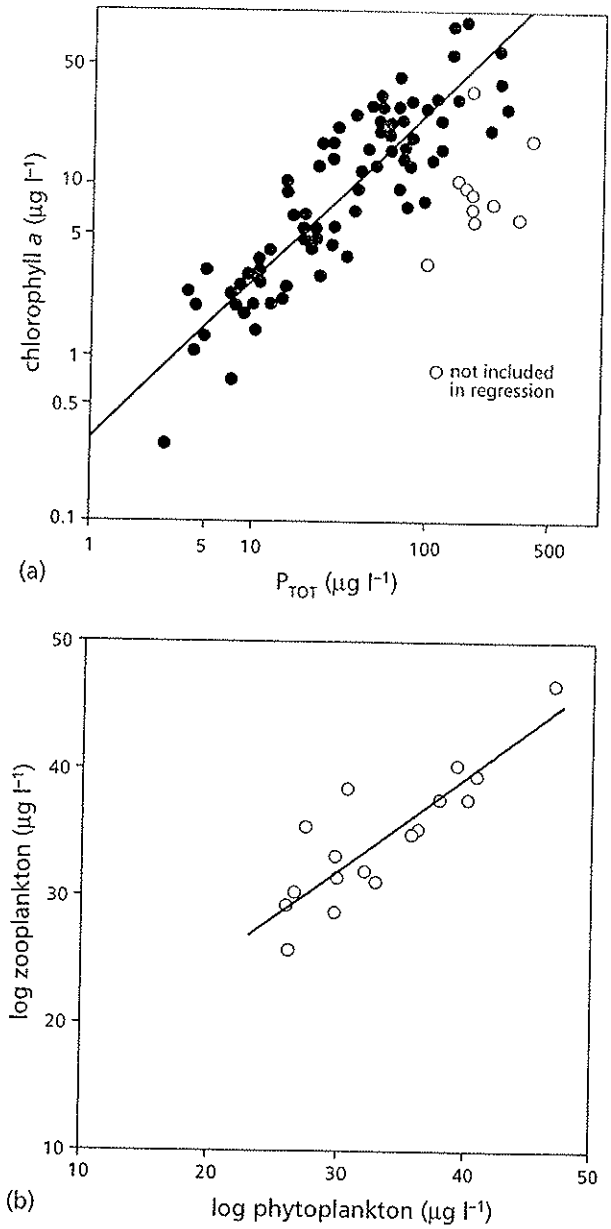


**Figure 22–42** Bottom-up control data from many lakes of various trophic status. (a) Phytoplankton biomass (as chlorophyll *a*) as a function of phosphorus. (b) Log zooplankton biomass as a function of log phytoplankton biomass. (a: Based on Vollenweider, 1982 ©Springer-Verlag; b: After McCauley and Kalff, 1981)

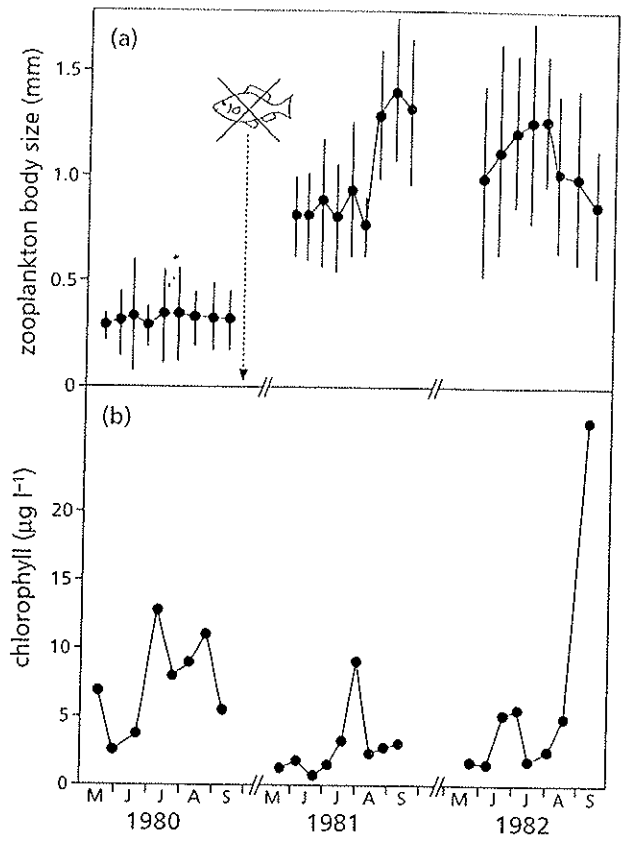


**Figure 22–43** Biomanipulation of Round Lake, Minnesota. The entire fish population was eliminated with rotenone in 1980. (a) The average body size of zooplankton increased after the elimination of planktivorous fish. (b) Phytoplankton (as chlorophyll) were reduced in 1981, but a massive bloom of the cyanobacterium *Aphanizomenon flos-aquae* occurred in 1982. (Data from Shapiro and Wright, 1984; figure after Lampert and Sommer, 1997 ©Georg Thieme Verlag)

In enclosure experiments, fish may be excluded, or added at various densities in combination with nutrient treatments. Fish generally reduce zooplankton (top-down) but nutrients increase phytoplankton (bottom-up) (Vanni, 1987). Brett and Goldman (1997) collected data from 11 enclosure studies that employed both nutrient additions and planktivorous fish manipulations. They performed a meta-analysis of all these data to examine the regulatory roles of both planktivores and nutrients. They found that both top-down and bottom-up controls were significant. Zooplankton were under strong planktivore control (top-down) but were only weakly stimulated by nutrients. Phytoplankton were under strong nutrient control (bottom-up) and were moderately controlled by fish through their effects on zooplankton. Specifically, phytoplankton biomass increased, on average, 179% in nutrient treatments, but 77% in fish treat-

ments where zooplankton were suppressed. Therefore both top-down and bottom-up control of phytoplankton occurs, but the consensus of these enclosure experiments is that bottom-up control was stronger than top-down control.

Results from whole-lake studies are more variable than results from enclosures. Whole-lake studies may involve natural experiments, where a mass mortality of fish has occurred, or artificial manipulation of fish stocks. In at least one class of lakes—small, shallow, eutrophic lakes—biomanipulations have been generally successful (Sondergaard, et al., 1990; Meijer, et al., 1990; van Donk, et al., 1990a). Initially, in summer, these lakes were dominated by blooms of cyanobacteria. Following removal of planktivorous and benthivorous fish, the zooplankton shifted from rotifers to larger *Daphnia* and a clear-water phase occurred. Submerged macrophytes reestablished themselves due to improved light conditions at the lake bottoms. The lakes remained clear because nutrients were taken up by the macrophytes. When the same manipulations were tried on larger (>100 ha) shallow eutrophic lakes, results were variable. Lake Breukeleveen, Netherlands, (180 ha) showed no improvement, due to wind-induced turbidity that prevented macrophytes from developing (van Donk, et al., 1990b), but Lake Christina (1619 ha), central Minnesota, U.S.A., improved dramatically because submerged macrophytes increased (Hanson and Butler, 1990).

Biomanipulations in other types of lakes are less predictable. Shapiro and Wright (1984) poisoned the entire fish stock of Round Lake, Minnesota (U.S.A.) with rotenone (Fig. 22–43). In 1980 the lake was dominated by planktivorous fish and small zooplankton. After fish removal, the zooplankton size increased and phytoplankton (as chlorophyll) declined. But two years after the manipulation, the grazing-resistant cyanobacterium *Aphanizomenon flos-aquae* bloomed, and chlorophyll levels were higher than previously.

In a seven year study of Lake St. George (Canada), McQueen, et al. (1989) found evidence of both top-down and bottom-up controls. In the winter of 1981–1982, low oxygen under the ice caused a winter fish kill (Fig. 22–44). Zooplankton quickly reached maximum body size and biomass, but they had no impact on the phytoplankton. The correlation coefficients show that piscivorous fish had a strong negative impact on planktivorous fish, which, in turn, had a negative impact on zooplankton. Nutrients had a strong positive impact on phytoplankton. Both top-down and bottom-up control occurred, with the effects diminishing as they passed up or down the food web. These results were supported by the meta-analysis of enclosure experiments discussed previously.

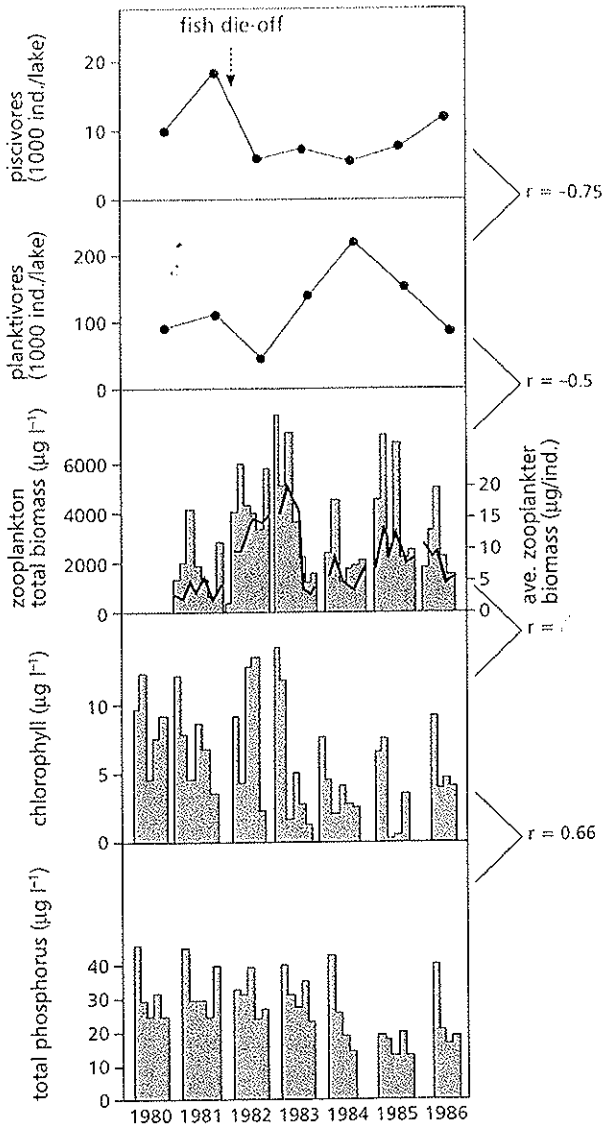


**Figure 22–44** Seven years of food web data from Lake St. George, Canada. In the winter of 1981-1982, a winter kill reduced all the fish populations. Zooplankton biomass and body size (center) increas... due to reduced planktivore pressure. The planktivores recovered quickly and reduced the zooplankton in 1983. Phytoplankton and phosphorus show little change. Correlation coefficients between adjacent trophic levels are shown on the right. (Data from McQueen, et al., 1989; figure after Lampert and Sommer, 1997 ©Georg Thieme Verlag)

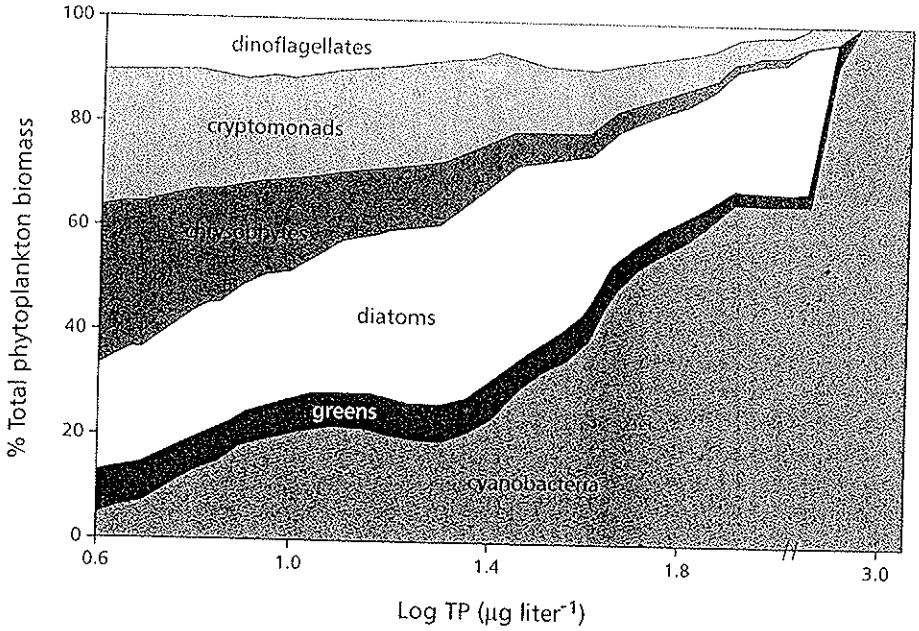


**Figure 22–45** Percentage contribution of taxonomic groups of phytoplankton to total summer biomass as a function of average total phosphorus of lakes. As log TP rises, cyanobacteria become increasingly dominant. (After Watson, et al., 1997)

The concept of top-down and bottom-up interaction has become increasingly recognized in the literature. In 1990, Vanni, et al., reported on the effects of a mass mortality of planktivorous fish in Lake Mendota, Wisconsin. After the fish die-off, the larger *Daphnia pulicaria* replaced *D. galeata mendotae* and generated a longer spring clear-water phase. These authors suggested that high phosphorus levels may reduce effects of trophic cascades on phytoplankton communities. In a comparative study of manipulations in Peter, Paul, and Long lakes, Michigan (U.S.A.), Carpenter, et al. (1996) concluded that the potential effects of phosphorus input on phytoplankton were stronger than the potential for controlling phytoplankton through food-web manipulation. In other words, phosphorus enrichment could overpower the mitigating effects of a trophic cascade and affect the success of a biomanipulation. If nutrient inputs have a stronger effect on phytoplankton blooms than does food-web manipulation, then effective phytoplankton management will require the difficult (and expensive) job of controlling nutrient inputs through erosion control, wetland preservation and restoration, and effluent treatment.

Is it top-down or bottom-up? Carpenter and Kitchell (1993) reply, "A simplistic view of trophic interactions (Is it top-down or bottom-up?) is insufficient and misleading." Clearly, both controls are important and interact with each other. Two current hypotheses have been proposed to address the interaction between nutrients and food-web effects (Carpenter and Kitchell, 1993). The "mesotrophic maximum hypothesis" states that food-web effects are greatest in mesotrophic lakes (Elser and Goldman, 1991). One study of fish removal from an oligotrophic lake, however, showed that significant food-web effects could occur even at low nutrient levels (Henrikson, et al., 1980). The "nutrient attenuation hypothesis" states that as nutrients increase, phytoplankton escape grazer control (McQueen, 1990). Watson, et al. (1997) examined patterns of phytoplankton taxonomic composition across temperate lakes of varying trophic status (Fig. 22–45). In summer, the taxonomic composition of the phytoplankton changes drastically with total phosphorus (TP) concentration. Lakes with high TP are dominated by cyanobacteria. *Daphnia* cannot survive in dense blooms of cyanobacteria (Gliwicz 1990). Therefore, once lakes are in the upper range of phosphorus enrichment, they will be dominated by cyanobacteria and grazing may have little effect. Recent work suggests, however, that *Daphnia* may be able to reduce the frequency of cyanobacterial blooms by recycling nitrogen (ammonium) and reducing $N_2$ fixation by cyanobacteria (MacKay and Elser, 1998). Biomanipulations in nutrient-rich lakes may even cause lake quality to deteriorate if they result in the transfer of nutrients from edible algae to inedible algae, as may have happened in the Little Round Lake manipulation. Carpenter and Kitchell (1993) conclude that our abil-

ity to predict the outcome of trophic level interactions will improve "in proportion to our mechanistic understanding of species interactions and life-history characteristics." In their study of biomanipulations in Peter, Paul, and Long lakes, Carpenter and Kitchell's (1993) trophic dynamic models did not predict the actual phytoplankton response largely due to some unknown species interactions and life-history characteristics of *Peridinium limbatum*.

## Patterns of Loss Processes

The previous sections have discussed a wide range of phytoplankton loss processes. All loss processes do not affect all species or taxonomic groups of phytoplankton to the same extent. Although the data collection is laborious, a few studies have attempted to evaluate the relative impact of various loss processes on phytoplankton populations. Jewson, et al. (1981) examined loss rates from sedimentation, parasitism, and grazing in two diatoms, *Melosira italica* and *Stephanodiscus astraea*, in Lough Neagh, Northern Ireland. Losses due to washout from the lake were estimated to lie between 0.25% and 0.5% $day^{-1}$. Parasitism was observed at 2% to 4% of the *M. italica* cells, and grazing by copepods was calculated at 0.05% $day^{-1}$ early in the spring to 0.15% $day^{-1}$ when the diatoms were declining. Once silica became limiting, calm weather led to 90% of the diatoms settling out of the water column. Although virtually the entire crop reached the sediment surface and formed resting stages, grazing by the benthic fauna removed all but 1% of the population. That 1% could provide an inoculum of 65 cells $ml^{-1}$ for the following year.

Reynolds, et al. (1982) examined a wider range of species of phytoplankton for loss processes in their enclosures in Blelham Tarn (U.K.). Estimates were made of net growth rate (r) and losses due to sedimentation and grazing. Small algae, such as *Ankyra*, *Chromulina*, and *Cryptomonas*, were heavily grazed. The diatoms, *Asterionella* and *Fragilaria*, were grazed very little—even when the populations were in decline. Sedimentation was the major loss process. Neither sedimentation nor grazing could account for losses of *Microcystis*. Here, a mechanistic study of death and lysis of *Microcystis* could contribute significantly to our understanding of bloom dynamics.

More recently, Hansson (1996) examined grazing, sinking, and algal recruitment from the sediments in four northern Wisconsin lakes. Sinking losses were negligible because the phytoplankton chosen for study were all motile. Grazing was the main loss process. Algal recruitment from shallow sediments in the littoral zones played a significant part in determining dominant species in the phytoplankton. Algae able to occupy the sediment surface had a refuge from grazing losses and could augment their populations in the water column by 10% to 50% per day. Studies of loss processes and recruitment among different taxonomic groups of phytoplankton underscore the importance of understanding species differences in predicting the outcomes of trophic-level interactions. Thus the characteristics and differences of individual species of phytoplankton can be important even at the level of aquatic management.

## Recommended Books

Harris, G. P. 1986. *Phytoplankton Ecology*. Chapman & Hall, London, UK.

Lampert, W., and U. Sommer. 1997. *Limnoecology*. Oxford University Press, New York, NY.

Reynolds, C. S. 1997. *Vegetation Processes in the Pelagic: A Model for Ecosystem Theory*. Ecology Institute, Oldendorf/Luhe, Germany.

## Answers:

### Box 22–1 Exponential and logistic growth

1. Culture #1: Y = 0.04692(X) + 9.2469 and r = 0.04692 $hr^{-1}$. Culture #2: Y = 0.04717(X) + 9.5380 and r = 0.04717 $hr^{-1}$. Culture #3: Y = 0.05285(X) + 8.9762. The average net growth rate of *Chlamydomonas* is 0.04898 $hr^{-1}$ or 1.175 $day^{-1}$.

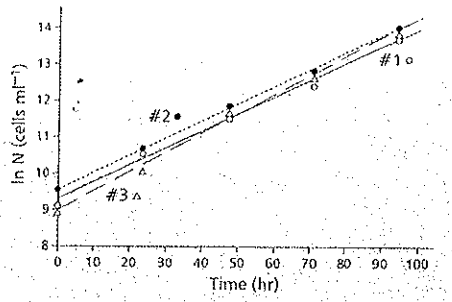


2. In the dark, Y = 0.02797(X) + 6.7091 so r = 0.02797 $hr^{-1}$ or 0.67 $day^{-1}$. In the light, Y = 0.03482(X) + 7.8708 so r = 0.03482 $hr^{-1}$ or 0.84 $day^{-1}$. Photosynthesis increased the net growth rate by 0.17 $day^{-1}$. The corresponding doubling times are 1.03 days in the dark and 0.83 days in the light. Thus, photosynthesis decreased the doubling time by 0.2 days.

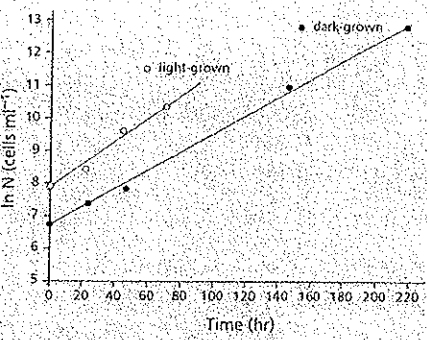


3. The net growth rate can be estimated from a linear regression of the first 7 data points (or the first 9). Refer to the figure (below) for this decision. The results are:

For n = 7: Y = 0.5612(X) + 10.0433 and r = 0.56 $day^{-1}$
For n = 9: Y = 0.5013(X) + 10.2387 and r = 0.50 $day^{-1}$

The last 4 or 5 data points can be used to estimate the carrying capacity K:

For n = 4, K = 8,949,870 and for n = 5, K = 8,821,480.

Which is used is a matter of choice, but a useful rule would be to accept the highest estimates consistent with a reasonable number of data points. Thus an estimate based on only two points is not as reliable as one based on three or more.

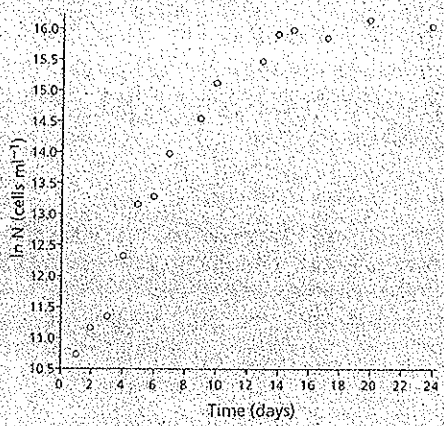


### Box 22–2 Nutrient uptake and growth

1. First take the reciprocals of the values of $SiO_2$ and ρ (see table below). Plot these values as shown in the accompanying figure. The regression is Y = 0.4676(X) + 0.06429 and the correlation coefficient is 0.993.

| x = 1/S | y = 1/ρ |
|---|---|
| 1.120 | 0.602 |
| 0.440 | 0.233 |
| 0.259 | 0.173 |
| 0.138 | 0.149 |
| 0.066 | 0.112 |
| 0.037 | 0.080 |

Now $1/\rho_{max} = 0.06429$ and so $\rho_{max} = 15.5 \times 10^{-9}$ $\mu$M cell$^{-1}$ hr$^{-1}$, $K_s/\rho_{max} = 0.4676$ and $K_s = 7.3$ $\mu$M $SiO_2$. These are quite close to the values reported in Tilman and Kilham (1976), who used nonlinear regression ($\rho_{max} = 15.1 \times 10^{-9}$ and $K_s = 7.5$). The uptake rate for silicate (15.5) is much higher than that for phosphate (5.4), but the half-saturation constant for phosphate uptake is much lower (0.83) than that for silicate (7.3). This means that *C. meneghiniana* can take up phosphate at much lower external concentrations than it can silicate.

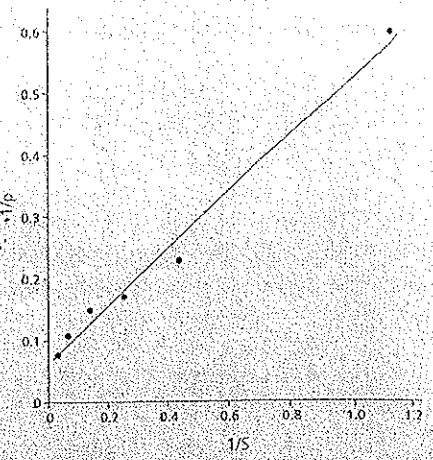


2. The equations are:

$$\frac{1}{\mu} = \frac{K_s}{\mu_{max}}\left(\frac{1}{S}\right) + \frac{1}{\mu_{max}} \quad \text{(a)}$$

| *Fragilaria* | *Synedra* |
|---|---|
| $\mu = 0.62\left(\frac{S}{1.5 + S}\right)$ | $\mu = 1.11\left(\frac{S}{19.7 + S}\right)$ |
| (b) | |

The plot is shown in the accompanying figure (right). According to these graphs, if the supply rate of $SiO_2$ is less than about 22 $\mu$M, *Fragilaria* should be able to outgrow *Synedra*. But if the silicate supply remains above 22 $\mu$M silicate, *Synedra* should be able to outgrow *Fragilaria*. This could lead to a replacement of *Synedra* by *Fragilaria* as silicate is depleted from well-mixed spring surface waters.

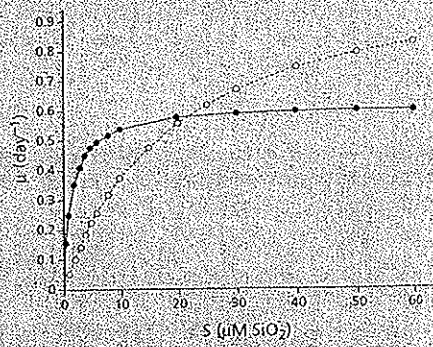


3. Take the reciprocals of the data in the table (below). Then plot the values of 1/S and 1/$\mu$ on graph paper as shown. Now take the linear regression of 1/$\mu$ on 1/S using equation a (above).

| x = 1/S | y = 1/μ |
|---|---|
| 0.2860 | 1.97 |
| 0.2700 | 1.94 |
| 0.1540 | 1.45 |
| 0.1430 | 1.43 |
| 0.0980 | 1.28 |
| 0.0758 | 1.23 |
| 0.0538 | 1.20 |
| 0.0454 | 1.07 |

The result is Y = 3.5982(X) + 0.9398 for which the correlation coefficient is 0.994. $1/\mu_{max} = 0.9398$ so $\mu_{max} = 1.06$ day$^{-1}$, $K_s = 3.5982$ ($\mu_{max}$) and therefore $K_s = 3.83\mu$M $SiO_2$. The values reported by Tilman and Kilham (1976) were $\mu_{max} = 1.06$ day$^{-1}$ and $K_s = 3.94$ $\mu$M.

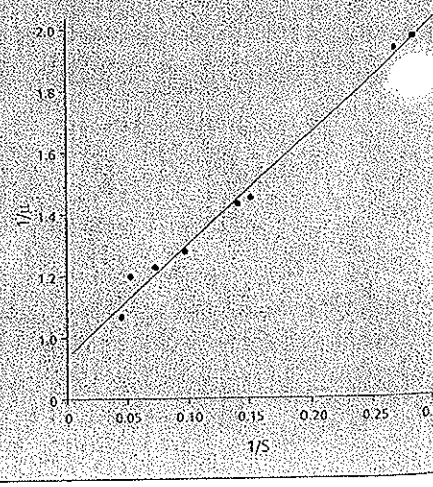

## Box 22–3 Sinking rates/Stokes' law

1. $v_s = 28.27\ \mu m\ s^{-1}\ \phi = 3.86$
2. $v_s = 0.75\ \mu m\ s^{-1}$. Small cells sink much slower than large ones.
3. $v_s = -13.09\ \mu m\ s^{-1}$ or $-0.047\ m\ hr^{-1}$. This ascent rate is much slower than the rates reported in the text, suggesting that cyanobacteria can achieve much lower densities through gas vacuoles than in this example.
4. Since g on Mars is (0.38) 9.8 m $s^{-2}$ or 3.72 m $s^{-2}$, *S. astraea* would sink at the rate of 9.49 $\mu m\ s^{-1}$, or 10.5 $\mu m\ s^{-1}$ if you used the observed value of Reynolds (1984).

## Box 22–4 Tilman's mechanistic model of competition

1. The graphs showing the Monod growth curves for each diatom and limiting nutrient are given below (a through d). The calculated values of R* for *Fragilaria* are: 0.005 $\mu$M $PO_4$ and 1.0 $\mu$M $SiO_2$. R* values for *Synedra* are: 0.002 $\mu$M $PO_4$ and 5.7 $\mu$M $SiO_2$. The following figure (e and f) shows the same resource plane with the consumption vectors based on the ratio of half-saturation constants.

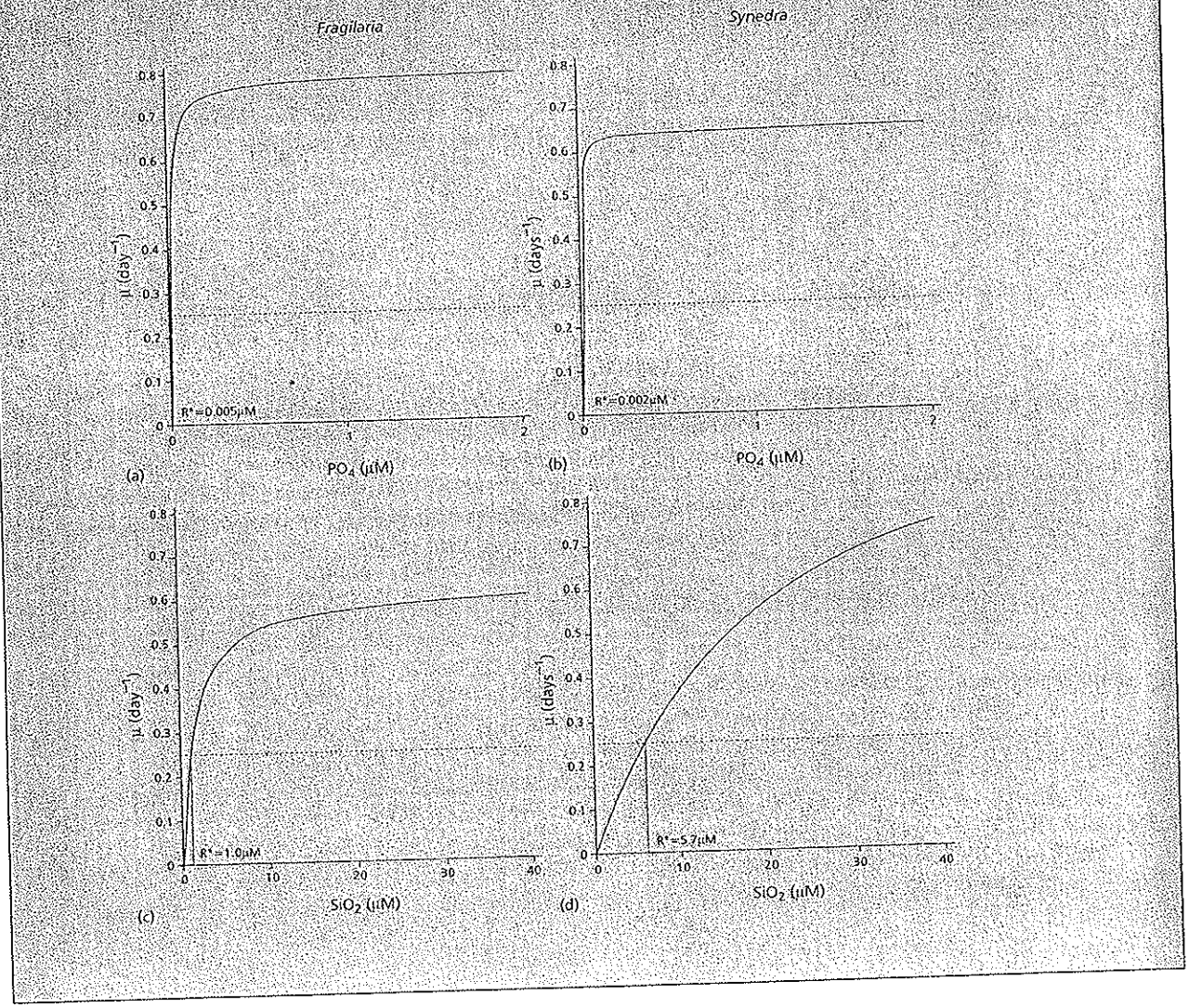

The resource plane with zero growth isoclines.

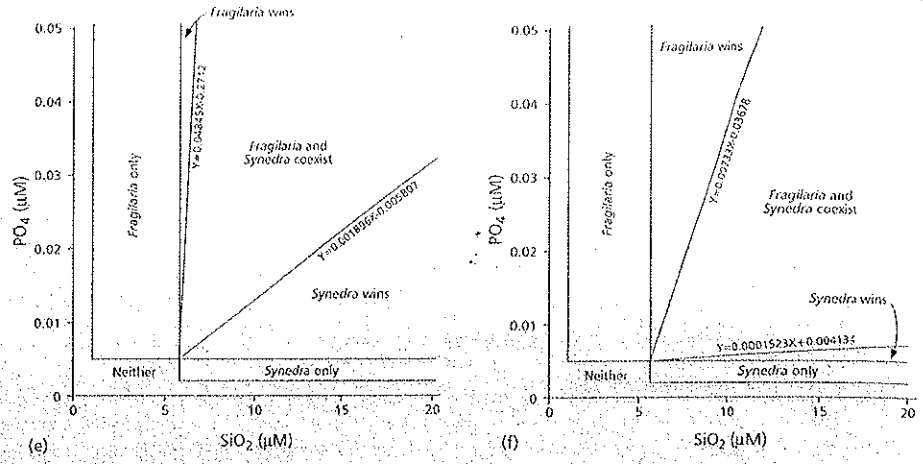


2. The values of R* for each species and nutrient are given in the table below. From these values the zero growth isoclines can be plotted as shown below:

| | R* (μM $NO_3^-$) | R* (μM $SiO_2$) |
|---|---|---|
| *Corethron criophilum* | 0.54 | 107.3 |
| *Nitzschia kerguelensis* | 0.64 | 71.5 |
| *Thalassiosira subtilis* | 1.50 | 9.5 |
| *Nitzschia cylindrus* | 3.10 | 6.2 |

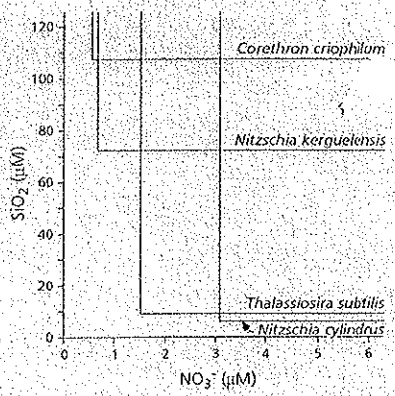


Zero growth isoclines.

There are three significant intersection points: (0.64, 107.3), (1.5, 71.5) and (3.1, 9.5) where the values are (μM $NO_3^-$, μM $SiO_2$). In addition, there are three other intersection points of the zero growth isoclines. These intersections only have meaning in two species interactions; in the four species system any population at these junctions would fall back to the isoclines further to the left.

There are two consumption vectors radiating from each of the significant intersection points listed above. The vectors have been plotted on the graph below. The equations of these lines radiating from each point of intersection are:

| point of intersection | | |
|---|---|---|
| | *Corethron criophilum* | *Nitzschia kerguelensis* |
| (0.64, 107.3) | Y = 200.3(X) – 21.9 | Y = 110.8(X) + 35.8 |
| | *Nitzschia kerguelensis* | *Thalassiosira subtilis* |
| (1.5, 71.5) | Y = 110.8(X) – 94.7 | Y = 6.33(X) + 62.0 |
| | *Thalassiosira subtilis* | *Nitzschia cylindrus* |
| (3.1, 9.5) | Y = 6.33(X) – 10.12 | Y = 2(X) + 3.3 |

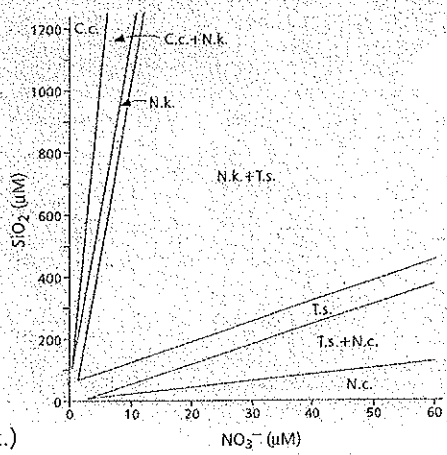


(Consumption vectors based on nutrient quotient.)